VEÐURSTOFA ÍSLANDS

Report
04014

Ragnar Stefánsson, Françoise Bergerat, Maurizio Bonafede, Reynir Böðvarsson, Stuart Crampin, Páll Einarsson, Kurt L. Feigl, Christian Goltz, Ágúst Guðmundsson, Frank Roth, Ragnar Sigbjörnsson, Freysteinn Sigmundsson, Peter Suhadolc, Max Wyss

PREPARED – first periodic report

February 1, 2003 - January 31, 2004

VÍ-ES-04
Reykjavík
May 2004

Contents

WP 1 Overall coordination of the project

Objectives

Scientific coordination and management of the PREPARED project.

Methodology and scientific achievements related to workpackages including contribution from partners

The input is reports on scientific progress in the various workpackages and management reports from the contractors.

The coordinator will through organizing workshops/coordinator meetings and special meeting sessions focus this multidisciplinary, multinational project towards results expressed in the objectives. A PREPARED website organized by the coordinator will also be a significant tool for this.

Every 6 months the coordinator compiles a Management Report about the progress of the project, an Executive Publishable Summary and a Periodic Progress Report after year 1 and year 2, and a Final Report and a Technical Implementation Plan (TIP) after year 2. Additionally he submits a Cost Statement Summary after year 1 and year 2.

The coordinator, which also provides a significant part of the data will try to ensure the other participants in the consortium with easy access to data and to results.

The coordinator which has warning duties in Iceland and which also operates and develops an early warning database will ensure that results of the project will be implemented for risk mitigating purposes in Iceland and be demonstrated for risk mitigating organizations elsewhere.

The first part of the project was a Kick-Off Meeting held in Reykjavík, Iceland, February 24-26, 2003. The minutes of the meeting can be found on the URL *http://hraun.vedur.is/ja/prepared_kick.html*. This meeting provided, besides getting acquainted with the state-of-the-art of geological and earthquake research in Iceland, an opportunity for the participants to meet each other in groups for preparing the various workpackages.

Another significant part for enhancing communication cooperation between the partners was the creation of the PREPARED website, *http://hraun.vedur.is/ja/prepared/* which was opened to the partners on February 14, 2003. The two parts of it, the open part and the closed part have all the most recent reports relevant for the progress of the project.

Informal meetings among attending PREPARED participants was organized during the EGS/AGU/EUG Joint Assembly in Nice, France, April 6-11, 2003.

A two day workshop, i.e. the PREPARED Mid-Term Meeting was organized in Reykjavík on January 30-31, 2004. The minutes of the meeting can be found on the URL *http://hraun.vedur.is/ja/prepared.*

This meeting was a summing up of the progress of the project. Lead contractors of the various workpackages gave presentations about the status of the work and laid the lines for the second part of the project.

The project leader, Ragnar Stefánsson, held an introductionary overview: About the state-of-the-art in providing earthquake warnings in Iceland. (see Stefánsson and Guðmundsson 2004).

Various meetings among participants were organized during January 29-31.

Meetings among scientists during the conference and workshop mentioned above as well as meetings especially organized at other occations are mentioned in the descriptions of the progress of individual workpackages.

The coordinator (IMOR) which has warning duties in Iceland is for its own cost developing an Early Warning and Information System in Iceland (EWIS) which applies the tools and methods of PREPARED in risk mitigation efforts.

The coordinator has provided easy access to much of the data which are basic for the project and communication of results and experiences achieved.

Two papers relevant for the project were presented by IMOR scientists at the EGS/AGU/EGU Joint Assembly in Nice 2003 (Vogfjörð 2003; Roberts et al. 2003). Two papers have been accepted for the EGU Assembly in Nice 2004, one for oral presentation (Stefánsson and Roberts 2004) and one for poster presentation (Roberts et al. 2004). These papers describe how time-dependent hazard assessments and earthquake warnings are realized in Iceland through joint work in the PREPARED and EWIS projects.

Socio-econimic relevance and policy implication

The social and economic impact of a destructive earthquake is enormous. Well established prognosis of what can be expected is a basis for decision on how and where man-made structures are built may lead to strengthening or removal of existing vulnerable buildings. It is a basis for various technical and social precautions and preparedness, that can mitigate the impact of earthquake hazards in various ways.

The PREPARED project is based on the experiences of the two M=6.6 earthquakes in the South Iceland lowland in year 2000. Earlier earthquake prediction research projects, like the SIL project 1988-1995 and the two PRENLAB projects 1996-2000, aimed at, by monitoring and research to prepare for that such an earthquake would occur. The successes in providing long-term hazard assessments for this region before the earthquakes as well as the success during these two earthquakes in providing useful warnings and earthquake information has fostered the hopes among scientists and the public that further progress is possible, and the faith in science to be able to mitigate risk by warnings and information. A significant and useful short-term warning was possible shortly before the second earthquake. In the ongoing work there are signs that practical short-term warnings for a “first earthquake” will be possible in the future in Iceland.

The faith in science for mitigating earthquake risk is already of enormous socio-economic significance and for the quality of life in this area. The experiences gained in PREPARED in Iceland can be applied in other parts of the world for encouraging work in this field and will create hopes that it is possible to obtain good results in earthquake prediction.

Discussion and conclusions

The project as a whole is progressing according to work plan.

Plan and objectives for the next period

There are no special changes from the original plan. During the next period the focus will be on merging together results from the various workpackages as was planned.

References

Kristín S. Vogfjörð 2003. Triggered seismicity following the June 17 Mw=6.5 earthquake in the South Iceland seismic zone. EGS-AGU-EUG Joint Assembly, Nice, France, April 6-11, 2003.

Matthew J. Roberts, Ragnar Stefánsson, Ebba Þóra Hvannberg, Bjarni G. Jónsson, Páll Halldórsson, Hafliði S. Magnússon, Gunnar B. Guðmundsson, Bergþóra S. Þorbjarnardóttir, Sigrún Gunnarsdóttir & Hjörleifur Sveinbjörnsson 2003. Digital warning system for geologic hazards in Iceland. EGS-AGU-EUG Joint Assembly, Nice, France, April 6.-11, 2003.

Matthew J. Roberts, Ragnar Stefánsson & Páll Halldórsson 2004. Internet-based platform for real-time geoscience during tectonic crises in Iceland. EGU General Assembly, Nice, France, April 25-30, 2004.

Ragnar Stefánsson & Gunnar B. Guðmundsson 2004. About the state-of-the-art in providing earthquake warnings in Iceland. *Icelandic Meteorological Office - Report.* In press.

Ragnar Stefánsson & Matthew J. Roberts 2004. Realization of time-dependent hazard assessments and earthquake warnings in Iceland. The ongoing PREPARED and EWIS projects. EGU General Assembly, Nice, France, April 25-30, 2004.

WP 2 Analysis of multiparameter geophysical data approaching the June 2000 earthquakes, assessing state of stress

Objectives

Analysis and linking together multiparameter geophysical observations expressing stress or strain induced variations with time approaching the June 2000 earthquakes and after these. Explain the possibly common source for these variations. Explain them physically. Formulate procedures to assess increase or decrease in probability of earthquake hazard on basis of observable multiparameter observations.

Methodology and scientific achievements related to workpackages including contribution from partners

The input is observations and results of evaluations in WP2.1-2.5, and evolving models and evolving crustal parameters in various other workpackages.

Lead contractors from WP2.1-2.5 work with the coordinator in a forum for analyzing the multidisciplinary observations. They will also be in close contact with other groups, especially the modellers. In Iceland there are many examples of apparent coupling between hazards at large distances. One attempt to explain this is that strainwaves originating from a large intrusive activity at depth, above the top of the hotspot in the center of Iceland or elsewhere, can cause such coincidences by triggering. Modern geophysical observations have also indicated such links between smaller events. Especially there are several indications of patterns that may be related to the strain build-up before the June 2000 earthquakes. Such patterns in space and time will be searched and analyzed in WP2.1-2.5 based on observations of microearthquakes, deformation and strain. Combining results of WP2.1-2.5 and new results of other workpackages, especially the modelling, will be applied to formulate procedures to assess the state of stress or increasing probability of earthquakes caused by crustal loading from outside the seismic zones or closeness to fractures criticality within the zone.

Much work within this workpackage has been used to evaluate enormous amount of data available at IMOR, to create a necessary database for work within WP2.1-2.5. Here the main work was to refine, evaluate further and organize a database of 170.000 microearthquakes which carry information which is of basic interest for most of the workpackages and partners of the project. During September 2003 this enormous base of seismic data could be made available for applications (Guðmundsson et al. 2003, Jakobsdóttir et al. 2002, Þorbjarnardóttir et al. 2003). There have been much contacts about applying the data and exchange of data among the partners. All the WP2.1-2.5 have obtained data from the coordinator and discussion has been about the data and interpretation, and modifications made in the database to make more information accessible and to constrain it. Special discussion was arranged among all the partners in connection with the Kick-Off Meeting and the Mid-Term Meeting as well as with many of the participants at the EGS/AGU/EUG Joint Assembly in Nice 2003.

Analysis of patterns in the seismic data

a) Indications from microearthquakes about stress build-up before the year 2000 earthquakes.

The main aim of this workpackage is to study geophysical data approaching the two earthquakes to try to find earthquake premonitory signs in the data and to explain these. Here the seismic data are most significant, and compared to all other information. In this area the seismic data are complete down to magnitude 0 (see Wyss and Stefánsson 2004; WP2.2 in this report).

Various information from small earthquakes are most likely to be our best indicators for stress build-up. Let us take a look at the two areas of SISZ where we had indications from small earthquakes about stress build-up before the earthquakes. How did the microearthquakes there behave before the large earthquakes? (Stefánsson and Guðmundsson 2004) (Figure 1).

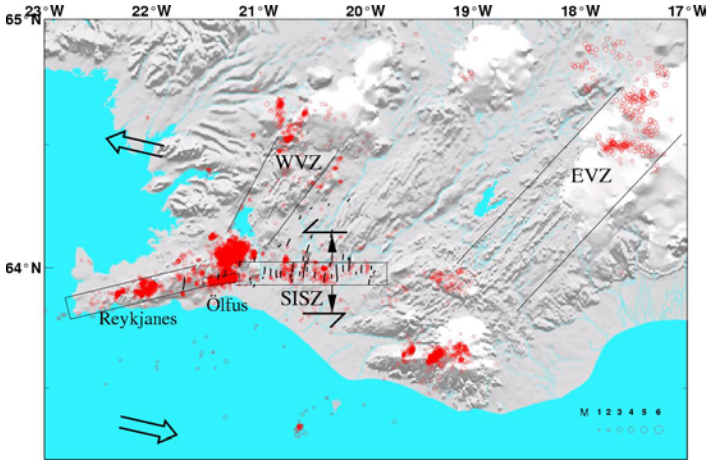

Figure 1. *The relation of the SISZ to the main features of the tectonics of SW Iceland. The western part of the seismic zone has a triple junction with the western volcanic zone and the Reykjanes peninsula. The eastern end of it links to the eastern volcanic zone. The two small seismicity clusters in the central zone are the sites of the two year 2000 earthquakes.*

In the next figure (Figure 2) we consider the time evolution of seismicity in the two clusters approaching the large earthquakes by plotting the number of earthquakes larger than zero.

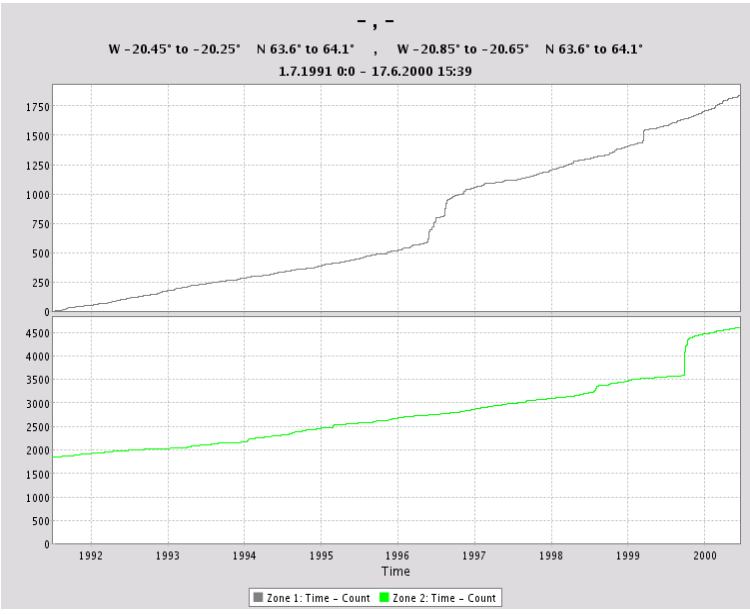

Figure 2. *The upper part shows the number of earthquakes larger than 0 in the eastern cluster (cluster 1), i.e. where the first of the two large earthquakes occurred. The lower part shows the evolution in the western cluster (cluster 2), i.e. where the second earthquake occurred.*

Since the start of microearthquake monitoring in the region in 1991 there is a clear rate increase in cluster 1, i.e. where the first Ms=6.6 earthquake occurred (Figure 2). The even build–up of this increase indicates stress increase in the area. However, we do not know how to use this for estimating even very roughly the time of onset of the probably impending event. In our study we hope to do better than that.

The area around the second M=6.6 earthquake shows no such rate increase in stress indicating microearthquakes (Figure 2). Certainly it has more release of large earthquakes near the end of the period. However, it is generally considered that stress build-up would be indicated by an even seismicity rate increase. This indicates that the second earthquake was not triggered by a gradual build-up of stress in its surroundings as was the first one. Its location was in the stress shadow of the asperity of the first earthquake, and then it was triggered by it. Even if the general stress build-up before the occurrence of the first M=6.6 earthquake does not tell us about the onset, there was a clustering of microearthquake activity along the becoming (expected) fault during the weeks before it, especially clustering near the hypocenter.

In the following we will study what microearthquakes indicate about fault weakening in the year 2000 earthquakes (Figure 3). We do not see the whole of the period of weakening or fault corrosion. We only see the last 9 years before the earthquakes, i.e. the SIL-period, when we observe magnitudes down to zero.

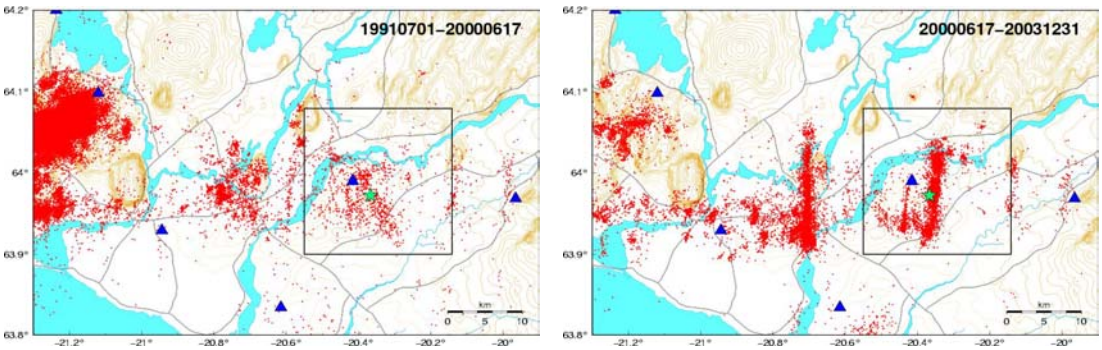

Figure 3. *Seismicity in the SISZ before and after the 2000 earthquakes.*

b) Seismicity changes studied in 3-D volumes around the hypocenter (Figure 4).

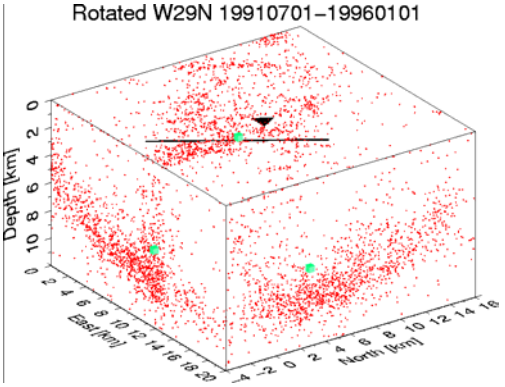

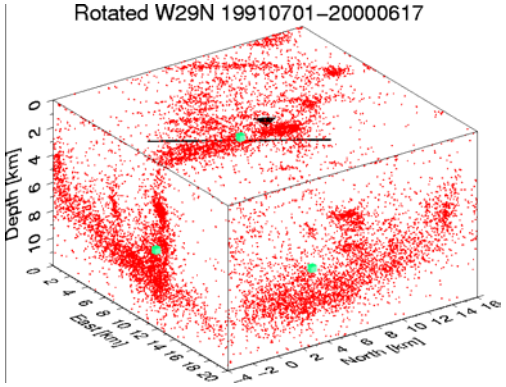

Figure 4a

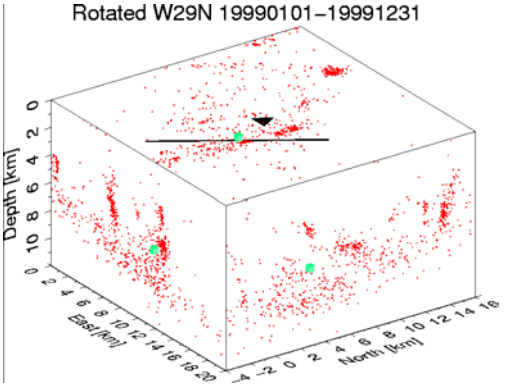

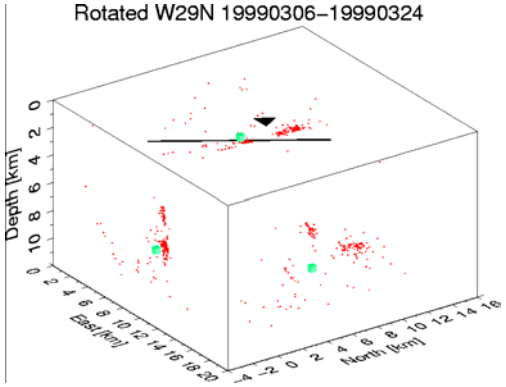

Figure 4b

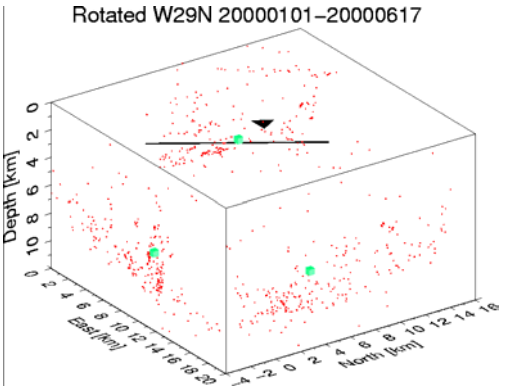

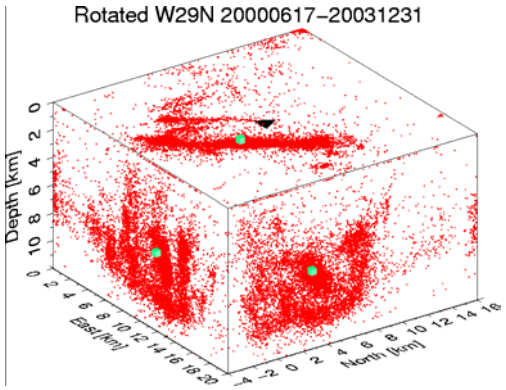

Figure 4c

Figure 4. *The studied 3-D boxes are oriented along the dilavolume, W29°N. The hypocenter (green dot) and the fault of the June 17 shock is also marked as well as SAU, a close seismic station. The two figures at the top (4a) show how the microseismic activity elevates closer to the surface by time. The two figures in the second row (4b) show an episodic shallowing of activity above the dilavolume. The*

figures in the bottom row (4c) show orientation of activity towards the fault plane, especially in the last figure, i.e. after the June 17 earthquake, where the dilavolume has disappeared.

c) Summary of observations in the hypocenter area of the June 17 earthquake.

In this area the everyday microseismic activity is located around 8 km depth in the crust, evenly distributed in time and space (Stefánsson 1993; Tryggvason et al. 2002). Here locally the everyday activity of small earthquakes is however elevated up to around 6 km into a volume which strikes 29° west of north. This volume crosses the middle of the impending earthquake fault below the hypocenter. We call this the dilavolume. A few episodes of larger earthquakes occur higher up in the crust, above both end segments of the dilavolume. Only shortly before the main shock the microearthquakes start to arrange along the impending fault plane. It appears that there is a clustering process for a couple of years in the seismicity, from spread activity towards more concentrated. This has to be studied more quantitatively.

A well defined boundary is observed at 3 km depth above the NW segment of the dilavolume, high number of earthquakes just below the boundary and just a few above. This boundary has a diameter of around 1.5 km.

The dilavolume could be a deep signature of a 300.000 years old fault which has been rotated towards a direction approaching to be perpendicular to horizontal compression axis, arround 50° east of north. Therefore it is not favourable for being released in a large earthquake crossing the zone. However, it had to be released and it preferred a fault which had a more favourable direction to the stresses, i.e. in a right-lateral fault striking 30-40° NW of the horizontal compression, on a fault 10-20° east of north. However, it can only break upwards through the crust in crust-through earthquakes until it is rotated about 10-20° to the west of north.. Then it seeks ruptures 10-20° to east. Generally the larger earthquake swarms occur on vertical faults higher up in the crust and of course the large crust-through earthquakes.

A comparable evolution also took place before the second earthquake.

Socio-economic relevance and policy implication

Being able to assess in a qualified scientific way that a large earthquake is approching, its location and size is very significant. It creates background for concentration of various risk-mitigating efforts in the area, like that of civil protection groups, strengthening of structures, etc. It also creates a basis for increased monitoring, earth watch and research to prepare for more definitie short-term warnings.

Discussion and conclusions

As seen in the enclosed reports, this WP as well as WP2.2, WP2.3, WP2.4 all show pattern of stress increase or of elevated stresses in the SISZ during 10 years of pre-earthquake observations. WP2.1 and WP2.5 have in studying the pre-earthquake activity developed methods or tools for studying and intepreting such changes. Modelling of fluid rock interaction and flow in the crust in WP2.4 and in WP6.2 are significant to explain the

observations. High pore fluid pressures near the bottom of the seismogenic crust appear as a central element in building up conditions for the release of the earthquakes. The earthquake preparation and nucleation process involves build-up of stresses in an area around the fault where fluids from below play a significant role. Approach in the release time of the earthquake the high pore fluid pressures within the system move from a volume distribution at depth within the crust towards the becoming fault and weakening it. The possibility for median-term or short-term predictions may probably be based on observing these changes in real-time.

Plan and objectives for the next period

The objective is to compare and merge the observations to obtain a tool for better time and size assessment of large earthquakes.

References

Bergþóra S. Þorbjarnardóttir, Gunnar B. Guðmundsson & Steinunn S. Jakobsdóttir 2003. Seismicity in Iceland during 2001. *Jökull* 52, 55-60.

Gunnar B. Guðmundsson, Kristín S. Vogfjörð & Bergþóra S. Þorbjarnardóttir 2003. SIL data status report. http://hraun.vedur.is/ja/prepared/reports/sdsr.pdf.

Steinunn S. Jakobsdóttir, Gunnar B. Guðmundsson & Ragnar Stefánsson 2002. Seismicity in Iceland 1991-2000 monitored by the SIL seismic system. *Jökull* 51, 87-94.

Ragnar Stefánsson & Gunnar B. Guðmundsson 2004. About the state-of-the-art in providing earthquake warnings in Iceland. *Icelandic Meteorological Office - Report.* In press.

Ragnar Stefánsson, Reynir Böðvarsson, R. Slunga, Páll Einarsson, Steinunn S. Jakobsdóttir, H. Bungum, S. Gregersen, J. Havskov, J. Hjelme & H. Korhonen 1993. Earthquake prediction research in the South Iceland seismic zone and the SIL project. *Bull. Seism. Soc. Am*. 83(3), 696-716.

Tryggvason, A., S.Th. Rögnvaldsson & Ó.G. Flóvenz 2002. Three-dimensional imaging of the P- and S-wave velocity structure and earthquake locations beneath Southwest Iceland. *Geophys. J. Int.* 151, 848-866.

Wyss, M. & Ragnar Stefánsson 2004. Nucleation points of main shocks in southern Iceland, mapped by b-value. Submitted.

WP 2.1 Pattern search in multiparameter seismic data

1 Objectives

The occurrence of earthquakes is a complex and highly variable process coupled in space and time. The resulting difficulty to separate superimposed seismicity patterns stemming from different causes impedes the search for anomalies possibly preceding large earthquakes. Within the ideal setting of the PREPARED project the objectives are twofold: confirmation and enhancement of the method on the one hand, application to seismicity in the SISZ on the other to detect long- term premonitory changes before the large events in 2000 and to search for precursors of impending events.

2 Methodology and scientific achievements related to Work Package 2.1 including contribution from partners

The earthquake catalogue (SIL data) since 1991 is of extraordinary quality for this work, with a magnitude completeness seemingly almost down to 0. Within the framework of PREPARED it is easy to rule out catalogue inconsistencies which might otherwise lead to spurious results. Close collaboration with WP 2.2 aided in this. After an initial analysis of the complete dataset using existing software, initial results are promising. Geological knowledge and data from other work packages will be incorporated to vary analysis parameters, enhancing the software in the process from now on. Correlation between observed anomalies and the occurrence of large events will finally lead to the establishment of a relation between anomaly characteristics and earthquake parameters.

The first elementary but important step in WP 2.1 was to familiarise ourselves with the data in view of various aspects. We began this task in June 2003 after the first part of data containing the period 1991 – 1995 was provided by the Icelandic Meteorological Office (IMO). The magnitude, time, depth and spatial distributions of the events were analysed. In September the second part of data including events until end of 2000 was delivered by IMO. Detailed analysis of the frequency magnitude distribution of different time intervals and the comparison between the two different measures of magnitude provided in the SIL data led to discussions about peculiarities of these magnitude scales especially with WP 2.2. Suspicious effects were observed in the frequency distribution of the moment magnitude (obtained from corner frequency) for the period 1996 – 2000. In the band $4 < m < 6$ the moment magnitude deviates significantly from a linear trend, reminiscent of characteristic earthquakes (Fig. 1). This effect can not be observed in the local magnitudes (obtained from amplitude and distance). Temporal variations in the seismic network and their effects on the completeness threshold were also studied. These observations were summarized in an internal report.

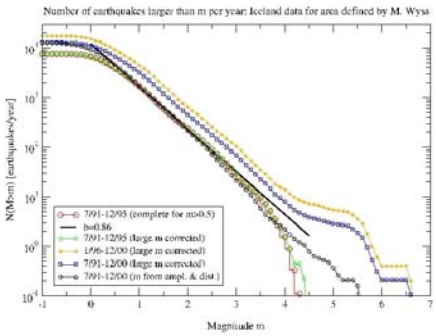

Fig. 1: Peculiarities of frequency-magnitude distributions in SIL data.

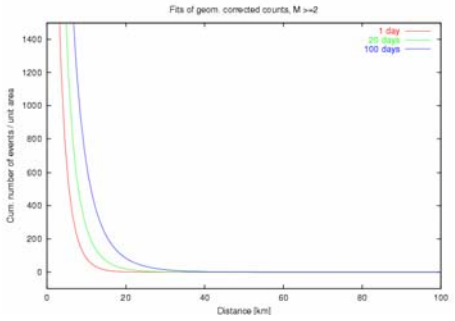

Fig. 2: Long-range correlation of seismicity in Iceland.

One of the prerequisites for the successful application of Principle Component Analysis (PCA) is the existence of coherent patterns in space and time, i.e. long-range correlations. We studied long range correlation among the earthquakes in Iceland to justify the search for such patterns. Using a modification of an approach that was just recently employed by Huc and Main (JGR, July 2003) to study global seismicity, we found that earthquake "interaction", i.e. "triggering" of earthquakes by earlier events is statistically significant up to distances of about 30 – 40km. This is illustrated in Figure 2 which shows the geometrically corrected number of earthquakes in a certain distance range for different time spans after the triggering event. We can thus expect to find coherent patterns of lateral extent up to 30 – 40km in pattern decomposition with PCA.

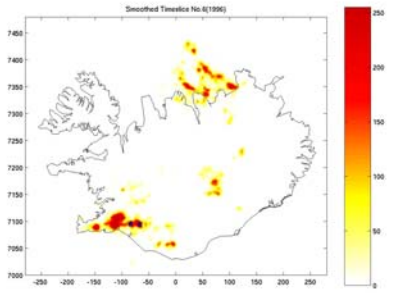

Fig. 3: Example of a time slice representing earthquake rates.

In preparation of PCA, software was developed to grid the data in space and time to create the *time slices* that constitute the input to PCA. Different from earthquake maps, the time slices contain the number of events in each cell, i.e. the rates, rather than the location of events themselves. An example is plotted in Figure 3.

It is obvious that the time slices are highly correlated and are hence a poor representation of independent constituents of the dynamics. PCA finds another representation of the data as uncorrelated *components* by first diagonalising the covariance matrix of the time slices and subsequently performing a coordinate system transformation such that the new axes point in the directions of maximum variance. The temporal information about the resulting patterns is provided by *loading graphs* that indicate the correlation of each component with all time slices.

We carried out PCA for the twelve time slices of the years 1991 too 2002. We used the catalogue irrespective of catalogue completeness since the aim of this first test is to investigate the technical capabilities of the method. Figure 4 demonstrates the usefulness of PCA. It shows the variance of the time slices that is explained by the respective components, i.e. the significance of the components, expressed in percent (100 % equals the total variance of the original data sets). These values correspond to the size of the eigenvalues of the covariance matrix. The fast decay indicates that the input images are highly redundant.

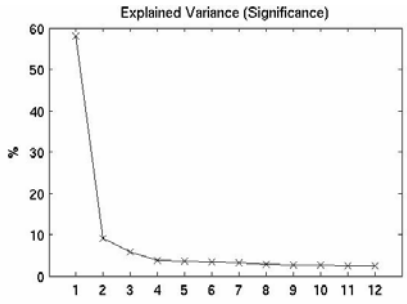

Fig. 4: Variance explained by respective components (1 – 12).

In the following some individual components will be discussed.

Component 1: Background Seismicity

The first component explains roughly 60% of the variance in the input data (cf. Fig. 4). This is the background seismicity present in all time slices. It looks roughly like a typical time slice (cf. Fig. 3). The correlation of component one with the time slices is fairly constant at a high level between 0.6 and 0.8 (Fig. 6). We thus isolate the most common pattern of Icelandic seismicity in this component. The Hengill and Ölfus areas show up as clear maxima but the South Iceland Seismic

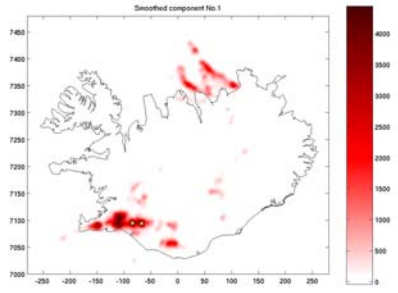

Fig. 5: Principal component 1.

Zone (SISZ), the Tjörnes Fracture Zone (TFZ), and the other well known areas of seismic activity are also present in this component.

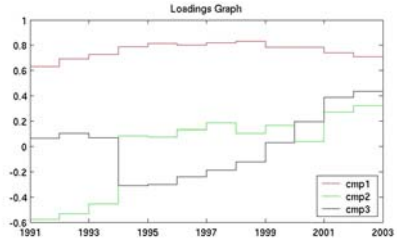

Fig. 6: Loadings graphs of components 1 – 3.

Component 2: Network Change

Component two, shown in Figure 7, reflects the pattern of most dramatic change. It accounts for about 10% of the overall variance in the time slices (cf. Fig. 4). A look at Figure 6 illustrates the temporal significance of this pattern. From 1991 to 1993 component two is quite strongly negatively correlated with coefficients around -0.5. From 1994 through 2000 the correlation is slightly positive around 0.1 and rises to about 0.3 in 2001 and 2002. This means that component two has strong negative impact from 1991-1993, is almost insignificant from 1994 to 2000 and gains significance in 2001 and 2002 again. Spatially, component two resides in Northern Iceland. The whole TFZ has high positive values. This feature in the north is thus superior to the small negative feature in the Hengill area. Combined with the information from the loadings graph, this component contains the fact that the activity in the TFZ was below the "normal" level of component one in 1991 to 1993. We conclude that component two represents the change in the network configuration that led to the detection of earthquakes in the TZF, i.e. installation of seismic stations in north Iceland. This effect is of course also visible as a difference between the 1993 and 1994 time slices.

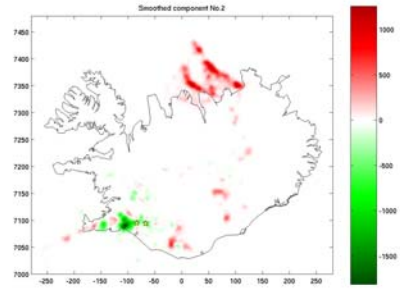
Fig. 7: Principal component 2.

Component 3: Volcanic Activity

Ascribing component two to artificial effects leaves component three (Fig. 8) as the most important natural change with a portion of about 6% explained variance according to Figure 4. This pattern is irrelevant from 1991 to 1993 (correlation coefficient of about 0.08). From 1994 onwards, however, the correlation rises constantly from a negative value of -0.3 in 1994 to above 0.4 in 2002 (cf. Fig. 6). This means that the pattern of component three becomes more and more important. The loading from 1991 through 1993 might be biased by an interplay with component two. A broad maximum is located in the area of Mýrdals- and Eyjafjallajökull in South Iceland. This component thus documents a strong increase in seismic activity in the Mýrdals- and Eyjafjallajökull area from a level below the average reported in component one in 1994 to a level far above average in 2002.

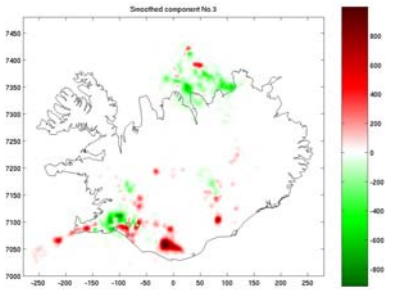
Fig. 8: Principal component 3.

Component 4: Possible Precursor?

This component (Fig. 9) essentially represents a pattern of activity on the Reykjanes Peninsula. There is a clear minimum around Kleifarvatn. The south eastern part of the Hengill / Ölfus area is highlighted by positive values, albeit of lower magnitude compared to Reykjanes. The loadings graph in Figure 10 reveals the temporal information associated with this pattern. Attributed to the

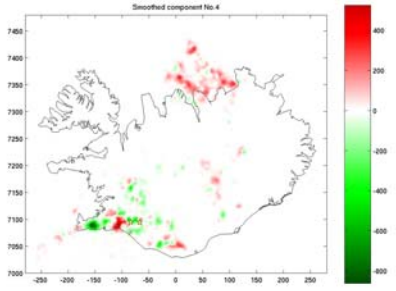
Fig. 9: Principal component 4.

negative anomaly around Kleifarvatn, the loadings can be interpreted in terms of seismic activity in three phases. At first the activity increases form 1991 to 1993, secondly the activity drops to a low level in 1994 followed by a gradual increase until 2000 similar to the increase observed around the Glaciers in the south (cf. component 3), and thirdly two years with low activity in 2001 and 2002. In view of the large events in June 2000 there might be some precursory information in this component because this pattern emerges in the run-up to these events and vanishes afterwards.

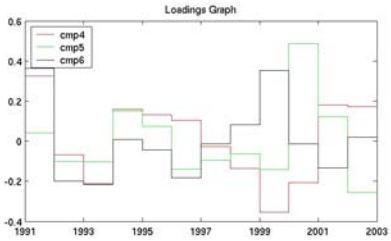

Fig. 10: Loadings graphs of components 4 – 6.

Component 5: Aftershocks

This component (Fig. 11) finally defines the aftershock activity of the June 2000 events. The loadings graph displayed in Figure 10 clearly shows very high correlation with the year 2000 time slice. The component highlights a wide area in south Iceland which indicates that this area was activated in 2000 well above the average level of component one. On the other hand the activity along the Reykjanes Peninsula which definitely increased in 2000 as well seems to be coupled weaker to the SISZ because it is not represented in component five together with the June 2000 events. In fact Reykjanes especially the Kleifarvatn area is represented in the separate component four.

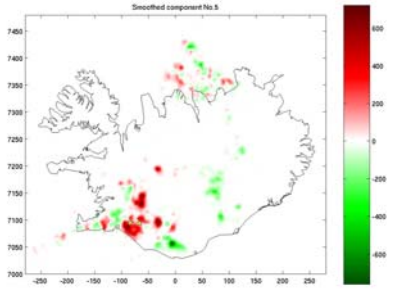
Fig. 11: : Principal component 5.

Higher Components

The remaining components show effects of smaller significance as can be seen in Figure 4. Together, components six through twelve explain less than 20% of the variance in the input data. At the moment, these components are of little interest but will be of importance in the next step which is to identify possibly subtle precursory effects.

3 Socio-economic relevance and policy implication

In the reporting period we justified our approach by showing the existence of long-range correlations and demonstrated that PCA may be successfully applied to this particular data. A first application proved the value of our method. Our software will provide the IMO with a tool for alternative analysis of seismicity.

4 Discussion and conclusions

We intensively studied the earthquake catalogue to exclude pitfalls in later work. Suspicious properties of the moment magnitude scale were discovered and changes in the catalogue completeness were estimated. Complementary long-range correlation analysis was carried out and revealed statistically significant “triggering” effects within distances up to 40km. The aim of PCA in this WP is to find a representation of the spatio-temporal earthquake dynamics that is better suited to the nature of seismicity than the standard way of e.g. mapping events that occurred within a certain period of time. We were able to show that PCA can provide such a representation. It is possible to isolate patterns associated with different tectonic processes as well as man made effects. Without PCA these patterns are superimposed in space and time and cannot be identified easily, if at all.

5 Plan and objectives for the next period

Further studies regarding PCA have to be carried out to deeper understand the interplay between the components and to investigate the limitation of the temporal resolution of the technique. The method will be extended to hypocenter depths information. The objective delineation and quantification of decomposed constituents (coherent patterns) will be a final step which has not been addressed in the qualitative interpretation up to now. We also plan the analysis of parameters such as Benioff strain in addition to earthquake rates, also in view of testing the hypotheses of growing correlation length and accelerated seismic moment release which are regarded as promising precursory phenomena. Development of software tools will continue to make PCA available to IMO and the public.

WP2.2 Seismicity patterns

a) Objectives: To determine if seismicity patterns allowed any sort of anticipation of the two M6.6 main shocks in southern Iceland in June, 2000.

b) Method and scientific achievements related to work packages.

The ratio of occurrence of small to large earthquakes in a seismogenic volume is measured by the b-value of the frequency-magnitude distribution (FMD)

$$\log N = a - bM \qquad (1)$$

(N is the cumulative number, a and b are constants, and M is the magnitude, (Ishimoto and Iida, 1939)). This power law is closely approximated by the observations in the vast majority of volumes other authors and we have investigated, regardless of size. If enough events are available (usually, we use 100 events for b-estimates), the data from the smallest volumes resolvable (approximately 1 km dimensions) obey equation (1).

Spatial variations of b, ranging from 0.5 to 1.5, are observed ubiquitously over distances of 1 to tens of kilometers (Wiemer and Wyss, 2002). Beneath volcanoes, anomalously high b-values map magma chambers (e. g. (Wiemer and McNutt, 1997), (Sanchez et al., 2003)); along fault zones, anomalously low b-values map asperities (Wiemer and Wyss, 1997; Wyss, 2001). A corollary of the latter observation is that the rupture initiation points of main shocks may be mapped by low b-value volumes (Wyss et al., 2000), and that recurrence times are estimated more correctly, if local b-values are used, rather than averages, derived by mixing seismicity from asperity with those from non-asperity volumes (Wyss and Matsumura, 2002; Zuniga and Wyss, 2001).

Evaluating the stationarity of b-value patterns is difficult in the presence of spatial heterogeneity. In a first rigorous search for violation of stationarity of local b-variations, it was found that in 85% of the volumes investigated, b-values were stationary over three decades in Parkfield (Schorlemmer et al., 2004).

Because b-value is inversely proportional to the mean size of earthquakes, as measured by their magnitude (Aki, 1965),

$$b = \log10(\exp)/(Mmean-Mmin) \qquad 2$$

(Mmin is the minimum magnitude used and Mmean is the mean magnitude in the sample), mapping b-values is equivalent to mapping mean magnitude. The cited evidence that great differences exist in mean magnitude between adjacent seismogenic volumes, means that the probability for a rupture, once initiated, to reach a given size is different in different volumes. Asperities, with their characteristically low b-values, produce more than average medium magnitude earthquakes, and main shocks are more likely to emanate from these volumes.

One of the main points of this paper is to determine whether or not the hypothesis of the correlation of main shock initiation points with low b-value volumes holds for southern Iceland. An associated question we investigated is: what are the dimensions of the b-value heterogeneity in southern Iceland? From these dimensions, we propose to derive the dimensions of the seismo-tectonic fabric. The third question we address is: Can we identify b-value anomalies as a function of time that could have been precursors to the M6.6 main shocks of June 2000.

We also seek more information on the possible association of high b-value anomalies with elevated pore pressure. Because fluids are known to play an important role in the tectonics and energy supply of Iceland, this data set offers an opportunity to verify this question.

The two main shocks of June 2000 constituted a major tectonic event in southern Iceland. Therefore, information is of interest that could contribute to understanding them, and possibly preparing for future such occurrences. Thus, the target for this study is the seismogenic zone of southern Iceland that generated these two main shocks.

Data: The heterogeneity of reporting as a function of time, space and magnitude is a major problem in all earthquake catalogs. Before studying seismicity patterns, we must define the part of any catalog that is homogeneous in reporting. Because we need as many events as possible for statistical resolution power, we seek to define the largest extent of the homogeneous part in the catalog as a function of time, space and magnitude.

First, we determined the onset of the high resolution catalog, using the assumption that the seismicity rate is stationary, except for swarms and aftershock sequences. This assumption is usually well fulfilled, even in relatively small volumes (Wyss and Toya, 2000). In southern Iceland, a strong increase of reported events in small magnitude bands is seen in 1994. However, this increase, and the associated evidence for magnitude changes at that time, is restricted to the west (Reykjanes peninsula). Magnitude shifts, inadvertent changes of magnitude scale, are a common problem in earthquake catalogs that can introduce errors in studies of seismicity rate and b-value (e. g. (Wyss, 1991; Zuniga and Wiemer, 1999)). To detect these, we scanned the catalog with the algorithm GENAS (Habermann, 1983) and applied magnitude signatures to evaluate the nature of reporting rate changes as a function of magnitude band (Habermann, 1987). In the area surrounding the 2000 main shocks, we found no signals that could be interpreted as magnitude shifts.

The spatial limits of the high-quality catalog depend on the distribution of seismograph stations. By mapping the minimum magnitude of complete reporting, Mc, (Wiemer and Wyss, 2000), we can determine simultaneously the range of magnitudes we can use and the spatial extent over which these magnitudes are reported completely. Using the catalog from 1991 on, Mc in the target area is approximately 0, whereas in the western part of southern Iceland it is substantially higher.

We define the high-quality catalog since 1991 as covering the southern Iceland seismogenic zone between 20.25°W and 21.3°W, and the magnitude range we used for the study is $Mw \geq -0.1$.

The seismicity studied in this paper is restricted to before June 2000 because we are interested in determining to what extent the main shocks in that year could have been anticipated. The few events with depths greater than 20 km are excluded because their hypocenter locations are suspect. The catalog used includes 6902 events.

Results: The seismo-tectonic fabric seems to be heterogeneous at the scale of about 1 km, as $b < 1$ changes to $b > 1$ horizontally and as a function of depth. Because of the tectonic complexity it is difficult to see patterns of b in relation to the two main shock hypocenters in the three dimensional view. In cross sections, it becomes clear that the hypocenters of the two main shocks are associated with low b-values. The EW cross section also shows that the bottom of the seismically strongly active crust is associated with anomalously high b-values.

Comparisons of the FMDs of 100 to 120 events in the vicinity of the main shock hypocenters with those in other, nearby volumes demonstrates first of all that the differences mapped are significant, and secondly that near main shock hypocenters the values are low.

As a function of time, we found no b-value anomalies near the 2000 main shocks.

c) Socio-economic relevance and policy implication.

Our results mean that likely locations of major earthquakes can be mapped by b-values. That is, they can be mapped by the locations that produce more medium sized micro-earthquakes

than other areas. In this way, locations can be identified where future earthquakes are to be expected. This does not guarantee that all locations that are so identified will produce major earthquakes soon, nor is it certain that all potential points of emanation of major ruptures can be identified. However, it means that there is great value in operating seismograph networks that are capable to detect very small quakes, because this allows the statistical analysis we need to find the asperities that generate the major earthquakes.

d) Discussion and conclusion.

With Mc = 0 in the core area , the earthquake catalog for southern Iceland shows a lower level of completeness than any other catalog we have analyzed (Wiemer and Wyss, 2000). This level of complete reporting is outstanding and provides an order of magnitude more events for detailed statistical analysis than the best regional catalogs worldwide.

As a function of space, the b-values vary strongly over distances of only 1 km, suggesting that the tectonic fabric is heterogeneous at a small scale. The same small scale heterogeneity is observed when inverting fault plane solutions for stress directions. Unless volumes with radii of about 1 km are used, the inversions show large misfits, indicating that stress directions are heterogeneous.

As a function of depth, b-values increase in California (Gerstenberger et al., 2001) and Japan (Wyss and Matsumura, 2002. In Iceland this trend also exists, but is obscured by pockets of high b-values at shallow depth. The method of {Gerstenberger, 2001 #1912) to systematically evaluate the increase of b with depth cannot be used here, because the thickness of the seismogenic crust increases from W to E in the middle of our study area. However, the close tracking of the bottom of the seismogenic layer with high b-values shows that smaller than average earthquakes are preferentially produces along the bottom of the seismogenic crust. This observation can be interpreted as being due to the presence of fluids under pressure.

Thus, the interpretation that high b-value anomalies are due to local high pore pressure in the Icelandic crust is our preferred choice. This choice is plausible because liquids under high pore pressure are known to be abundant in the study area. Thus, we interpret the patterns of high b-value anomalies as due to liquids that penetrate the crust from below and establish pockets of high pore pressure at mid-crustal levels.

One of the main topics of this paper, the possible correlation of low b-values with the source volumes of the two M6.6 main shocks, seems clear, in spite of the otherwise choppy variations of b. We found that the hypocenters of the two main shocks are clearly located in areas of low b-values. The comparison of the FMDs from the volumes surrounding the hypocenter of the three main shock (including the M4.5 event of September 1999), also show the contrast clearly. The way one samples around the hypocenter for FMD data does not influence the results much. One can select the nearest 100 to 150 earthquakes in a circle or one can select them by a rectangle parallel to the aftershock zone, the result is about the same. For the definition of the b-value in the main shock source volumes, only events that occurred prior to the respective main shocks were used, because the main shocks themselves and their aftershocks would introduce a bias favoring low b-values, if they were used. The Utsu test (Utsu, 1992) judges the contrasts to be highly significant.

We conclude that after the fact it is clear that main shocks in southern Iceland emanate from low b-value volumes with radii of approximately 1 km. This observation agrees with the hypothesis that asperities, as preferred main shock initiation points, can be mapped by anomalies of short recurrence time, which are mostly controlled by low b-values (larger than average mean magnitude). This has been documented in California (Wiemer and Wyss, 1997), Japan (Wyss and Matsumura, 2002) and Mexico (Zuniga and Wyss, 2001). However,

it may be difficult to identify such spots before the main shocks occur because of the small-scale b-value heterogeneity and because of the small dimensions of these asperities.

Inspection of the b-values as a function of time in the vicinity of the two M6.6 main shocks did not reveal any pronounced changes. Thus, we conclude that b-values are approximately stationary in southern Iceland and do not change before main shocks.

e) Plan and objectives for the next period. In the next period, we will evaluate the possibility that seismic quiescence has preceded the two main shocks in June 2000 in southern Iceland. The hypothesis of precursory seismic quiescence states that many main shocks are preceded by statistically significant reduction of microearthquakes in or near the source volume.

WP 2.3 Long-term deformation in the South Iceland seismic zone (SISZ) inferred by joint interpretation of GPS, InSAR and borehole strain data

(a) Objectives

The objective of the work package is to evaluate the long term 3D deformation in S Iceland prior to the June 2000 earthquakes, using existing geodetic data. The 3D deformation map will be used to derive a strain map for S Iceland prior to the June 2000 earthquakes, and to search for long-term precursors in geodetic signal.

(b) Methodology and scientific achievements related to workpackages including contribution from partners

We have re-analysed all campaign and continuous GPS data collected in South Iceland prior to the June 2000 earthquakes, from 1992-1999, using the GAMIT/GLOBK software (King and Bock, 2003; Herring, 2003), in collaboration with P10 (Kurt Feigl). The reason for re-analysis of the data were issues with different reference stations used in the older surveys (ARNA was used as a reference station in the 1992, 1993, 1998 surveys, LJOS and VEID were used as a reference stations in the 1995 and REYK in the 1999 surveys. Previous studies used different reference frames (ITRF91, ITRF93 and ITRF97), whereas the GAMIT/GLOBK solution is in the ITRF2000 reference frame. The re-analysis also ensured that the data were analysed in a coherent self-consistent manner, whereas previous analysis used somewhat different schemes for obtaining the solutions. The GAMIT/GLOBK software estimates velocities and co-seismic/co-eruptive offsets due to different sources during the time period, hence the difference in the velocities for some stations.

This GAMIT/GLOBK solution describes station motions in terms of absolute velocities (over time intervals) and displacements (at instantaneous points in time, i.e. “epochs”). The velocities represent the average “pre-seismic” velocity, equivalent to the slope of the position time series estimated from the GPS observations performed before June 17, 2000. The displacements represent the instantaneous co-seismic offsets in position estimated at the epochs of the two earthquakes on June 17 and June 21, 2000. To realize the reference frame for the GPS positions and velocities, we used the “stabilization” procedure described by McClusky et al. [2000]. This approach minimizes the residual positions and velocities for a globally-distributed ensemble of up to 28 stations, for which the coordinates and velocities are well determined in ITRF2000. Following this stabilizing minimization, the post-fit residual scatter for these stations is 1.6 mm/yr, indicating that the reference frame is determined to within the same amount.

The horizontal velocity field for the pre-seismic period, derived using GAMIT/GLOBK, relative to the continuous GPS station in Reykjavík (REYK) is shown with blue vectors in Figure 1.

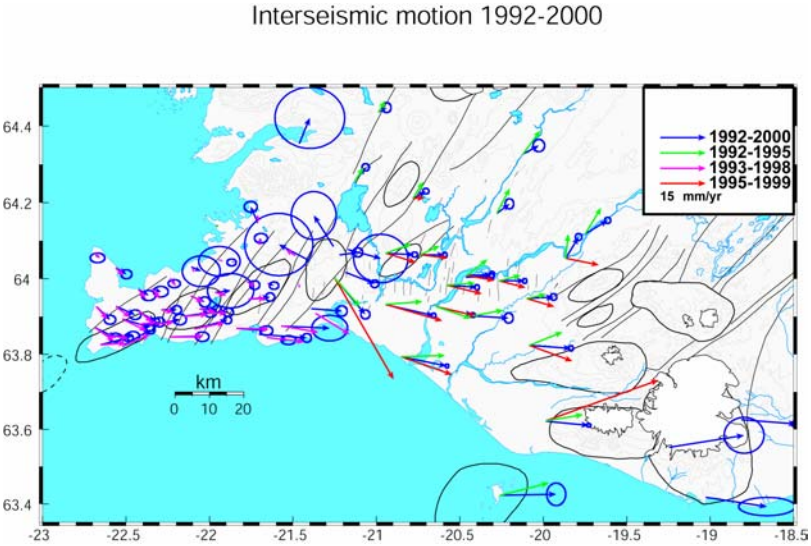

Figure 1. Horizontal velocity field obtained from GAMIT/GLOBK analysis (blue vectors), compared with solutions from Bernese analysis by different researchers. The 1992 station locations are from Sigmundsson et al. (1995), the 1995 and 1999 solution is from Árnadóttir et al. (2001), and the Reykjanes 1993-1998 velocities are from Hreinsdóttir et al. (2001).

The GAMIT/GLOBK velocities compare well with previous solutions. Most of the differences can be explained by the different parameterizations. The GAMIT/GLOBK solution allows offsets for co-seismic and co-eruptive displacements, thereby diminishing the average velocities (in absolute value).

Figure 2 shows comparison of the vertical velocity signal between the GAMIT/GLOBK solution (blue vectors) and previous solutions relative to the continuous GPS station REYK.

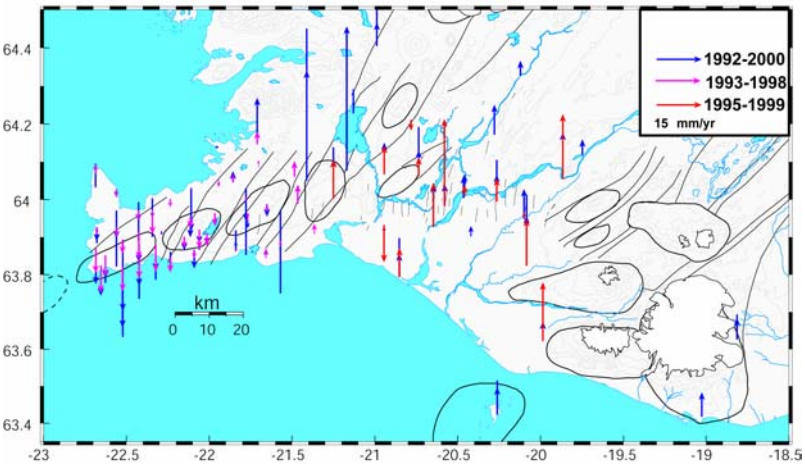

Figure 2. Vertical velocity field obtained from GAMIT/GLOBK analysis (blue vectors), compared with solutions from Bernese analysis by different researchers. The 1995-1999 solution is from Árnadóttir et al. (2001), and Reykjanes 1993-1998 solution from Hreinsdóttir et al. (2001).

The horizontal velocity field in the pre-seismic period is fairly uniform. To better visualize the relative plate motion, we assume that REYK moves at half Nuvel1A plate motion (i.e. add the velocity vector (-9.6, 2.1) mm/yr to the GAMIT/GLOBK solution). The resultant velocity field is shown in Figure 3.

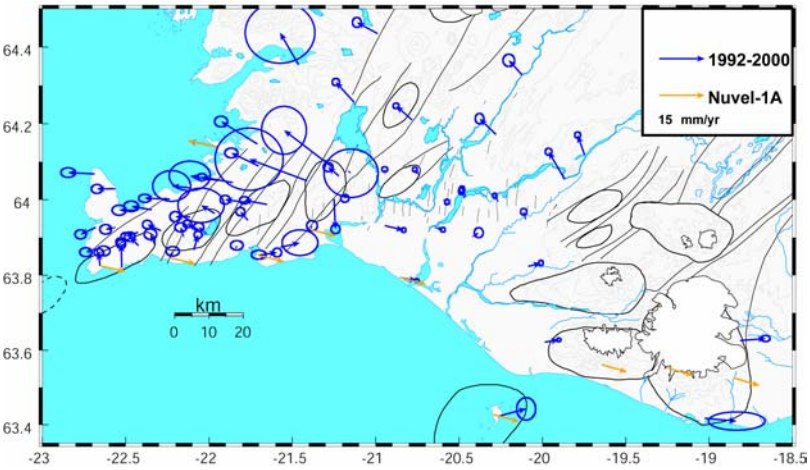

Figure 3. Relative plate motion in South Iceland, assuming that REYK is moving at half Nuvel1A velocity.

Figure 3 shows that the motion in the central part of the South Iceland Seismic Zone (SISZ) is small, indicating that these stations are close to the plate boundary. Stations to the north of 64N move north-westward, suggesting they are on the North American plate, and stations further south and east (e.g. HEIM on the Vestman Islands) have an easterly component of motion as we get further east, indicating that they are located on the Eurasian plate.

We examine how well the velocity field in the SISZ fits a simple trans-current motion model in a uniform elastic half space. We use a simple 1D screw dislocation model (see equation 1), assuming that the plate motion is accommodated by motion on an E-W left-lateral transform that is locked down to a depth D, and moving with velocity (V) below D (e.g. Savage and Burford, 1973). The surface velocity perpendicular to the plate boundary is then described by:

$$u(x) = V/\pi \arctan(x/D) \qquad (1)$$

where u(x) is the observed surface velocity, V is the slip rate below the locking depth D, and x is distance along the profile. In our study, the component of the observed surface velocities (u), that is parallel to N104E (i.e. the Nuvel-1A plate motion direction), is plotted in a NNE-SSW profile across the SISZ (see Figure 4a and 4b). We calculate the predicted surface velocities using Equation (1) and the misfit, i.e. the difference between the observed and model prediction for a range of locking depths (D) and velocities (V) (see Figure 4c). The minimum misfit is obtained for a range of locking depths (D=14-24 km), and velocities (V=17-23 mm/yr), but two parameters are highly correlated, and the locking depth is less well constrained than the velocity. These values for the locking depth and velocity for the SISZ are larger than values obtained for the Reykjanes Peninsula using the same model, i.e. there the locking depth was estimated as 6.5 km and deep slip rate was 16.5 mm/yr (Hreinsdóttir et al., 2001). The crustal thickness, estimated from depth of earthquakes in the SISZ is greater in the SISZ than on Reykjanes Peninsula.

Figure 4 shows an N-S velocity profile through the SISZ, plotting the velocity component parallel to the Nuvel1A spreading direction (N104E). We calculate the residual, i.e. the difference between the observed velocities and model prediction, and find that the velocity profile can be fitted with a simple screw dislocation model with a locking depth no less than 14 km, and velocity of about 19 mm/yr.

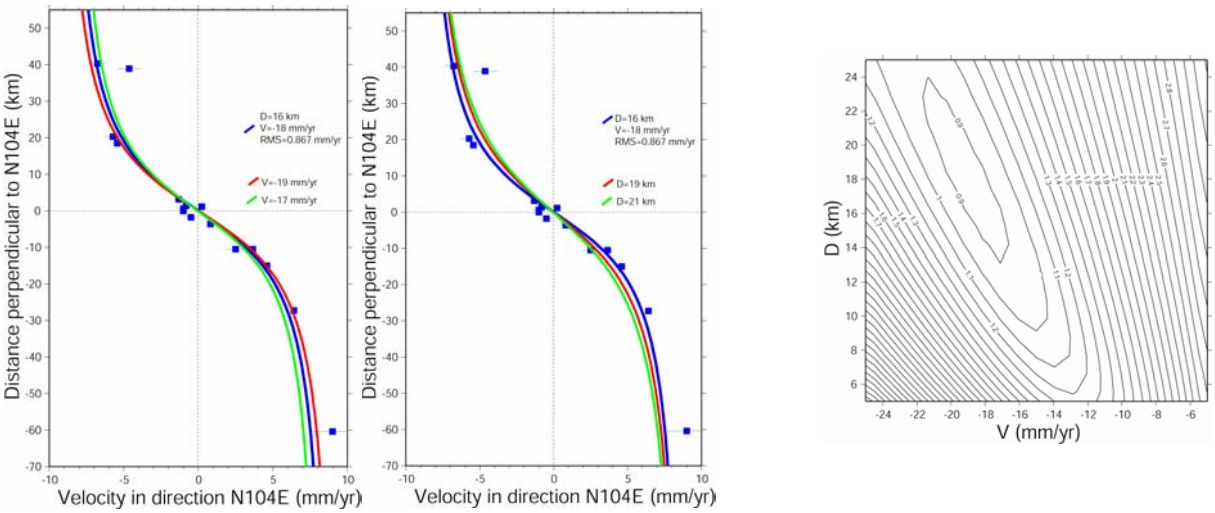

Figure 4. An N-S velocity profile for the SISZ from Figure 3. The data are shown with blue squares. Color curves show model predictions for simple screw dislocation models with: (a) a fixed locking depth, D=16 km and a range of velocities (V=17, 18, 19 mm/yr), (b) a fixed velocity, V= 18 mm/yr and a range of locking depths (D=16, 19, 21 km). (c) Results of a grid-search across the 2-dimensional parameter space of locking depth D and deep slip rate (V). The contoured values are normalised RMS misfit to the observed surface velocities plotted in the previous figure.

We use the GAMIT/GLOBK solution to calculate the strain field in South Iceland in the pre-seismic period 1992-1999. The shear strain rate is composed of several components of the gradient of the velocity field in different directions. We find that the northward gradient of the eastward velocity component, i.e. dVe/dN is most indicative of left-lateral motion on an E-W transform, or right-lateral motion on an N-S fault, as observed in the SISZ. Figure 5 shows this component of the strain tensor. We see that the strain rate is high in the center of the SISZ, and decreases as we move north or south from 64N. This is the pattern demonstrates that strain was concentrated in the SISZ prior to the June 2000 earthquakes. The green stars show the locations of the June 17 and June 21 main shocks. The black color around the Hengill area indicates very high negative strain rates, as expected for this period due to the high rate of deformation during this time period. It is somewhat surprising to see that the strain rates are generally higher in the Reykjanes Peninsula, than in the SISZ. Previous studies estimated the average strain rate across the Peninsula to be of the order of 0.2 □strain/yr (Hreinsdóttir et al., 2001), but our calculations indicate an even higher strain rate, up to about 0.5 □strain/yr. It is noteworthy that three M5 earthquakes were dynamically triggered on Reykjanes Peninsula on June 17, 2000, located in areas where we estimate high strain rates (Pagli et al., 2003).

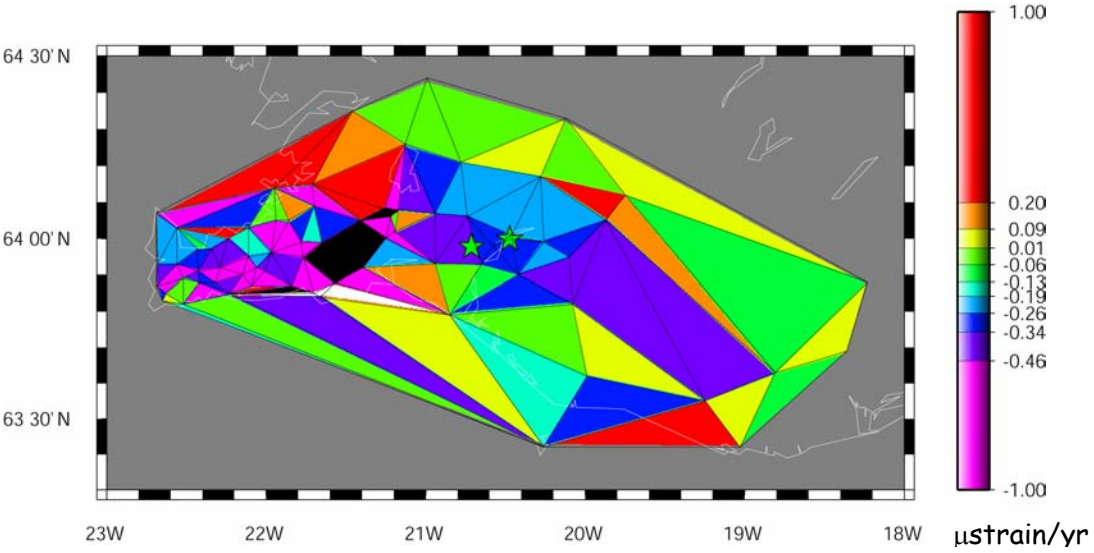

Figure 5. Gradient of the eastward component of the velocity (Ve) in the northward direction (N), i.e. dVe/dN.

(c) Socio-economic relevance and policy implication.

Evidence of strain precursors prior to the June 2000 earthquakes would be valuable information that could be used with other information in earthquake prediction.

(d) Discussion and conclusions

We have re-analysed GPS data from 1992-1999 and derived a 3D velocity field and strain field for South Iceland. The GPS network is too sparse to allow detailed interpretation of spatial variation of the strain within the SISZ. We see that the strain rate is high in the center of the SISZ, and decreases as we move north or south from 64N, as we would expect since strain is concentrated in the SISZ prior to the June 2000 earthquakes.

(e) Plan and objective for the next period

We plan to continue the analysis of the strain field from available geodetic data and compare with other data, e.g. seismic data and previous studies using EDM data (Lindman, 2002). Results from InSAR data analysis will be incorporated in the strain analysis as they become available (see report from P10). The final deliverable in this work package is an evaluation of earthquake precursors (at M18), which we expect to be on schedule. We will also continue our work of studying post-seismic deformation observed with GPS in the years following the June 2000 earthquakes.

References:

Árnadóttir,Th., Hreinsdóttir,S., Gudmunsson, G., Einarsson, P., Heinert, M., and C. Völksen, Crustal deformation measured by GPS in the South Iceland Seismic Zone due to two large earthquakes in June 2000, *Geophys. Res. Lett., 28*, 4031-4033, 2001.

Herring, T.A., GLOBK: Global Kalman filter VLBI and GPS analysis program version 4.1, Mass. Inst. Technol., Cambridge, 2003.

Hreinsdóttir, S., P. Einarsson, and F. Sigmundsson, Crustal deformation at the oblique spreading Reykjanes Peninsula, SW-Iceland: GPS measurements from 1993 to 1998, *J. Geophys. Res., 106*, 13803-13816, 2001.

King, R.W., and Y. Bock, Documentation for the GAMIT Analysis Software realease 10.1, Mass. Inst. Technol., Canbridge, 2003.

Lindman, M., Strain precursors for the June 2000 earthquakes, South Iceland: A study of crustal deformation 1984-1995, MS thesis, Lulea University, 2002.

McClusky, S., S. Balassanian, A. Barka, C. Demir, S. Ergintav, I. Georgiev, O. Gurkan, M. Hamburger, K. Hurst, H. Kahle, K. Kastens, G. Kekelidze, R. King, V. Kotzev, O. Lenk, S.

Mahmoud, A. Mishin, M. Nadariya, A. Ouzounis, D. Paradissis, Y. Peter, M. Prilepin, R. Reilinger, I. Sanli, H. Seeger, A. Tealeb, M.N.T.o.z. Toksoz, and G. Veis, Global Positioning System constraints on plate kinematics and dynamics in the eastern Mediterranean and Caucasus, J. Geophys. Res., 105 (B3), 5695-5720, 2000.

Savage, J. C., and R. O. Burford, Geodetic determination of relative plate motion in central California, *J. Geophys. Res., 78*, 832-845, 1973.

Sigmundsson, F., P. Einarsson, R. Bilham, and E. Sturkell, Rift-transform kinematics in south Iceland: Deformation from Global Positioning System measurements, 1986-1992, *J. Geophys. Res., 100*, 6235-6248, 1995.

WP 2.4 Space and time variations in crustal stress using microearthquake source information from the South Iceland seismic zone

1 Objectives

The main purpose of the WP 2.4 is to utilize the unique data set provided by the SIL-network to analyze the SISZ using various type methods and algorithms. In this report we will show results from four type of processing techniques and algorithms: a) Time-window Local Earthquake Tomography, b) Spectral Amplitude Grouping, c) Stress Tensor Inversion and d) Seismicity Ratio with Applied Mechanism.

2 Methodology and scientific achievements

2.1 Time-window Local Earthquake tomography

Background Seismic tomography is a powerful tool for imaging the structure of the crust in three dimensions. In Iceland previous studies have shown that other effects than composition are controlling factors for the seismic velocities, e.g. temperature and pore fluid effects are important (Tryggvason et al., 2002). Whereas temperature changes can be expected to transport themselves slowly through the crust, stress changes and changes in pore fluid pressure may take effect more rapidly. Local Earthquake (LE) tomography has rarely - if ever - been used to monitor changes in seismic velocities with time. One reason might be the lack of data. Many times there simply is not enough seismicity to allow for a big enough dataset to accumulate for performing tomographic inversions in a short time window. What is important, besides the number of earthquakes, is their distribution. If the seismicity is narrowly concentrated in certain small source regions, this will limit the possibilities to select enough earthquakes, even though the number of events may be large. In South Iceland the seismicity is distributed among several seismic active zones, and is also abundant. During year 2000 more than 110000 events occurred on the Reykjanes Volcanic Zone, the Hengill area and in the South Iceland Seismic Zone. This seismicity rate is very much larger than normal for the region, and is in all likelihood related to the two magnitude 6 earthquakes that occurred there in June 2000. South Iceland therefore seemed to be well suited for an experiment aimed at exploring the possibilities that changes in seismic velocities with time could be detected.

Seismic tomography The LE tomographic inversion was conducted with the same parameters as the previous study in the area by Tryggvason et al., (2002) which was based on data from 1973-98. The model was parameterized in 4 by 4 km horizontal and 1 km vertical cells. Below 6 km depth the cells were 2 km thick. The algorithm used (PStomo_eq) simultaneously solves for the P- and S-wave velocity fields as well as the earthquake locations. Data from different time windows were selected, as shown in Figure 1.

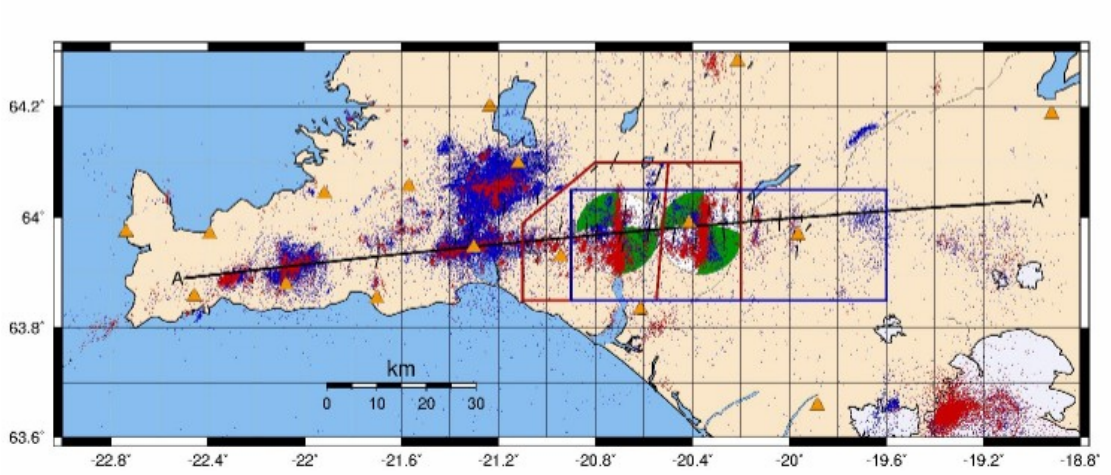

Figure 1. Map of southwest Iceland. Yellow triangles are SIL seismic stations, blue dots earthquakes before the June 17, 2000, event, red dots earthquakes after the June 17 event, mechanisms of the large events are from the Harvard CMT catalog. The black AA' line denotes the local earthquake tomography profile, the red boxes are the areas used in the SAG and stress analyzes, and the green box is the area used for the SRAM analysis.

When performing the tomography, the seismic velocity models from the previous time window were used as starting models. Before an inversion for the seismic velocities is performed the events are relocated in the starting model, which takes care of most of the data residual. To explain the remaining data residuals slight changes in the seismic velocity field is needed. In Figure 2 the Vp/Vs ratio in a cross-section (A-A' in Fig. 1) through the model region is shown. The Vp/Vs ratio is computed by taking the ratio of the P- and S-wave models, and only model cells which are hit by both a P- and an S-wave are shown. The Vp/Vs ratio relative the previous model is shown, and anomalies as large as 3% appear in and near the volcanic systems.

Results In Figure 2a is shown the relative change in Vp/Vs ratio during 1999 compared to 1998. In the cross section four anomalies are shown. The two strongest anomalies are the one beneath the Krisuvík volcanic system and the one where the profile crosses the southern end of the Hengill fissure system. Two minor anomalies occur in the South Iceland Seismic Zone. The two yellow stars are the locations of the two large earthquakes of June 2000, thus it seems that the anomalies of -1% are situated east of the faults of the coming large earthquakes. Figure 2b shows the relative change during year 2000 up until June 17, the date of the first of the two large events. Figure 2c shows the model based on data from just 4 days, from June 17 to June 21 which is when the second large event occurred. During those four days more than 22000 events occurred. From this time slice we can see an increase in the Vp/Vs ratio in the same region as we could see a decrease during 1999. In Figure 2d the Vp/Vs ratio is stable, we can however observe large changes (-3% to 1%) in the Reykjanes Volcanic Zone. In the final slice (Figure 2e) we observe very small changes.

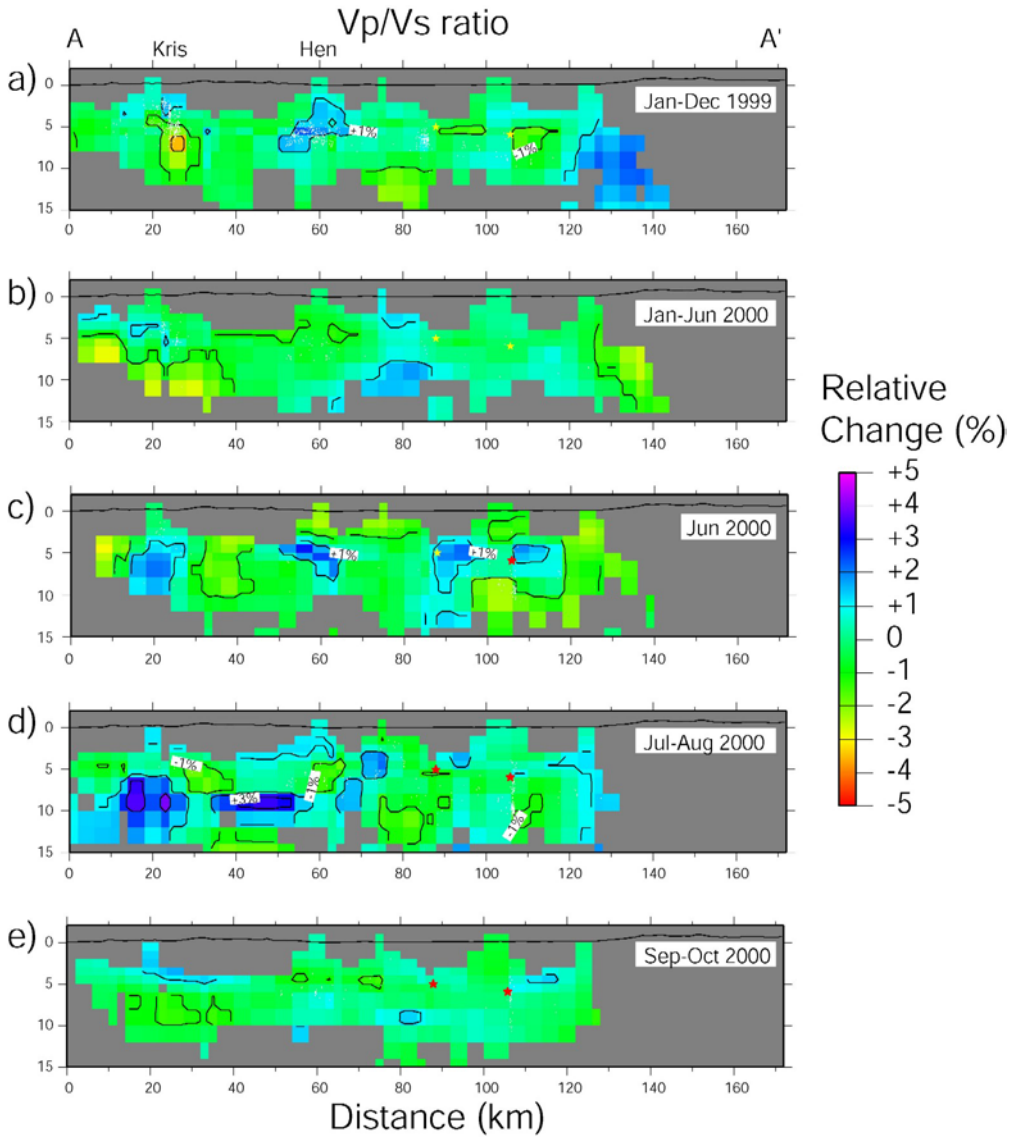

Figure 2: The cross sections (A-A' in Fig. X) show the relative changes in the Vp/Vs ratio, starting in 1999 in a), and ending in Oct 2000 in e). The data used in every tomographic inversion is shown in Table 1. Kris marks the location of the Krisuvík volcanic system and Hen marks where the profile crosses the southern part of the Hengill fissure system. The stars mark the locations of the large events of June 2000, yellow before they occur and red after.

Time period	Total no of Events	Selected Events
1/1 - 31/12	-99	11600 6362
1/1 - 17/6	-00	22000 1200
17/6 - 21/6	-00	22000 1845
21/6 - 31/8	-00	23000 4200
1/9 - 31/10	-00	23000 1300

Table 1: The number of events occurring in the region for the different time intervals used in the tomographic inversions, and the number of selected events.

Outlooks What we report here are, however interesting, very preliminary results. We think we can observe changes in the seismic velocities which can be related to the two big earthquake of June 2000 in the South Iceland Seismic Zone. What remains to be done is a thorough data analysis to see if the observed anomalies are coincidental. A plausible physical model to explain the observations is also not ready yet. This work will be done during the final stages of the project.

2.2 Temporal Spectral Amplitude Grouping variations:

In order to investigate temporal variations in microearthquake focal mechanisms we used the Spectral Amplitude Grouping (SAG) method (Lund and Bödvarsson, 2002) in temporal mode. The algorithm then uses a fixed size memory, in this case of 250 events, which events are correlated and grouped and the result recorded as the number of solitary events, i.e. events that have focal mechanisms dissimilar to other events, and the number of groups. The next event, in time, in the data set is then incorporated into the event memory and the oldest event in the memory discarded. The correlation and grouping is repeated, the new numbers recorded and after processing the entire data set the result is presented as in Figure 3. Figure 3 shows the number of solitary events (red line) and the number of groups (blue line) as a function of time for the area of the June 17 earthquake, see Figure 1. The data set consists of 8375 events recorded at at least four stations. The seismicity rate is very low during the first years and we do not fill the 250 event memory until May, 1992, this initiation period should thus be disregarded. We see in Figure 3 that the number of solitary events is rather constant at 130-140, approximately 50% of the memory size, until early 1996, when a distinct, gradual decrease starts. We also see that the number of groups increase slightly during the first half of 1996, i.e. there are more events with similar focal mechanisms although some of the groups are quite small. In late September, 1996, there was a magnitude 5.6 earthquake and a large volcanic eruption under the Vatnajökull glacier. These events abruptly change the SAG pattern, during the next six months events become increasingly dissimilar. It is interesting to note that the number of groups decrease dramatically some time before the large earthquake/volcanic eruption, as if the seismicity conforms to just a few varieties of focal mechanisms. The next large earthquakes and volcanic eruptions in southern Iceland do not influence the SAG pattern in any obvious way, not until the two large events of June 2000, when the number of solitary events drops dramatically in the aftershocks, and the number of groups increase. In order to properly interpret the results of the SAG analysis further research is needed. We aim to have a better interpretation during the cause of the PREPARED project and we are very optimistic about the possibilities of the SAG analysis to provide input to an earthquake forecasting system.

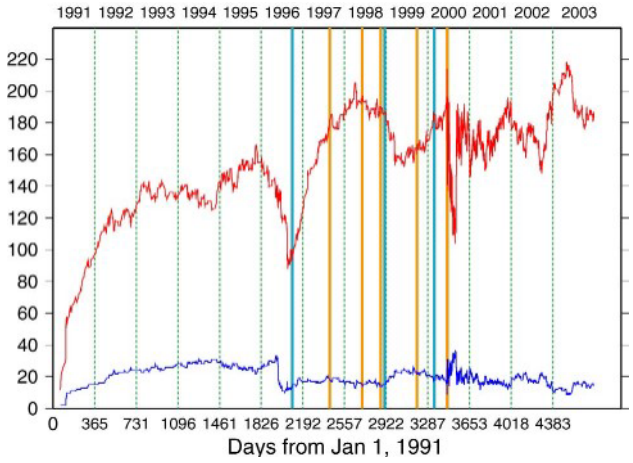

Figure 3. Result of Spectral Amplitude Grouping (SAG) of 8375 events in the June 17 earthquake source area. The number of solitary events (red line) and the number of groups (blue line) for an event memory of 250 events are plotted in time. Years are noted at the top and delineated by green dashed lines. The vertical, light blue lines correspond to times of volcanic eruptions in south/central Iceland and yellow lines correspond to times of major earthquakes, above magnitude 4.5.

2.3 Stress Tensor Inversion of Earthquake Focal Mechanisms.

In order to investigate the temporal evolution of stress in the source areas of the two large earthquakes of June 2000, we used the SAG method to form groups of 50 events that do not have similar mechanisms. The groups are formed in time order, with each group having 50% event overlap with the preceding group. The events' focal mechanisms were then inverted for the causative state of stress using the method of Lund and Slunga (1999). In Figure 4 we plot the temporal evolution of the estimated maximum horizontal stress in the June 21 earthquake area. We see during the early years that the horizontal stress is rather well constrained at approximately N50E, the stress field is disturbed by the Vatnajökull eruption and turns northerly, and is then quite varying during the rest of the time period. If we zoom in on the year before the June 2000 events there seems to be a northerly rotation of the maximum horizontal stress before the first large event. Analysis of misfit and residuals show that these stress inversions are well constrained. Further work is needed in order to properly interpret the apparent rotation and to statistically analyze its significance.

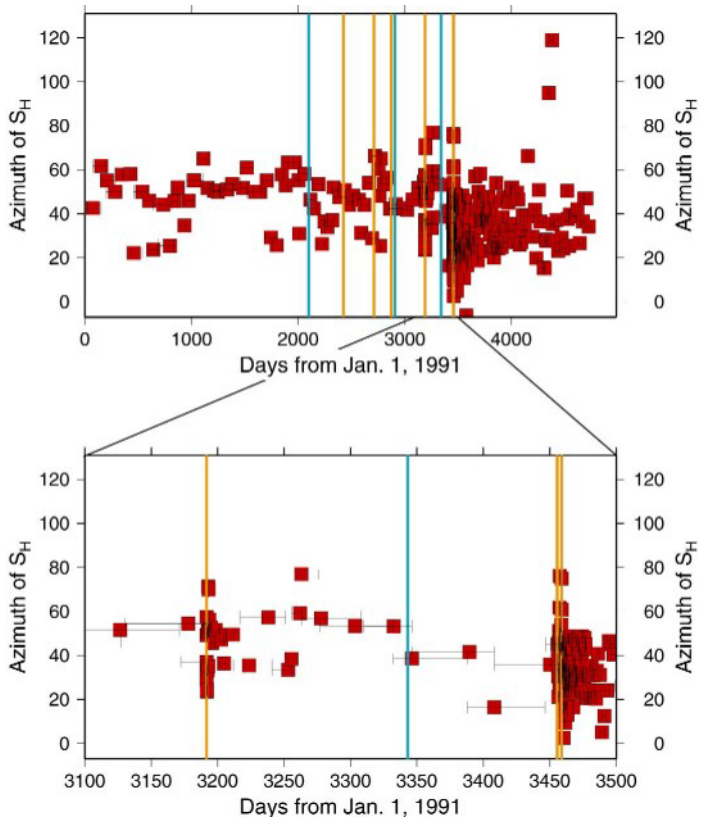

Figure 4. Azimuth, from north, of the direction of maximum horizontal stress from stress tensor inversion of earthquake focal mechanisms in the vicinity of the June 21 earthquake source region, see Figure X. Each square is an inversion of a group of 50 events, the groups overlap 50% in time and the horizontal bar on the squares shows the time span of the events in the group. The upper plot shows 371 groups of events during the time of operation of the SIL network. The lower plot is zoomed in during the year prior to the large June 2000 events. Large earthquake occurrences are denoted by yellow lines, volcanic eruptions by light blue lines.

2.4 Seismicity Ratio with Applied Mechanism

A new algorithm for seismicity analysis has been developed. In this simple algorithm we analyze the seismicity in the SISZ area by looking at the ratio between the number of earthquakes in the compressive and tensile quadrants at any given point in a grid of points covering the SISZ. The purpose was to check if the seismicity pattern could be made more sharp by adding this a priory knowledge of mechanism of the large earthquakes in the area.

In the analysis we use data from 1991 through May 2000 and the results are shown in Figure 5. In this figure we see two major anomalies, the strongest located in the vicinity of the June 17th earthquake and the the other anomaly in the vicinity of the second earthquake. When running the algorithm on various periods between 1991 and 2000 gave similar results already in 1993 although with less pronounced anomaly, particularly around the second event. We will develop the algorithm further and do some more detailed analysis in the second part of the project.

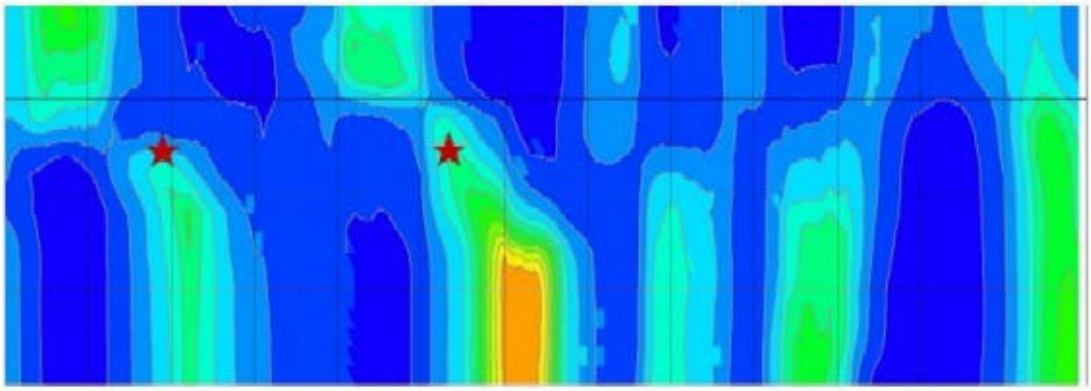

Figure 5. Results from the SRAM analys in the SISZ. The red starts are the location of the two large earthquakes.

3 Socio-economic relevance

This research is a contribution to a better understanding of the deformation processes in the SISZ and other seismic areas in general. This can be of importance for possible future earthquake predictions which would be of important value for the society.

4 Discussion and conclusion

In this mid-term report we have tried to give information on the ongoing research and the very preliminary results that we have available. We feel that the preliminary results from the various methods described above are promising and will contribute to a better understanding of the ongoing processes in the seismogenetic crust in SISZ.

5 Plan and objectives for the next period

We will continue working according to our original plans as we now have access to the recalculated database. The plans for the work using the different methods are discussed at the end of each sub-chapter in section 2. We will participate in the PREPARED meetings and some international meetings. We are also preparing papers to be published in international journals.

References:
Lund, B and R. Bödvarsson, Correlation of microearthquake body-wave spectral amplitudes, Bull. Seis. Soc. Am., 92, 2410-2433, 2002.

Lund, B and R. Slunga, Stress tensor inversion using detailed microearthquake information and stability constraints: Application to Ölfus in southwest Iceland, J. Geofys. Res., 104, 14947-14964, 1999.

A. Tryggvason, S.Th. Rögnvaldsson, and O.G. Flovenz, 2002. Three- dimensional imaging of the P- and S-wave velocity structure and earthquake locations beneath Southwest Iceland, Geophys. J. Int. 151, 848-866.

WP 2.5 Using shear-wave splitting above small earthquakes to monitor stress in SISZ

3.1) OBJECTIVES (CAPS), RESULTS & DELIVERABLES (lower case)
3.2) METHODOLOGY AND SCIENTIFIC ACHIEVEMENTS

1) CONTINUE MONITORING SHEAR-WAVE SPLITTING
2) EVALUATION OF STRESS INDUCED CHANGES IN SHEAR-WAVE SPLITTING:
3) IDENTIFY THE BUILD-UP OF STRESS:

1,2,3a) Continued monitoring, evaluation, and identification of build-up of stress (Deliverables D28, D30):

Time-delays in Band-1* of the shear-wave window have been monitored at those few stations above persistent swarms of small earthquakes. Indications of increasing stress have been observed at BJA and SAU in the SISZ (Fig. 2.5i) and at FLA, GRI and HED in the Tjörnes Fracture Zone in Northern Iceland (increases at these stations are similar to those in Fig. 2.5i. We have no information for distinguishing whether these increases indicate accumulating stress before earthquakes or before volcanic eruptions.

*Band-1 is the double-leafed segment of the solid angle of ray paths making angles between 15º and 45º either side of the average vertical plane of the cracks. It is this band of the effective shear-wave window which shows the effects of increasing stress.

a) **b)**

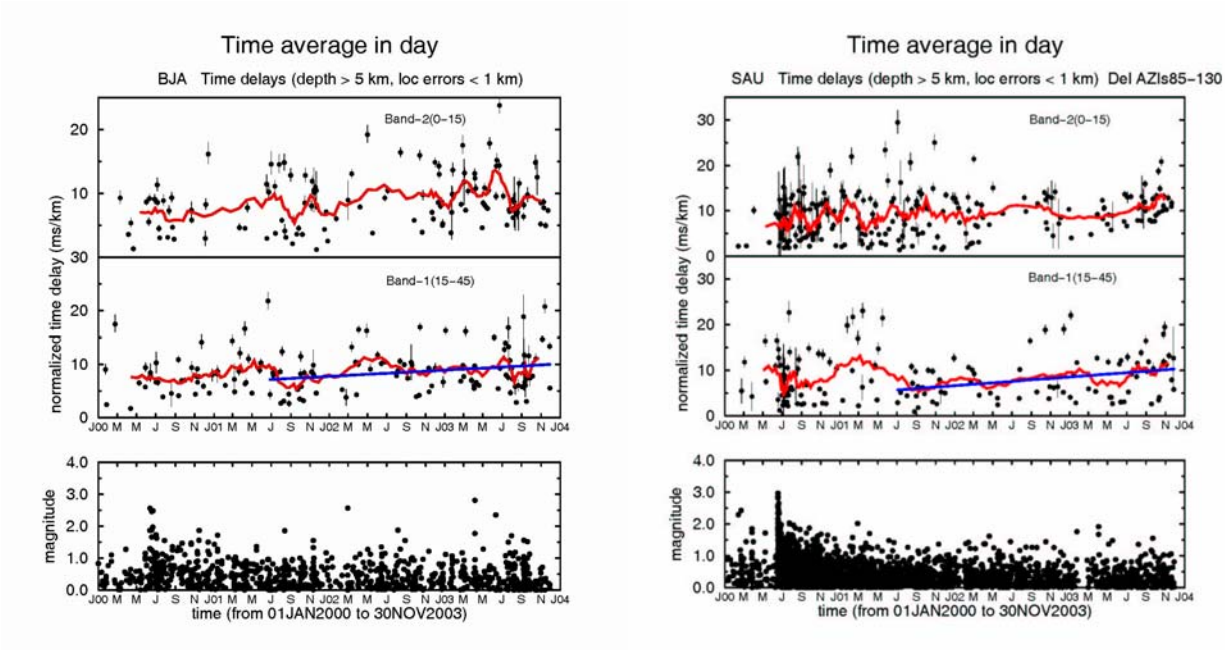

Fig.2.5i. Variations of time-delays between split shear-waves at stations BJA and SAU in SISZ. Note that to avoid the effects of anomalous weighting at concentrations of earthquakes, the normalised time-delays are averaged to one per day. Please see previous issues for discussion of these diagrams. The blue lines are averages in Band-1 directions thought to indicate increasing stress.

Fracture criticality, when rocks fracture and earthquakes occur is generally believed to occur at between normalised delays of 10 and 12 ms/km. So the increase does appear to indicate the accumulation of stress before an earthquake or eruption expected to occur comparatively soon. Note the widespread occurrence of the increase does not give any information about the site of the event.

3b) Collaboration between partners in imaging stress variations (D31):

The stress directions indicated by the polarisations of shear-wave splitting and the principal stress directions from fault-plane mechanisms obtained by Jacques Angelier (UPMC) are quite closely similar in the SISZ. There are however significant differences in stress directions derived from shear-wave splitting at stations BRE, FLA, and HED adjacent to the Húsavík-Flatey Fault and fault-plane mechanisms in northern Iceland. This is an interesting phenomenon and we shall collaborate with Reynir Bödvarsson (UPP) and Jacques Angelier (UPMC) in investigating the anomaly.

One of interesting phenomena is that the shear-wave polarisations at BRE, FLA, and HED show fault-parallel 90º-flips in direction thought to be caused by the high pore-pressures pervading all seismically-active faults. The stress directions of UPMC appear to be intermediate between the approximately NE to SW shear-wave polarisations at almost all seismic stations in Iceland and the 90º-flips immediately adjacent to the Húsavík-Flatey Fault.

3c) Stress-relaxation before earthquakes (D30):

Because of its probable significance, we further discuss the stress-relaxation reported previously. For information, we reproduce figures from the previous 6-month report and also see Gao & Crampin (2004).

a) **b)**

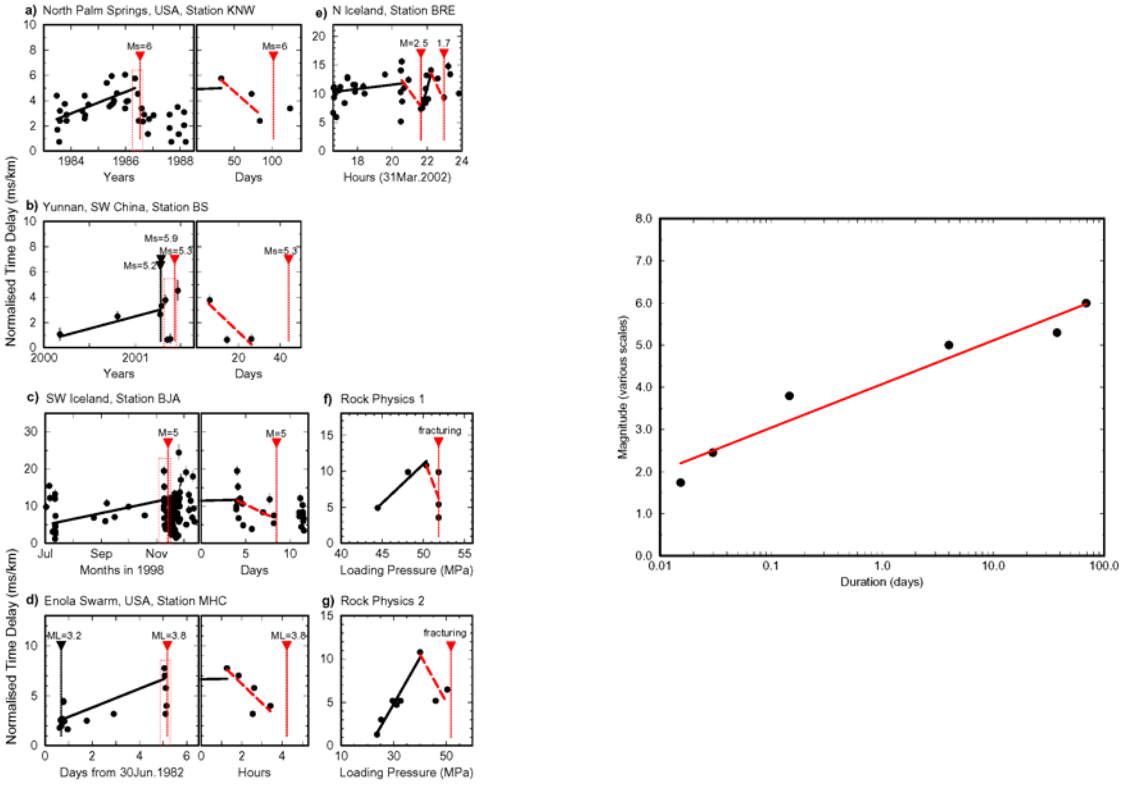

Fig. 2.5ii. (a) Precursory delays in field and laboratory. For details see Gao & Crampin (2004).
(b) Logarithm of duration of precursory delays and earthquake magnitude. (Gao & Crampin, 2004).

We interpret these precursory delays in the time-delays of shear-wave splitting as indicating some form of stress relaxation before earthquakes occur. Note three possibly important phenomena:

1) Although there are only a limited number of examples in Fig, 2.5ii (six earthquakes and two laboratory experiments), this is all earthquakes that display sufficient time-delays immediately before earthquakes for the precursory delay to be measured. There are no known exceptions.
2) The delays appear at substantial distances from the eventual earthquake focus, so the precursory delays appear to be as pervasive in extent as the increasing time-delays, and appear to be caused by the effect of changing stress on the ray path rather than the effect of the immediate source zone. Again demonstrating the sensitivity of the fluid-saturated microcracked crust to small stress changes at substantial distances.
3) The precursory delays before the 1988 *Ms*6 North Palm Springs Earthquake on the San Andres Fault in Fig.2.5iia-a, and before the two swarm events at BRE on the Húsavík-Flatey Fault in Fig.2.5iia-d are all from records which show 90º-flips in shear-wave polarisations at the surface. That is half the number of earthquakes displaying precursory delays are from records which show 90º-flips.

This appears to have important implications for the behaviour of the stressed rock-mass. The stressed volume reaches fracture criticality over an extensive volume but the eventual earthquake fractures on usually pre-existing faults which appears to trigger a relaxation again over an extensive volume. We suggest this has important applications for short-term earthquake precursors.

4) DEVELOP AUTOMATIC ANALYSIS OF SHEAR-WAVE SPLITTING BY NEURAL NETWORK (ANN) TECHNIQUES:

4a) Report on progress of ANN measurements of shear-wave splitting (D32):

Although we have made some progress in the development of ANN measurements of shear-wave splitting, we have been diverted by the success of more widely applicable automatic techniques for automatic measurement. (We are also discouraged by the difficulty of choosing suitable training sets for ANN, see Item 5, below. This is a critical handicap.) It seems that currently ANN techniques are not the best way to automatically measure parameters of shear-wave splitting, and we are discontinuing their development in favour of alternative automatic techniques.

5) DEVELOP TRAINING SETS FOR ANN THAT PRESERVE INTERPRETER'S EXPERIENCE:

5a) Report on experience of selecting training sets for ANN (D33):

We now know that observations of shear-wave splitting above small earthquakes are complicated by the large scatter (±80%) in shear-time delays, caused by the critically-high pore-fluid pressures on all seismically-active fault-planes causing 90º-flips in shear-wave polarisations (Crampin *et al.,* 2004). Thus the scatter is geophysical in origin and cannot be removed. ANN techniques require large (20+) training sets of selected seismograms for each seismic station, which have been manually read by an experienced observer, so that the observer's experience can be characterised by ANN. The scatter in shear-wave splitting caused by 90º-flips means that all observations of shear-wave splitting above small earthquakes, at any particular station, are necessarily subject to a large ±80% scatter. This means that there is wide variation of shear-wave splitting parameters at any seismic station, even above a persistent swarm of similar small earthquakes, which might otherwise be thought to be a stable source of shear waves.
This variability and instability of parameters means that ANN training sets for measuring shear-wave splitting would need to be extremely long, possibly upwards of 40 earthquakes for each seismic station. These are unwieldy and much of the flexibility and adaptability of ANN for automatically measuring the parameters of shear-wave splitting is taken away, so that ANN techniques no longer look so attractive, in comparison to a good generally applicable automatic technique for reading shear-wave splitting, and the effort planned for ANN (Objectives 4 & 5)

have been diverted to developing other automatic techniques, which are beginning to look very rewarding

3.3) SOCIO-ECONOMIC RELEVANCE

Monitoring of shear-wave splitting imaging the build-up of stress before earthquakes, and the precursory decrease immediately before the earthquake, appear to given effective long-term and short-term predictions of earthquakes (and/or volcanic eruptions). Note however that this would only be possible in those exceptional areas such as Iceland where persistent swarms of small earthquakes can be monitored by seismic stations within the shear-wave window. Such stress-forecasting elsewhere requires controlled shear-wave source experiments in the Stress-Monitoring Sites such as the EC SMSITES Project at Húsavík in the Tjörnes Fracture Zone in northern Iceland.

3.4) DISCUSSION AND CONCLUSIONS

In the first year of PREPARED, WP2.5 has established two possibly-important scientific results: (1) recognised that the large scatter in shear-wave time-delays above small earthquakes is caused by the effects of critically-high pore-fluid pressures on all seismically-active faults; and (2) recognised that all earthquakes show stress-relaxation before earthquakes, where the log of the duration of the decrease is proportional to earthquake magnitude. In conjunction with the increase in time-delays, these are important precursory phenomena for large earthquakes.

WP2.5 continues to monitor shear-wave splitting in the SISZ and elsewhere in Iceland and recognises what appears to be a consistent build-up of stress over two years in both the SISZ and in the Tjörnes Fracture Zone.

WP2.5 is developing what appears to be a successful automatic technique for reading shear-wave splitting on 3C seismograms. Note that the inherent large scatter (see Item 1, above) in shear-wave time-delays, means that ANN (automatic neural network) techniques require excessively-lengthy training sets to cover all eventualities at each seismic station. Such training sets would be inflexible and unwieldy and seriously disadvantages any possible advantage of ANN analysis. Consequently, the ANN development has been diverted into the development of other automatic analysis techniques.

3.5) PLAN AND OBJECTIVES FOR THE NEXT PERIOD

The objectives, as listed above, are unchanged, except that the development of ANN techniques (Objectives 4 and 5) have been diverted into the development of automatic techniques for reading the parameters of shear-wave splitting.

UEDIN is planning collaboration with UPMC and UU comparing stress, as determined from shear-wave splitting, and stress from fault plane mechanisms (Deliverable 31).

It will be interesting to see the conclusion of the implied build-up of stress in Fig.2.5.
With SMSITES I managed to avoid producing a TIP until the Project was completed.

WP 3 Short-term changes/precursors

Objectives

Analysis of observed short-term changes in various measurements, especially before the large earthquakes. Test and develop multidisciplinary short-term warning algorithms.

Methodology and scientific achievements related to workpackages including contribution from partners

The input here is basically analysis and deliverables of WP3.1 and WP3.2. Also related deliverables from several other workpackages of the project which provide results applicable for developing new warning algorithms, such as WP2.1, 2.2, 2.3, 2.5, 4.1, 5.5 and 6.2.

Automatic warning procedures of different types are already operated by IMOR. An alert system based mainly on seismicity rate has been operated there for 9 years. New algorithms based on work in the PRENLAB projects have been in operation during the last year. They are based on besides the character of the seismicity also on microearthquake source information and wave path information. These warning procedures have shown to be significant, especially for activating and assisting the seismologists in evaluation of signs of possible impending hazards.

WP3 is a forum for integration of all results of the PREPARED project which can help in developing and testing enhanced short-term warnings. Besides the methods for warnings that will be especially studied in WP3.1 and WP3.2, many other workpackages can be expected to rend results which will be significant contribution to this work of developing and testing short-term warning methods. To mention examples there were hydrological changes and deformation rate changes before the first earthquake, that possibly may be related to it, which are analyzed in other workpackages.

WP3 will coordinate these activities in general and work on merging the multidisciplinary methods by analysis and testings into operative warning algorithms to be implemented into the Icelandic early warning system, and provides information which can help in developing similar warning algorithms into comparable warning systems elsewhere.

The main work in this workpackage is to create and edit tools on short-term hazard assessments or warnings based on results from various other WPs. Most of the WPs of PREPARED will provide results which will be a significant input to this work. Most significant input in WP3 up to the present comes from WP3.1-3.2, WP2.1-2.5 and WP6.2. Special discussion and exchange of results for the interactive work of these partners have been during the two regular PREPARED meetings and during the EGS-AGU-EGU Joint Assembly in Nice in 2003. Models for penetration of fluids from below, causing high pore fluid pressures in the seismogenic part of the crust and rock fluid interaction is together with the observations gradually leading to new understanding on the earthquake stress build-up and nucleation process.

The seismic work, which is basic for the short-term warnings, is based on a unique database created by IMOR in WP2 and WP4.1, released in September 2003 (Guðmundsson et al. 2003). This database is unique as it carries information on earthquakes in the area well below magnitude zero and is complete (WP2.2) down to magnitude 0. This provides high resolution information on crustal conditions, near continuous in time and space. It is also unique in such

a way that besides the usual information on magnitude and location it contains information on fault plane solutions and various source parameters. This is basic for studying processes approaching the large earthquakes, not least to study the short-term changes. This database makes it possible to see causal relationship on a small scale within the earthquake zone, migration of activity probably often caused by migration of fluids and migration of pore fluid pressures deep in the crust, below the hydrostatic sphere. A qualitative analysis has been ongoing by the lead contractor in observing and finding such causal relationships in distribution and migration of small earthquakes to prepare for a more quantitative analysis including the use of fault plane solutions and source parameters especially in cooperation with WP3.1 and WP2.4. This work very much relies on and is inspired by modelling work in WP6.2 and WP3.1.

Analysis on short-term patterns in the seismic data

a) Some indications on pre-earthquake short-term crustal processes from studying the distribution of seismicity (Figure 1).

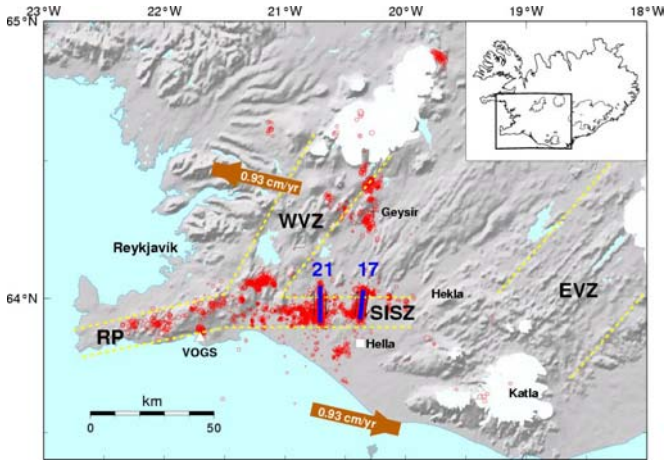

Figure 1. *SW Iceland. The whole of Iceland is indicated in the upper right corner. The South Iceland seismic zone (SISZ), the eastern and the western volcanic zones (EVZ, WVZ as well as the Reykjanes zone (RP) are indicated. Red dots show small earthquakes and the blue lines marked 17 and 21 show the earthquake faults, i.e. of the June 17 and June 21 earthquakes, respectively. The heavy arrows indicate the plate motion according to the NUVEL 1A plate model (De Mets et al. 1994).*

b) Seismicity long-term changes studied in 3-D volumes clustering towards the fault direction of the June 17 earthquake (Figure 2).

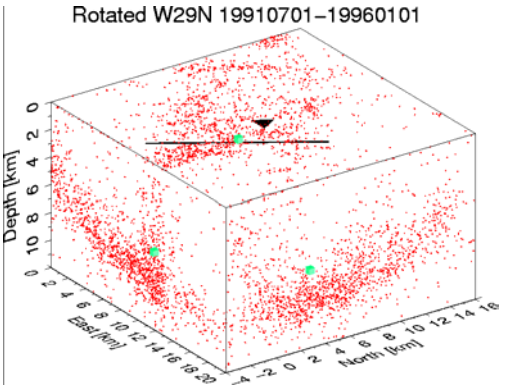

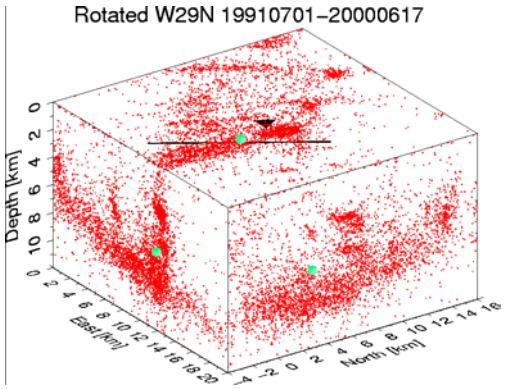

Figure 2 a

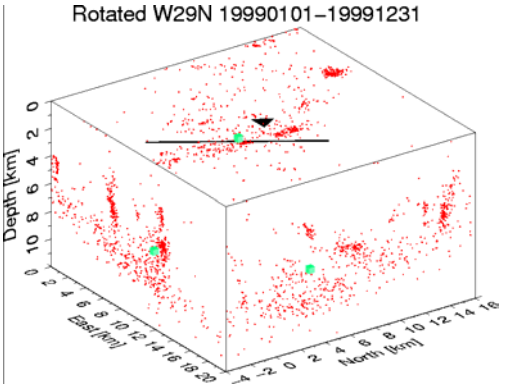

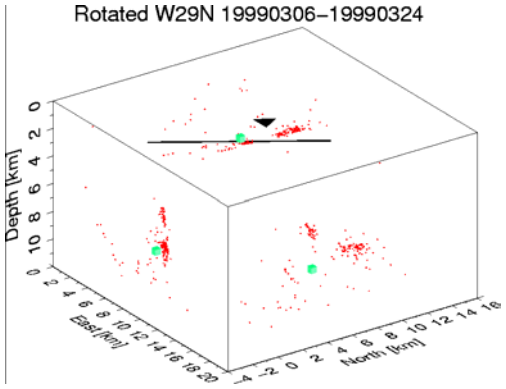

Figure 2 b

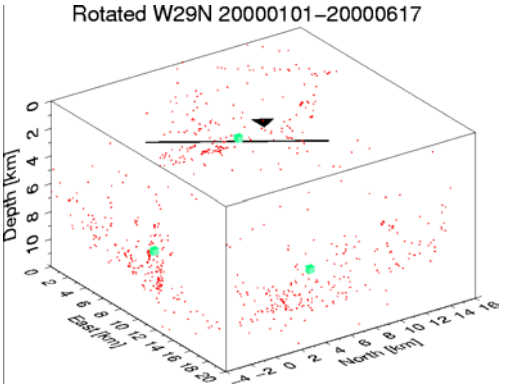

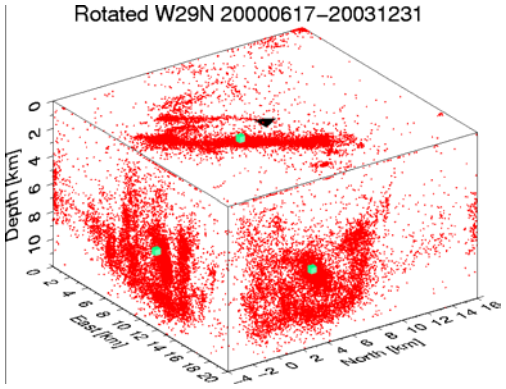

Figure 2 c

Figure 2. *The studied 3-D boxes are oriented along a seismic volume elevated from the usual ductile brittle boundary, here called the dilavolume. It is probable that the dilavolume consists of anomalously high pore fluid pressures. It strikes 29° west of north. The hypocenter (green dot) and the fault of the June 17 main shock is marked as well as SAU, a close seismic station. The two figures at the top (a) indicate relative shallowing of activity by time. This remains though to be confirmed by a special study. The two figures in the second row (b) show an episodic shallowing of activity above the dilavolume. The figures in the bottom row (c) show orientation of activity towards the fault plane, especially in the last figure, i.e. after the June 17 earthquake, where the dilavolume has disappeared.*

b) Short-term orientation of seismic activity towards the June 17 earthquake shortly before and after it occurred (Figure 3).

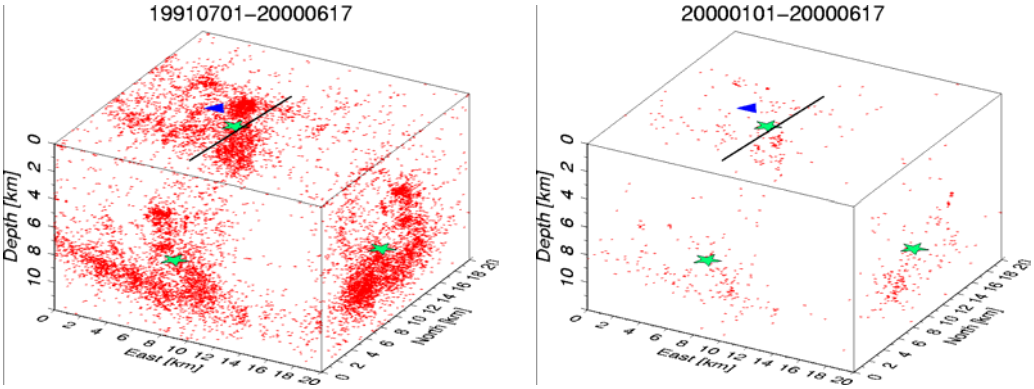

Figure 3 a

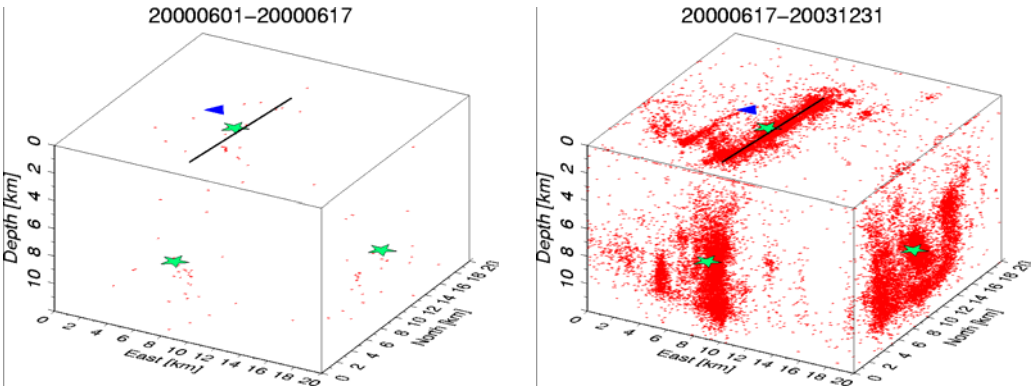

Figure 3 b

Figure 3. *Looking along the June 17 fault as the seimicity changes from pre-earthquake towards post-earthquake situation. Clear orientation towards the fault direction is seen during the last 17 days before the earthquake. After the earthquake the seismicity is oriented along the fault and the N29°W dilavolume has disappeared*

c) Observations relevant for short-term warning before the June 17 earthquake.

For the general interpretation of what is seen in these figures see WP2. On a short-term basis a clear clustering towards the line of the becoming fault and to the hypocenter, i.e. the 1-2 km diameter asperity, shortly before the earthquake.

d) Approaching the June 21st 2000 M=6.6 earthquake.

Parallel observations are made in analyzing the seismic patterns shortly before the second earthquake, i.e. the June 21, M=6.6 earthquake. The main difference is though that the June 21 earthquake was triggered by the June 17 earthquake. It did not have an asperity or one could say that the asperity of the first earthquake was a common asperity of both earthquakes. Linearization of seismic activity around the becoming earthquake fault was observed in the days between the earthquakes, compared to the spread activity well before both earthquakes. The second earthquake was in fact forecast 26 hours ahead, as immediate, right size and fault plane position (Stefánsson and Guðmundsson 2004).

e) Other WPs already arriving conclusions significant for short-term warning.

From detailed studies of b-values in WP2.2 patterns of high b-value anomalies are interpreted as due to liquids that penetrate from below and establish pockets of high pore pressures at mid-crustal levels.

Research in WP2.5 leads to the conclusions that large scatter in shear-wave time delays above small earthquakes is caused by the effects of critically high pore fluid pressures on all seismically active faults, and that all earthquakes show stress relaxation before their occurrence.

Studying the stress tensor inversion of earthquake focal mechanisms in WP2.4 a north rotation of the horizontal stress axis was observed shortly before the first large earthquake.

In WP3.2 studies of radon anomalies in water samples from geothermal wells in the SISZ revealed, common for many sampling stations, anomalies related to the 2000 earthquakes, before, during and after these.

In WP3.1 a new method has been developed to assess the absolute stress level, and will among other things be included in an early warning algorithm, EQWA (often called Slunga warning), developed within the PRENLAB projects (1996-2000).

Modelling work in WP3.1 and WP6.2 which treat rock-water interaction and pore fluid pressures and fluid flow deep in the crust creates a basis for explaining the observation of the microearthquakes before the earthquakes, especially to explain the short-term changes which are observed.

Socio-economic relevance and policy implication

It is of economic and social significance to be able to provide short-term warnings before earthquakes. It makes it possible to prepare people and rescue infrastructure before the event.

The short-term warning does not only include saying that an earthquake is probably impending within hours or days. Short-term warnings are issued when real-time monitoring and investigations reach a certain level of probability. Shortly before the earthquake it can be expected that knowledge on the exact fault position and intensity will have reached a level that is of enormous significance even if warning of the exact time of rupture would fail. Knowledge of progress in this field increases the quality of life in any earthquake-prone area.

Discussion and conclusions

Progress in the various involved WPs, provides various examples of observable processes approaching the 2000 earthquakes. Modelling work emphasizes that understanding of fluid migration and of high porous fluid pressures is of fundamental significance in providing the observed forerunning signals.

Plan and objectives for the next period

The main activity in WP3 in the next period is to test the indications obtained in the qualitative seismic analysis described shortly above and to merge together the results of the various other WPs providing short-term indicators or adequate modelling into overall short-term forecasting or warning tool.

References

DeMets, C., R. G. Gordon, D. F. Argus & S. Stein 1994. Effect of recent revisions to the geomagnetic reversal time scale on estimates of current plate motions. *Geophys. Res. Lett.* 21, 2191-2194.

Gunnar B. Guðmundsson, Kristín S. Vogfjörð & Bergþóra S. Þorbjarnardóttir 2003. SIL data status report. http://hraun.vedur.is/ja/prepared/reports/sdsr.pdf

Ragnar Stefánsson & Gunnar B. Guðmundsson 2004. About the state-of-the-art in providing earthquake warnings in Iceland. *Icelandic Meteorological Office - Report.* In press.

WP 3.1 Foreshocks and development of new warning algorithms

A. Objectives

During the PRENLAB projects an earthquake warning algorithm, EQWA, based on the statistics of the microearthquakes was designed. The following microearthquake parameters were included: hypocenter location, origin time, seismic moment, slip size, static stress drop, and fault radius. The EQWA is described by Slunga (2003a). Within PREPARED there is an intention to go into a more physical analysis of the microearthquakes preceeding an earthquake which possibly will increase the predictive value of the EQWA. The improved EQWA will then be made operational and implemented within the routine system.

B. Methods and achievemnts.

A simple method of estimating the complete rock stress tensor from the microearthquakes has been investigated in the first stage of this workpackage. As is well known the use of Bott's criterion together with fault plane solutions gives four constraints on the rock stress tensor. It gives the orientation of the principal stresses (three angles) plus the shape factor relating the intermediate principal stress to the maximum and minimum principal stresses. The stress tensor contains 6 parameters. One additional constraint is given by setting the vertical stress equal to the lithostatic stress. Another constraint is given by Coulomb failure criterion. If the stress changes slowly enough one can assume that the shear stress equals the shear strength as given by Coulomb. If slip directions are used it is obvious that the shear strength has been exceeded. The only problem is then that the Coulomb failure criterion requires knowledge about the water pressure.

In the NORFA summer school in Geysir in Iceland 2004 a simple way of estimating the pore pressure from the rock stresses and rock parameters was presented, Slunga (2003b). The model was also discussed in the Nordic Geological Winter Meeting in Uppsala, Slunga (2004). In short the idea is to use the relation for a waterfilled fracture between the contact normal stress, Sc, the water pressure, p, and the normal rock stress on the fracture, Sn:

$$Sc * (1-k) + p * k = Sn,$$

where k is the ratio between the non-contact area and the total normal area of the fracture. For basalt laboratory measurements have given values close to 1.0 while values in the range 0.85-0.95 have been estimated for granites in the crust. The stresses increase with depth leading to increased Sc and possibly reduced k. As long as the fractures are open the water pressure has to be hydrostatic. There is an upper limit for Sc given by the strength of the contact points, Sc(lim). Although both Sc(lim) and k are uncertain there is a simple way to find reasonable combinations of these by checking their consistency with the rock wall strength values JCSo and the uniaxial compressive strengths as reported in the literature. When Sc(lim) is exceeded the fracture will close unless the water pressure can be increased. However the water pressure can only exceed the hydrostatic value if the fracture is not connected with the surface. Figure 1 and 2 shows the situation for different depths if Sc(lim) equals 1.9 GPa and k equals 0.99 for basalt and 1.2GPa and 0.90 for granite. For these values the water pressure will be hydrostatic down to 4 km depth in basalt and down to 20 km depth in granite. The figures also show approximately the effective normal stress at the fracture. The peak value for basalt is 60 MPa and for granite 320 MPa. The basalt value is in agreement with the JCSo values while

the granitic value is a little high, around 200 MPa is more reasonable which would mean that hydrostatic pressure in granite is only possible down to 10-15 km depth.

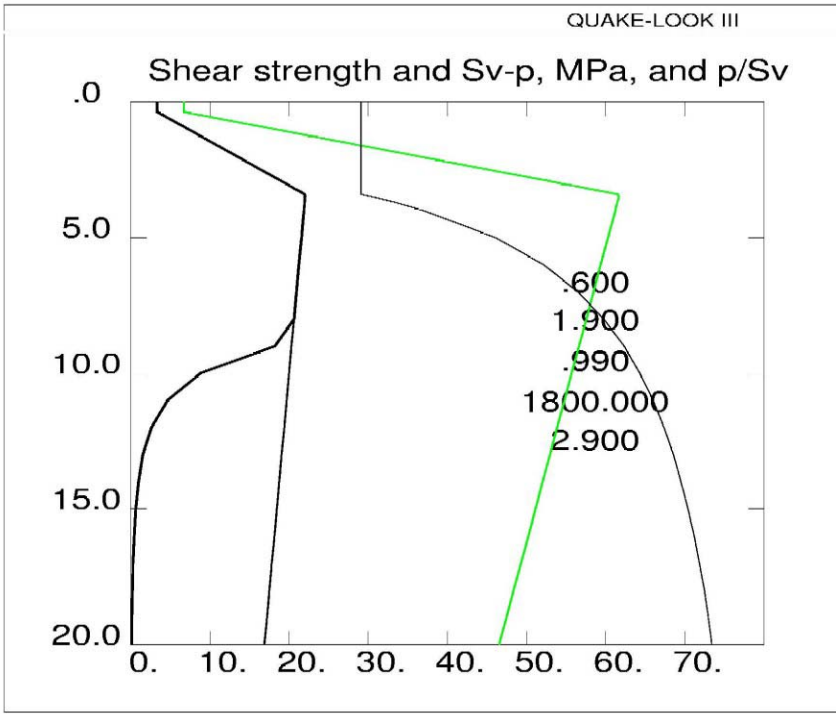

Figure 1. The two thick line curves to the left show the shear strength of the crust. The curved lower part of the thickest line is due to the strength reduction due to temperature and strain rate. The water pressure divided by the lithostatic pressure is given by the line constant to a depth of about 3.5 km (hydrostatic pressure) where it gets confined and the pressure starts to increase. The remaining curve peaking at a value of about 60 MPa is the effective normal stress. This figure is computed for a normal faulting stress regime. The parameter values are: friction 0.6, k 0.99, Sc(lim) 1800 MPa, and density
2.9 g per ccm.

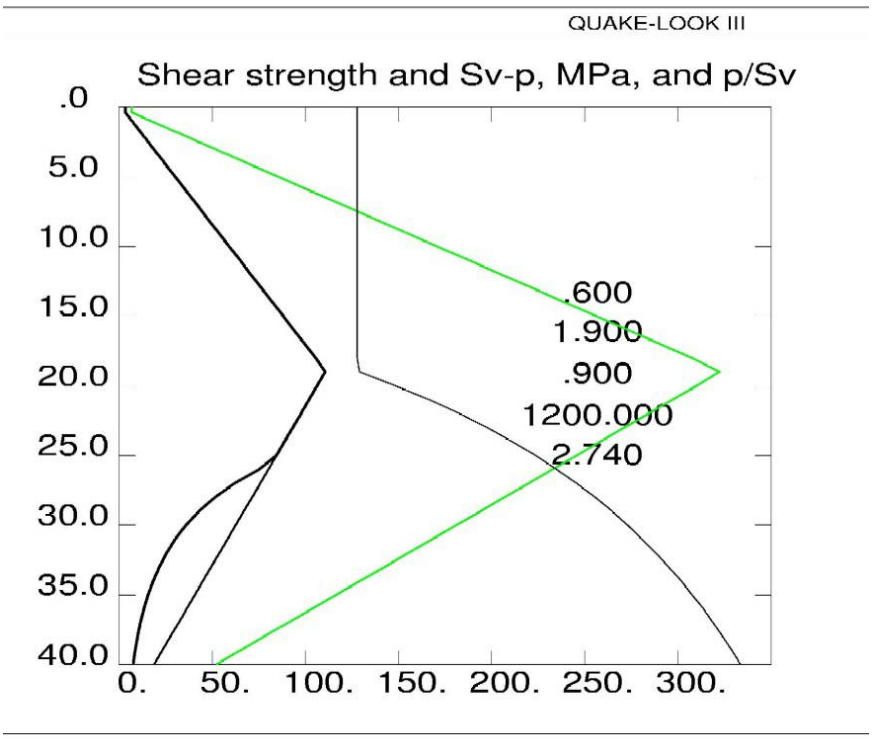

Figure 2. As figure 1 but now for parameter values reported for granite. Sc(lim) is here 1200 MPa and k is 0.90. Note that the effective normal stress is over 300 MPa which is more than normally reported. A more reasonable value would be about 200 MPa which would give hydrostatic pore pressure down to only 12 km. Hydrostatic pressure in granitic crust has been found to such large depths.

The consequences for the water below the depth where its connection to the surface is lost and the pressure will increase are interesting. The water will flow from fractures with higher normal stress to fractures of lower normal stress and tend to be accumulated in fractures with normals parallell with the direction of smallest principal compression.
When the water in a fracture is surrounded by fractures of higher normal stresses the water will stay and only slowly diffuse through the rock mass. For this reason the water pressure at confined depths is related to the smallest principal stress through the equation above with Sc replaced by Sc(lim).
A rotation of the stress tensor is enough to cause instability as it will lead to increased water pressure in the previously favoured fractures. Another consequence is that a sudden release of shear stresses will always cause an immediate increase in water pressure everywhere around the shear slip as the minimum principal compression will increase. This is one important cause to aftershocks. In order to test this concept of estimating the absolute rock stresses from microearthquake observations the activity prior to the June 4 1998 earthquake was chosen due to the large number of foreshocks. First the auxiliary planes were eliminated by combined use of FPS and high accuracy relative locations leading to groups of earthquakes having common fault planes. In the second step Bott's criterion was used for groups of closely spaced events and the result was combined with the constraints of the vertical stress and the Coulomb criterion. This gave a number of stress tensors and water pressures. Figure 3 shows the water pressure, the shear stress, and the stress level (the sum of the three principal stresses divided by the vertical stress) as a function of depth. The water pressure is typically 0.75-0.9 of the lithostatic. The shear stress is 11-13 MPa but observe that this is a consequence of the values of Sc(lim) and k. Any value in the range 10-25 MPa is reasonable. The stress level should be 3.0 for hydrostatic conditions, values above 3 indicate increased stress level.

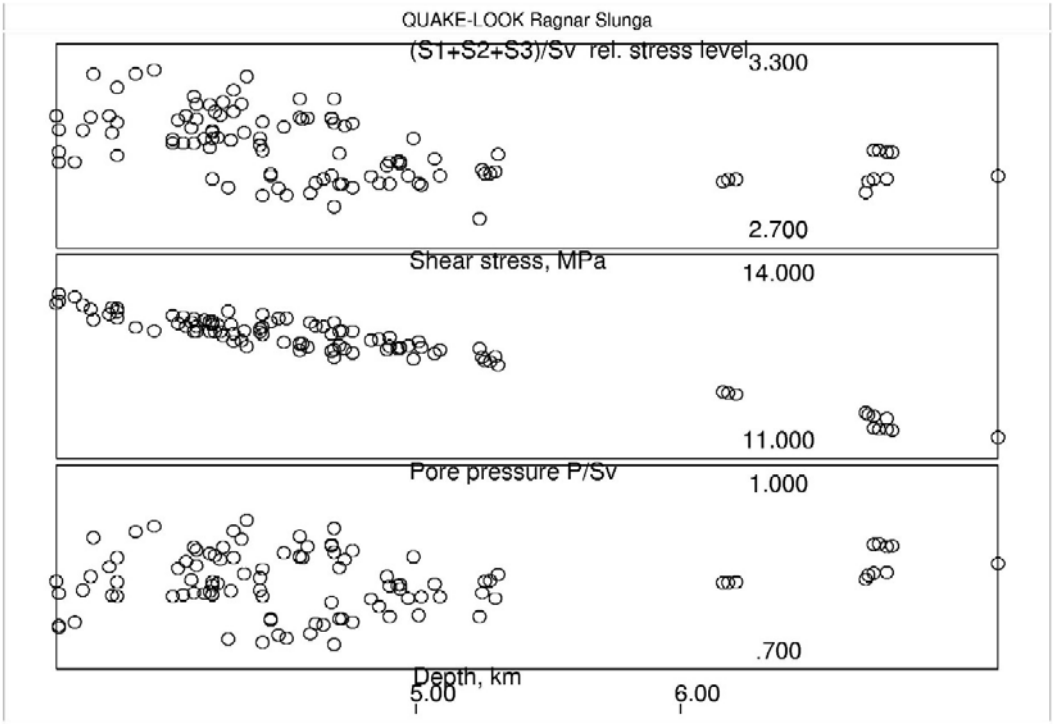

Figure 3. The results of some 110 rock stress tensor inversions before the June 4 1998 earthquake. The water pressure, the shear stress, and the stress level are given as functions of depth. The ranges are for pore pressure 0.7-1.0 of the lithostatic, for shear stress 11-14 MPa, and for the sum of the principal stresses (stress level) 2.7-3.3 of the lithostatic pressure.

Figure 4 shows the positions of the stress tensor estimates around the fault of the 1998 EQ. The sizes scales with the stress level and we see high levels in the compressive quadrant as theoretically expected. The highest levels are 2km northeast of the hypocenter and shows actually the epicenter of the largest foreshock about 40 hours before the main event. In conclusion the picture given by figure 4 is promising.

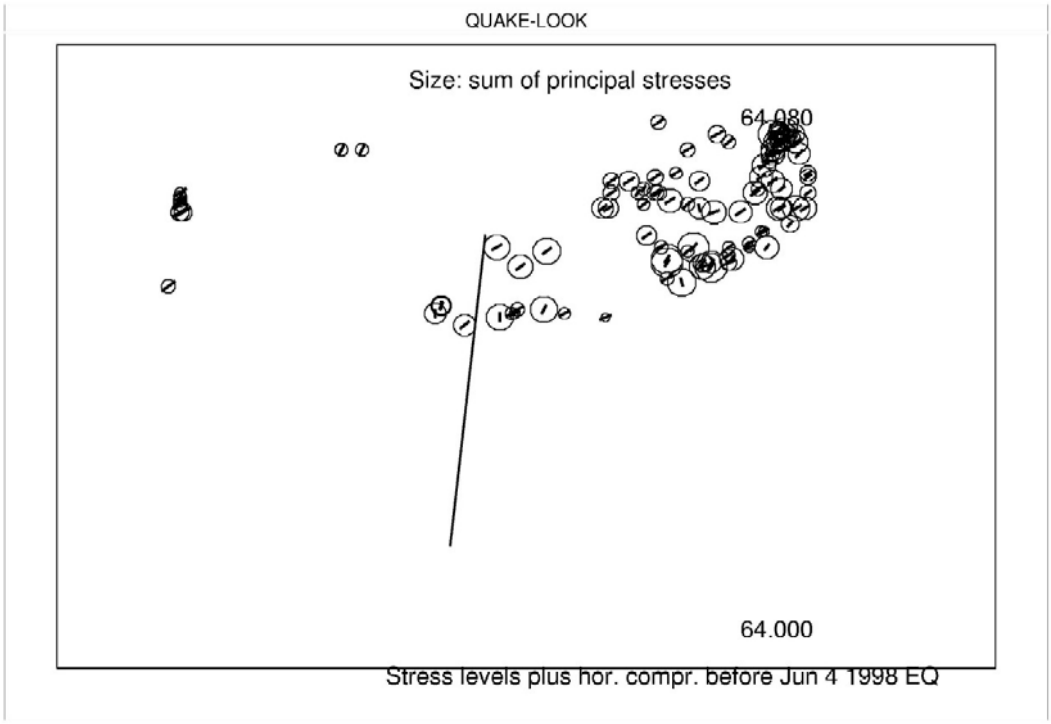

Figure 4. This is a map of the epicentral area of the June 4 1998 earthquake. The latitude is from 64.0 to 64.08 degrees north and longitude 21.38W to 21.22W. The fault is shown by the line. Each circle marks the position of one rock stress tensor, the line shows the direction of the horizontal principal compression, and the size of the circles marks the compressive stress level, see figure 3. The largest compressive stresses are at places of the largest forshock (2-3 km NE of the central fault) and later at the compressive quadrant of the earthquake.

The first of the two large earthquakes in June 2000 had only 5 foreshocks in the epicentral area during the last 24 hours. This means that the activity rate itself is not enough for an EQWA. Based on the results in figure 4 a test was done for the epicentral area of the June 17 2000 earthquake. In figure 5 an analysis of the absolute stress level is shown and for this area we see that we do indeed observe high stresses for the last 2-3 months before the earthquake.

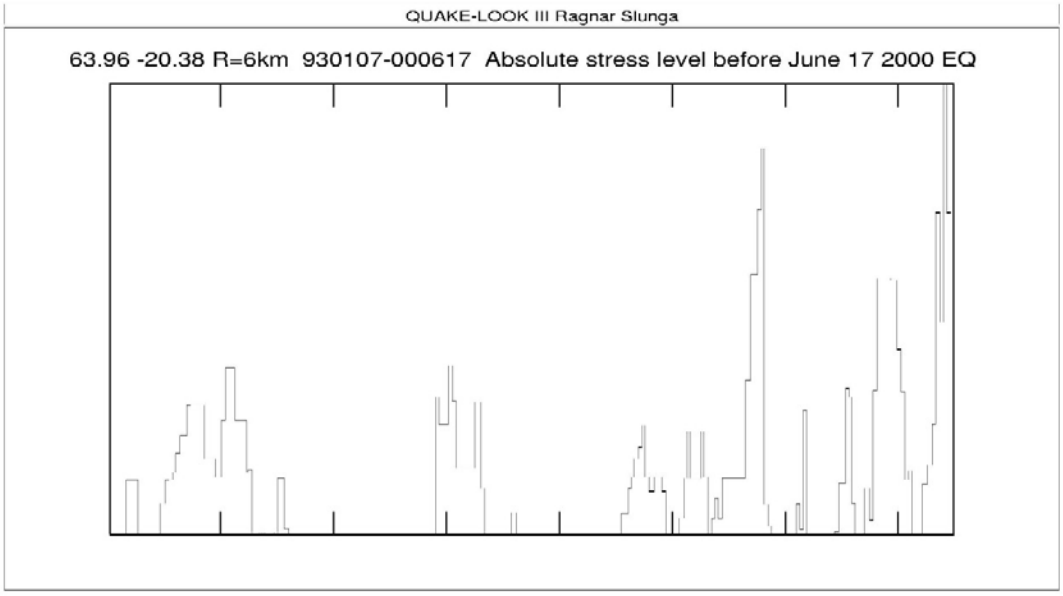

Figure 5. The earthquakes in the epicentral area of the June 17 2000 earthquake have been used for monitoring the absolute stress level. The statistical deviation (increase) in the stress level is computed from groups of 60 microearthquakes. This test shows that the value of this stress level parameter is increased during about 3 months before the EQ. The years are marked at top and bottom of the figure.

C. Social and economic effects.

If the promising resukts can be utilized in a well working EQWA it means that life can be saved and also some economical losses can be reduced. The value can be compared to the meteorological storm warnings even if storms normally affects larger areas.

D. Discussion and conclusions.

The absolute stress level is a new aspect on the EQ warning and is independent of the previous EQ parameters used. This can possibly lead to a significant improvement of the EQWA. The preliminary investigations are promising. E. Plan and objectives for the remaining time period.

The detailed study of the foreshocks before all larger EQ in the area will continue and be completed. The potential value of the stress level monitoring will be evaluated during this work. The results of these investigations will be incorporated in the coming version of the EQWA.

The work is proceeding according to the plan and time schedule.

References:

Slunga R (2003a) Microearthquake Analysis at Local Seismic Networks in Iceland and Sweden and Earthquake Precursors, Lecture Notes in Earth Sciences 98, editors: T Takanami and G Kitagawa, Springer Verlag Berlin 2003.

Slunga R (2003b) Microearthquake analysis, lecture note presented at the NORFA Summer School in Geysir, Iceland, 2003.

Slunga R (2004) Rock-water interaction in the crust, abstract, 26th Nordic Geological Winter Meeting, Uppsala University, Jan 6-9, 2004.

WP 3.2 Radon anomalies

Objectives:
To establish the significance of the radon anomalies that occurred prior to the June 2000 earthquakes by comparing them to earlier results of the radon monitoring program in South Iceland and other results world-wide. Characteristics of the anomalies will be determined with the aim of developing a warning algorithm.

Deliverables:
1. Time series of radon at all measuring stations in South Iceland since 1977.
2. Paper in a refereed journal on the radon anomalies identified.
3. Presentation of the radon results at 2 international meetings.
4. Warning algorithm.

Milestones:
3 months: Time series ready for study
12 months: Presentation of first results at a meeting
20 months: Manuscript of paper submitted to a refereed journal
24 months: Final results and warning algorithm presented at a meeting.

Methodology and scientific achievements:
The relationship between radon and earthquakes in this area has been studied since 1977 when Egill Hauksson of the Lamont-Doherty Earth Observatory installed the first equipment for this purpose (Hauksson, 1981, Hauksson and Goddard, 1981). The instruments were operated until 1993. A summary of the results until then was given by Jónsson and Einarsson (1996). A very clear relationship could be established and a number of premonitory radon anomalies were identified.

The positive results spurred further work and a new instrument was designed and tested for the purpose of radon monitoring. The instrument is based on a novel liquid scintillation technique where counting only Bi-218/Po-218 pulse pairs gives high sensitivity with a simple construction. The system represents a significant progress in the radon measuring technique (Theodórsson, 1996, Theodórsson and Guðjónsson, 2004).

A new program of sampling from geothermal wells in the South Iceland Seismic Zone was initiated in 1999, a year before the destructive earthquakes of June 2000 occurred. The two M6.5 earthquakes originated in the middle of the sampling network. These events were preceded by clear anomalies at six out of seven stations (Theodórsson et al. 2000, Kerr, 2001, Einarsson et al., 2004). Four types of change could be identified in the radon time series in association with the earthquake sequence of June 2000:

1. Pre-seismic decrease of radon. Anomalously low values were measured in the period 101-167 days before the earthquakes.
2. Pre-seismic increase. Spikes appear in the time series 40-144 days prior to the earthquakes.
3. Co-seismic step. The radon values decrease at the time of the first earthquake. This is most likely related to the co-seismic change in ground water pressure observed over the whole area.
4. Post-seismic return to pre-seismic levels about 3 months after the earthquakes, probably also linked with the pressure change in the geothermal systems reported by Jónsson et al. (2003).

These results are clearly seen in Fig. 1 where the time series of all stations are shown on a common time axis, normalised to the station mean.

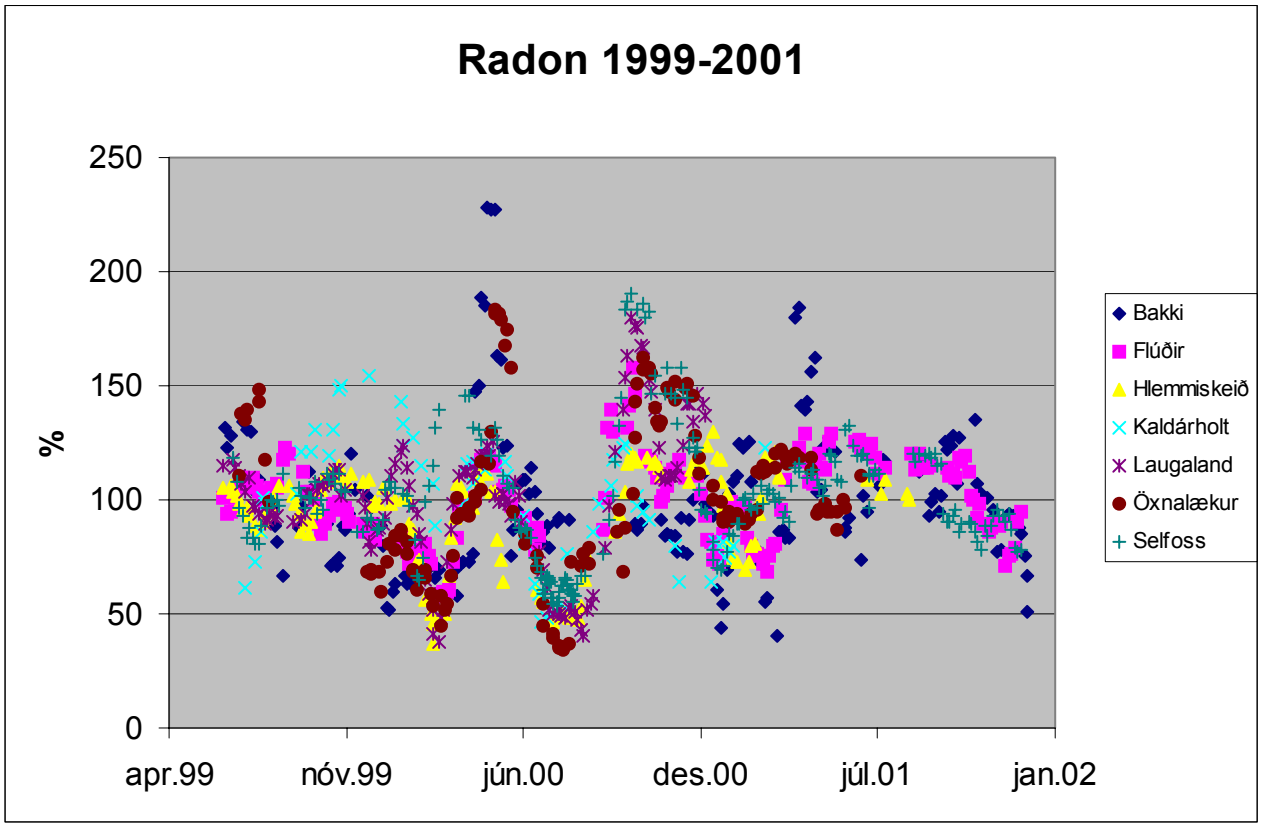

Fig. 1. *Radon time series of South Iceland normalised to the mean value at the respective station. The series are highly correlated, especially around the time of the Hekla eruption in February and the SISZ earthquakes in June 2000.*

In view of the positive results of the project we are developing and testing a new, automatic radon instrument, Auto-Radon, based on the same design, that continuously monitors the radon concentration in the geothermal ground water (Theodórsson and Guðjónsson, 2004). The instruments are situated at the drill hole stations, taking 4 radon readings each day. Four stations have been installed so far.

A research assistant, Ásta Rut Hjartardóttir, was hired to study the data from the three data sources listed above, integrate them and do statistical tests. She worked half time from September to December 2003 and will continue full-time in 2004.

Work delivered so far:

1. Paper on the premonitory anomalies to the 2000 earthquakes has been submitted for publication in Geophysical Research Letters (Einarsson et al., 2004).
2. A BS-thesis has been written on the 1999-2000 radon time series and their relations with earthquakes in South Iceland (Hjartardóttir, 2003), supervisor Páll Einarsson.
3. The time series for the discrete sampling of 1977-1993 and 1999-2003 have been assembled and can be distributed (Hjartardóttir et al. 2004).
4. A report on the time series was given at the PREPARED Mid-term Meeting in Reykjavík in January 2004 (Einarsson, 2004).

Socio-economic relevance and policy implication.

So far the radon program is a purely scientific endeavour. Its socio-economic relevance and policy implications are impossible to judge at this time.

Discussion and conclusion.

The most significant finding of this study is the high correlation between the radon time series over the entire area in the time period 1999-2001. Stations that are tens of kilometres apart show very similar fluctuations in the concentration of radon. Considering the short half-life of radon these fluctuations can hardly be ascribed to material transport between the stations. A common origin of the fluctuations must be assumed. Two significant events occurred in the crust of South Iceland during this time, the Hekla eruption of February 26 – March 8 and the earthquake sequence of June. It must be considered very likely that these events were the causal agents for the radon fluctuations. This conclusion is further strengthened by the temporal correlation of the post-earthquake radon recovery with the pore-pressure recovery and its poro-elastic response observed by Jónsson et al. (2003). We believe these observations are of crucial importance for the understanding of the physical mechanism of premonitory radon anomalies.

Plan and objectives for the next period.

1. Prepare a time series for earthquakes in the SISZ that fulfil the magnitude-distance criteria set by Hauksson (1981).

2. Find a statistics test for significance of correlation between the radon and the earthquake time series.

3. Work on an algorithm that detects radon anomalies in a time series.

References:

Einarsson, P., Radon anomalies. Paper given at PREPARED Mid-term Meeting, Reykjavík, January 30, 2004.

Einarsson, P., P. Theodórsson, G. I. Guðjónsson. Radon anomalies prior to the earthquakes sequence in June 2000 in the South Iceland Seismic Zone. Geophys. Res. Lett., submitted, 2004.

Hauksson, E., Radon content of groundwater as an earthquake precursor: Evaluation of worldwide data and physical basis. J. Geophys. Res., 86, 9397-9410, 1981.

Hauksson, E., and J. Goddard, Radon earthquake precursor studies in Iceland. J. Geophys. Res., 86, 7037-7054, 1981.

Hjartardóttir, Á. R. Radonfrávik sem fyrirboðar Suðurlandsskjálftanna 2000. (Radon anomalies occurring before the earthquakes of 2000 in South Iceland, in Icelandic). BS-thesis, Department of Natural Sciences, University of Iceland, 35 pp and Tables, 2003.

Hjartardóttir, Á. R., P. Einarsson, P. Theodórsson and G. Jónsson. Radon Data from the South Iceland Seismic Zone, 1977-1993 and 1999-2003. Report and CD, Science Institute, University of Iceland, 2004.

Jónsson, S., and P. Einarsson. Radon anomalies and earthquakes in the South Iceland Seismic Zone 1977-1993. In: Seismology in Europe (Ed. B. Thorkelsson et al.), European Seismological Commission, Reykjavík, p. 247-252, 1996.

Jónsson, S., P. Segall, R. Pedersen, G. Björnsson. Post-earthquake ground movements correlated to pore-pressure transients. Nature, 424, 179-183, 2003.

Kerr, R. A. Predicting Icelandic fire and shakes. Science, Jan. 26, 2001.

Theodórsson, P., Improved automatic radon monitoring in ground water. In: Seismology in Europe (Ed. B. Thorkelsson et al.), European Seismological Commission, Reykjavík, p. 253-257, 1996.

Theodórsson, Páll, Páll Einarsson, Guðjón I. Guðjónsson. Radon anomalies prior to the earthquake sequence in South Iceland in June 2000. Am. Geophys. Union, Fall Meeting, Abstract in Eos, 81, p. 891, 2000.

Theodórsson, P. and Guðjónsson, G. I. A simple and sensitive liquid scintillation counting system for continuous monitoring of radon in water. *Advances in Liquid Scintillation Spectrometry*, 249-252, 2003

WP 4 A model of the release of the two June 2000 earthquakes based on all available observations

Objectives

To model the source process in time and space of the two large earthquakes based on multidisciplinary information.

Methodology and scientific achievements related to workpackages including contribution from partners

The main input here is results and deliverables of WP4.1, WP4.2, WP4.3 and WP4.4., and results from other WPs like the modelling packages WP6.1 and WP6.2 as well as WP5.5.

A significant part of the modelling is a dynamic modelling based on teleseismic data, local seismometer data and acceleration data as described in WP4.1 and WP4.2 which will carry out a full moment tensor inversion assuming point sources and slip distribution on a fault, respectively, i.e. related to the short (several seconds) earthquake process.

Observations by microearthquakes and by geological methods will reveal independently the size and the orientation of the fault plane, as well as the detailed postseismic slip and possibly volume changes. Although these observations express process over a longer period of time, they will as well as the various deformation measurements put extra constraints on the short-lived earthquake modelling.

Another part of modelling the earthquakes is based on observations of the earthquake process as a process lasting for weeks, i.e. including pre- and postseismic process. This involves the possibility of a significant role of shallow or from great depth in the earthquake process. Such a modelling is very significant in light of the possibility that such strike-slip earthquakes can be considered a part of a large and longer lasting aseismic process.

WP4 is a forum with representatives from WP4.1–4.4 as well as from other workpackages in the project, to merge together results and discuss interactively the progress in revealing the overall source process during the project period.

There has not been much work in WP4 as such, so far. The work has mainly involved discussion meetings with various participants of the project that are gradually releasing results that are significant for the multidisciplinary source modelling of WP4. Modelling has been carried out based on deformation data (GPS, InSAR), both as takes to the slip process and fault size of the two earthquakes, but also as takes to the process on a larger spacial scale, taking to the whole of the seismic zone towards the Reykjanes peninsula (see other workpackages). Mapping of faults along the whole seismic zone, by seismic methods and by surface studies is ongoing and rendering new and significant results. The seismic database applied was released in September 2003. Intensive work has been going on since then on the seismic data. Besides the mapping of subsurface fault patterns of seismicity before the earthquakes are being analyzed and already provide confirmation of the significance of high pore fluid pressures exerted by fluids rising from below the brittle crust. Work on utilizing fault plane solutions and source parameters is emerging and will provide constraints on the more traditional pattern studies based mainly on location and time of the microearthquakes. Hydrological studies have already provided significant results especially for interpretation of

various deformation measurements on the surface. Studies of historical seismicity and paleoseismicity will render information which will complement the geologically short time of geophysical information. The emerging results from the various WPs have urged the modellers to study the effect of high pore fluid pressures below the area of hydrostatic pressure conditions, stemming from fluids upflow from below the ductile brittle boundary in the crust and the upper mantle.

The emerging results from the various workpackages makes it more and more obvious that the modelling of the source process of the two earthquakes in time and space will benefit from results in all other WPs in the project. The premonitory process of the earthquakes is observed several years before it. The earthquake fault zone involved in the source process is more than 100 km long, and the process is linked to processes in the eastern volcanic zone, to the center of the Iceland hotspot, and in west to the Reykjanes ridge. The two earthquakes are linked together in such a way that the first triggers the second.

Analysis of microseismicity and its relevance for modelling

Figure 1 describes the area involved as illuminated by aftershocks of the two large earthquakes.

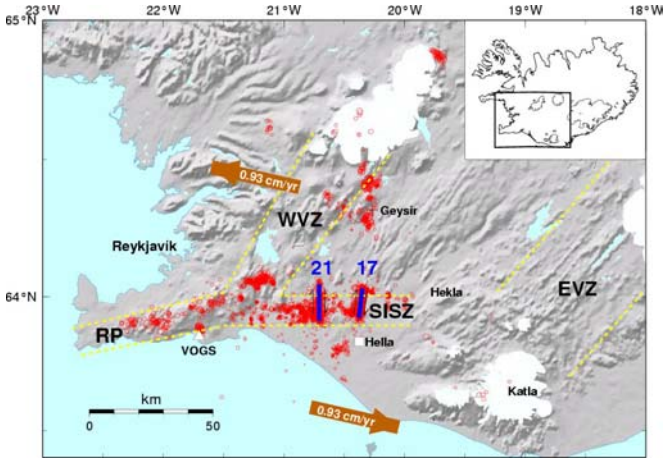

Figure 1. *SW Iceland. The whole of Iceland is indicated in the upper right corner. The South Iceland seismic zone (SISZ), the eastern and the western volcanic zones (EVZ, WVZ as well as the Reykjanes zone (RP) are indicated. Red dots show small earthquakes and the blue lines, marked 17 and 21 show the earthquake faults.The heavy arrows indicate the plate motion according to the NUVEL 1A plate model (De Mets et al. 1994).*

The angle of the transform SISZ to the NUVEL 1A plate model motion indicates a 1.8 cm/year left-lateral motion along the EW zone and, significantly, 0.4 cm/year NS, opening across the zone. A plausible parallel is that fluids participate in the process of opening, and of weakening a 10 km wide zone. (Stefánsson and Guðmundsson 2004). Pores originating in the ductile or semiductile material below the crust seek their way gradually or episodically up through the crust, bringing upward high lithostatic pressures. Lithostatic pressure is contained below a few kilometers depth and thus creates pockets of high fluid pressure. Pores with high fluid pressures most probably originating from below are gradually increased at the brittle ductile boundary and in the brittle crust until they are released during small- or large-scale pore fluid connections or ruptures and fluid flow along these ruptures or pervasive material.

A tentative sketch (Figure 2) describing these conditions was discussed during the PRENLAB projects (*http://hraun.vedur.is/ja/prepared/reports/*).

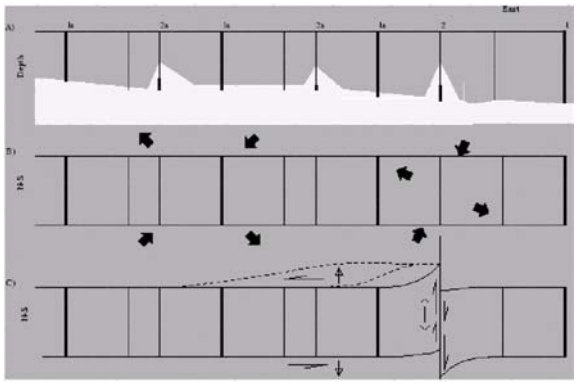

Figure 2. *The uppermost part of the figure shows a depth section from west to east along the SISZ. Heavy vertical lines (marked by 1) indicate faults of recent earthquakes, i.e. earthquakes which have released strain in the area and significantly also, pore pressures. The lighter horizontal lines (2) and the elevated white area indicate areas where pore pressures are building up from below and the predicted fault of a near future earthquake. The lower sections of the figure are horizontal sections, before and after earthquake stress release.*

The model (Figure 2) predicts increased pore pressures migrating from below up into the elastic/brittle crust most probably during a long time, possibly hundreds of years at sites where there has not been a large crust-through or other pore pressure releasing event for that period. Where we have recently had earthquakes (marked by 1) the high pore pressures are not reaching as high up into the brittle crust.

The fluids are episodically and gradually rising closer to the surface increasing pore pressures and corroding larger and larger surface of the fault until the earthquake is released. The high pore pressures weaken the area near the becoming fault so it breaks because of the 100 year strain build-up.

Socio-economic relevance and policy implication

It is significant to understand the source mechanism of earthquake processes in the SISZ. Earthquakes reaching magnitude 7 are expected there and have through historical times caused huge destruction. After the M=6.6 (Ms) earthquakes of the year 2000 a challenging question is if the sequence is over, can more be expected and where. A sequence of 5 large earthquakes (Ms > 6) broke through the central and the western part of the SISZ in the year 1896. 16 years later, in the year 1912, a magnitude 7 earthquake broke through the easternmost part of the zone. West of what usually is called the SISZ on the Reykjanes peninsula there is a region where in 1929 an earthquake of magnitude 6.3 occurred, only 15-20 km from the city of Reykjavík. What can be expected in that area is of enormous interest to know.

It can be expected that the project will render innovative results concerning earthquake nucleation and release process in general and thus can be of social and economic benefit for earthquake-prone areas in general.

Discussion and conclusions

There are no conclusions except that the multidisciplinary observations and evaluation in many WPs of the first-term of PREPARED provides information that will render a well constrained and innovative model of the earthquake processes in the SISZ.

Plan and objectives for the next period

The second term of the project will involve several meetings among many of the partners in the project during the EGU Assembly in Nice in April, during the ESC Assembly in Potsdam in September and before a final meeting of all the partners in the project near the end of 2004. To finalize the WPs several papers are in preparation, which will join together results of the various working parts. The lead contractor did visit Uppsala University in February/March for discussing progress and defining tasks and writing of a paper that can be expected to appear from that special cooperation with Uppsala. In general deliverables are expected to be in agreement with what was planned in the Description of Work.

References

Ragnar Stefánsson & Gunnar B. Guðmundsson 2004. About the state-of-the-art in providing earthquake warnings in Iceland. *Icelandic Meteorological Office - Report.* In press.

WP 4.1 Source mechanisms and fault dimensions of the June 17 and June 21 earthquakes determined from mapping of aftershocks

Objectives

To determine the source mechanisms and fault dimesions of the two large earthquakes on June 17 and June 21, using local events. That is:

1) Define the locations, dimensions and possible sub-fault details in the fault planes of the J17 and J21 earthquakes, by relatively locating the thousands of aftershocks on each of the two faults.

2) Map the post-seismic slip as a function of location and time on the two large faults in order to understand the evolution of the post-seismic stress.

Methodology and scientific achievements related to workpackages including contributions from partners

Interactively analyzed events are fed into a multievent relative location algorithm, in order to map the fault dimensions and finer subfault details of J17 and J21. The method used cross correlation of seismic wave forms recorded at a station, with the waveforms of its neighbouring events to determine relative travel times with subsample accuracy. The method is based on the assumption that the difference in travel times from a group of closely spaced events to a station at a greater distance is mainly due to the relative location difference of the events, as they propagate essentally along the same ray path to the station. The wave forms are sampled at 0.01 s and the timing accuracy of the clocks is 1 ms. Therefore the location accuracy achiveable with good data is on the order of tens of meters.

Joint interpretation of the revised hypocenter distribution and the possible fault-plane solutions of the individual microearthquakes is performed, in order to study the finer details of post-seismic slip on the two large faults as a function of time and space.

Nearly five thousand earthquakes have been interactively analyzed on the J17 (Holt) fault and roughly six thousand on the J21 (Hestfjall) fault. The relative location software can handle up to 1800 events simultaneously, so each fault is divided into four time-sections with approximately the same number of events. The time periods are listed in Table 1.

Holt Fault		***Hestfjall Fault***	
Time period	***Number of events***	***Time period***	***Number of events***
1: 1. Jan. - 20. June	1208	1: 1. Jan. - 22. June	1534
2: 21 June - 5. July	1350	2: 23. June - 1.July	1542
3: 6. July - 22. Sep.	1471	3: 2. July - 19. Sep.	1540
4: 23. Sep. - 31. Dec.	1160	4: 20. Sep. - 31. Dec.	1534
Total:	5189	Total:	6150

Table 1. *Time periods and numbers of events.*

In each inversion for relative location, the events are divided into overlapping groups of 40 events. So each event's waveforms are correlated with the waveforms of the remaining 39 events in the group. Each group is restricted to events within a circle of 2.8-3.0 km radius and the distance between the centers of groups is 2.0-2.2 km. The exact choice of parameters is determined by the overlap desired; that is, most events should be in 6-8 groups and therefore be well constrained. The total number of groups in each inversion is 200-240. Wave forms from stations at distances up to 100 km are used for correlation, with window lengths of 100 and 200 s around the first P and S arrivals.

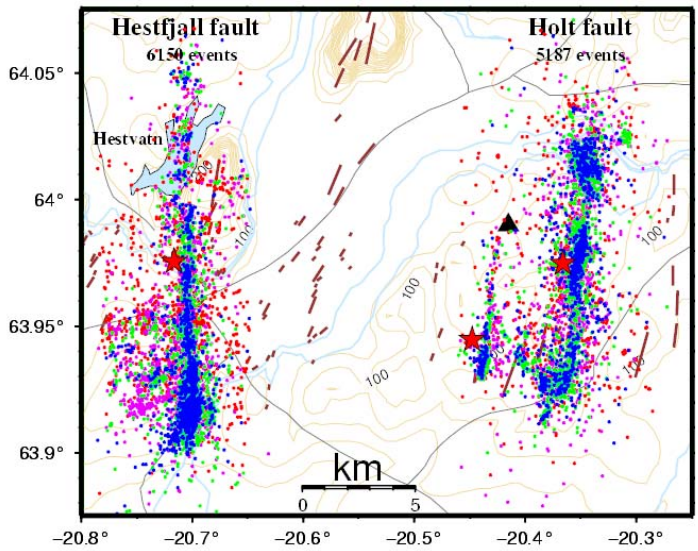

Figure 1. *Relative locations of events recorded during the year 2000, color coded according to time period (1=red, 2=purple, 3=green, 4=blue). Epicenters of the main events are shown (red stars) and previously mapped surface faults are also outlined (brown).*

Results from the inversions on the two faults are shown in Figure 1, color coded according to time period. There is considerable scatter in the locations, especially in the first time period. Still, the general strikes of the two faults are clearly defined. The activity on the Holt fault (J17) is not contiguous, but appears to be concentrated in the center and at the edges. Activity on the Hesfjall fault (J21) is not as patchy, but the fault bends westward at the southern end, a feature possibly also apparent on the Holt fault. The epicenter locations of the two main events and the second Holt event, 2 minutes after J17, are also shown on the map. Both main-events' epicenters are near the fault centers, and aftershocks are much more frequent south of the J21 epicenter, than to the north of it. To clarify the features of the faults, events with relative location errors in latitude and longitude ≤50 m, and in depth ≤100 m, are shown in Figure 2. The patchiness of the activity on the Holt fault is now even clearer and the westward bending of both faults at their southern ends is less obscure. Superimposed on the map is the mapped surface rupture following the large earthquakes (Clifton and Einarsson 2004) they follow closely the trends of the two Holt faults.

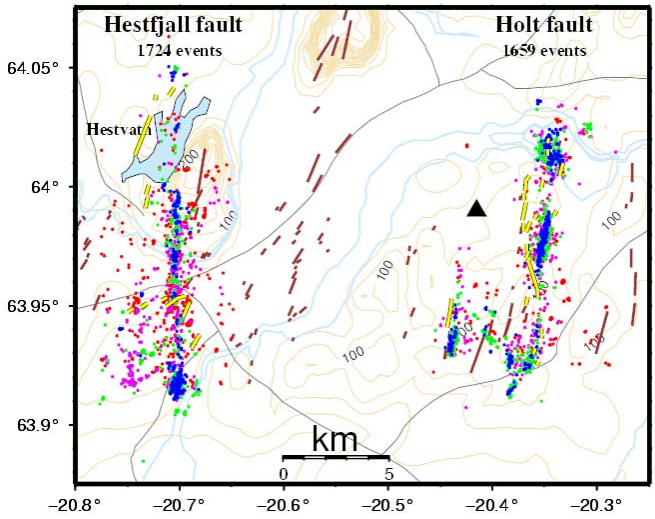

Figure 2. *Selected events, with relative errors in latitude and longitude ≤50 m; in depth ≤100 m. Older mapped faults are shown (brown) and fresh surface rupture mapped following the two large events are also superimposed (yellow).*

The Holt Fault

The total fault length of the Holt fault is approximately 11.5 km, with overall strike of 7° Fault width is 10 km with a small apparent dip to the west. The central patch is only 3 km long and 3 km wide, and has a more easterly strike of 14° and 85° dip to the west. Fault direction at the southern end also appears to have a more easterly direction than the overall trend of the fault. Event distribution at the bottom of the fault is more smeared out in the EW direction, and the lower half of the fault may possibly dip slightly to the east. The concentration of the aftershocks at the fault edges and the central patch is more clearly displayed on Figure 3, which shows a 3D view from southwest of the select event distribution from Figure 2.

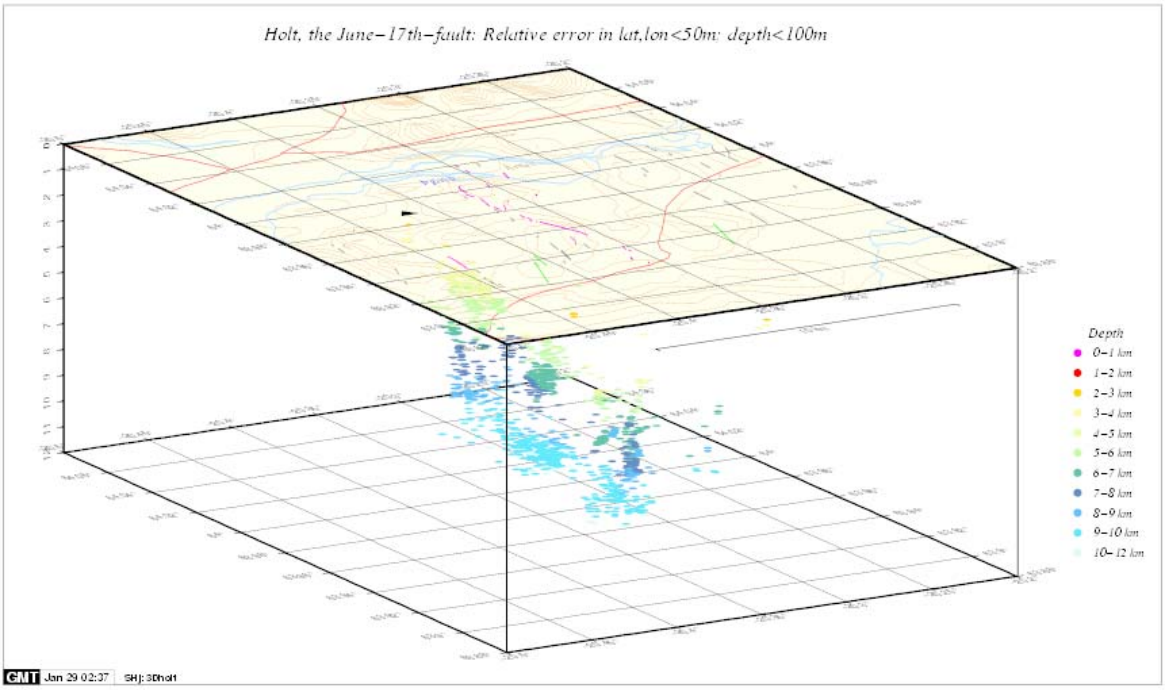

Figure 3. *3D view of the Holt-fault (J17) aftershocks viewed from the southwest. The events are the same as displayed on Figure 2. Event depths are color coded, with the color palette defined on the right. The activity on the central patch is separated from the seismicity along the edges. The fault-bottom activity at 10 km depth appears smeared out in the EW direction.*

The Hestfjall Fault

Total fault length of the Hestfjall fault (J21) is approximately 16.5 km, striking 359° and dipping 88° to the west. Fault width is variable, increasing from 6 km in the north, to 9 km in the south. The fault dip, as definded by the event distribution, does not show the same variation as that observed on the Holt fault, but is nearly constant throughout. At the southern end, the fault appears to bend rather sharply to the west, and a heavy concentration of aftershock activity is observed there. A large part of the activity is also clustered along the bottom of the fault. Figure 4 shows the event distribution on the fault from the second time period, both in map-view and vertical cross-section, viewed from the east. The Figure (and Figure 2 as well) show clear southwesterly off-shoot faults from the main fault. Some of these off-shoot faults appear to correlate with the strike direction of the observed surface faults. Widening of the fault by 3 km, from north to south is clearly displayed on the vertical cross section.

Socio-economic relevance and policy implication

Large earthquakes in the South Iceland Seismic Zone (SISZ), like J17 and J21 can be devastating for the inhabitants of the farms and small towns in Southern Iceland. Knowledge about the behaviour of faults and the character of faulting in the SISZ can lead to clearer regulations on building standards and building sites in S-Iceland. It may also lead to increased awareness in the communities of the reality of living on top of a major transform zone, and may thus help people prepare for and cope with the effects of destructive earthquakes.

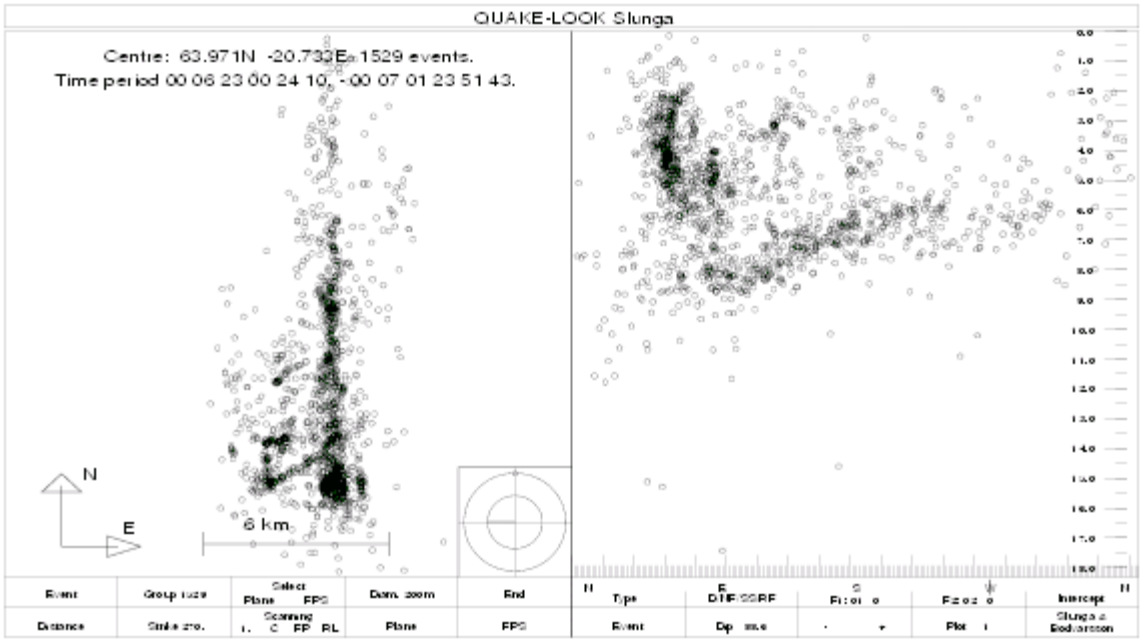

Figure 4. *Map-view (left) of the event distribution from the second time period on the Hestfjall fault. Vertical cross-section (right) viewed from the east shows increase in fault width from 6 km in the north to 9 km in the south, as well as a concentration of seismicity along the bottom and up along the southern edge.*

Discussion and conclusion

Initial relative relocation of aftershocks on the two main faults of June 2000 have been performed, revealing their overall sizes, strikes and dips. On the Holt fault the seismicity is confined to a central patch and to the edges of a near rectangular fault. Strikes on the southern and central patches appear more easterly than the overall strike of the fault. Activity on the bottom of the fault also appears smeared-out in the EW direction. On the Hestfjall fault, strike and dip are more constant along most of the fault, although strike suddenly becomes more easterly at the southern end. Like on the Holt fault, a heavier concentration of seismicity is observed along the bottom and up along the southern edge, but no central patch of activity is observed. The width of the fault is not constant, but increases from about 6 km in the north to 9 km in the south.

Plan and objectives for the next period

In the remaining months the fault mapping will be finalized, with a closer look taken at the finer details of subfaults. A joint interpretation with the focal mechanisms of individual events will also be performed to analyze the slip of the patches in space and time.

A point-source moment tensor inversion of teleseismic waveforms from the two events will be delayed.

References

Clifton, A.E. and P. Einarsson 2004. Styles of surface ruptures accompanying the June 17 and 21, 2000 earthquakes in the South Iceland Seismic Zone. Submitted to *Tectonophysics.*

WP 4.2 Analysis, inversion and estimation of strong ground motion from extended-earthquake fault models of the two June 2000 Iceland events

1 Objectives

1) Inversion of strong ground motion (accelerograms) data related to the two June 2000 events in Iceland using particular station distributions to retrieve the slip distribution on the fault. 2) Analysis of the reliability of the above inversions using particular station distributions and different physical constraints. 3) Estimation of the strong ground motion due to the June 2000 events in localities with no instrumental recording and assessment of their damage potential, in strong collaboration with Icelandic engineers.

2 Methodology and description of progress and scientific achievements

The task is to perform the research summarised in the objectives above, in particular:
To retrieve the slip distribution on the fault of the two June 2000 events based on the analysis and inversion of strong motion records in the South Iceland Seismic Zone (SISZ) that have recorded them.
Estimate on the basis of the retrieved fault model the strong ground motion in the surroundings of the two events, i.e. also at sites of interest that have no records.

Part of the topics under both a) and b) have been dealt with and are reported below. A vital item for the progress of this work is:

ESTIMATION OF THE ABSOLUTE TIMING OF STRONG MOTION RECORDS. Using the absolute time of the nucleation of each event and the a seismic structure model provided by Kristin Vogfjord from the Icelandic Meteorological Office, (IMO) we ray-traced the first arrival waves to each recording station. This allowed us to estimate the absolute arrival time of the P-wave at each station and, knowing the threshold level at each station, to estimate the absolute time of start of each record. This will permit the inversion of waveforms for the slip on the finite fault of each earthquake (work to be done in the second year). A more detailed report on this topic has been given in the six-month report.

A) RETRIEVAL OF SLIP DISTRIBUTION

We have collected the necessary input data, in particular:

structural models related to the region
aftershock catalogue of the two events
focal mechanisms of the main events

a) accelerometric waveforms related to the two events

This part of the work was conducted in close co-operation with both the Icelandic Metereological Office, Department of Geophysics, in Reykjavik (dr. K. Vogfjord, dr. R. Stefansson) and with the University of Iceland, Engineering Research Institute (prof. R. Sigbjorsson, dr. S. Olafsson). The strong motion data have been downloaded from the Internet based Strong Motion Database (ISESD), a product of a previous EC Project.

The computations of synthetic ground motion have been made using the modal summation method (Panza, 1985; Panza and Suhadolc, 1987; Florsch et al., 1991).

Forward modeling of strong motion waveforms due to the Iceland earthquakes of June 17 and June 21, 2002

From the stations that have recorded the two events we have first separated the ones located on bedrock from the ones that have evident site effects (e.g. Hver C, Selfoss H, Hella, Selsund). The first ones have been instrument corrected and Gausian filtered between 0.25 and 1 Hz.

Because the observed records did not have absolute timing (except for two stations) we have decided to make a forward modelling of the peak ground acceleration (at 1 Hz) due to the two events. In the meantime we have estimated the absolute timings (see Section C) so the inversion will be performed in the second year.

The main shock (nucleation) parameters have been retrieved from NEIC and Harvard determinations.

Point-source approximation modelling

In order to select the most appropriate structural model for the computations, we first computed the acceleration field of the June 17, 2000 event due to a scaled point source.
Three structural models have been taken into account: the one derived from the CRUST 2.0 database (Laske et al., 2003), the one derived from the EurID database (Du et al., 1998) and the one proposed by Vogfjord (personal communication), estimated on the basis of travel times of local events in the SISZ area. The first model (CRUST2.0) was too coarse, so it was discarded. The computations made with the other two models showed, that the Vogfjord model better reproduced the observed PGA of the June 17, 2000 event (misfit of 28% vs. 68%). For the June 21, 2000 event, the obtained misfit is 33%.
Therefore, all further computations were made using the Vogfjord structural model.

Finite-source approximation modeling

June 17, 2000 earthquake

On the basis of the observed aftershock distribution, empirical relations (Wells and Coppersmith, 1994) and previously proposed models (e.g. Stefánsson *et al.*, 2003), we have created four possible finite-fault models. Some of them rupture up to the free surface, for some of them the rupture ends 1 km below the free surface:

- Fault n° 1: 20×11 *km* fault dipping from the surface (inferred from Wells and Coppersmith, 1994)
- Fault n°2: 16×10.5 *km* fault dipping from the surface (inferred from aftershocks distribution)
- Fault n°3: 12×9 *km* fault dipping from 1 *km* depth (from Stefánsson *et al.*, 2003)
- Fault n°4: 12.6×10.5 *km* fault dipping from the surface (modified from the previous model)

For a uniform slip distribution on the fault, tapered to zero at its borders, fault number 3 gave the smallest misfit (69%).

Based on the aftershock distribution along the fault plane, we have also proposed a non-uniform slip distribution: a smooth-asperity model. The best results in terms of misfit have been obtained with the two-asperity model on the above fault: misfit 45%. This is higher than the one obtained from the scaled point source, however the synthetic seismograms generated by a finite-fault source resemble by far better the observed ones than those of the scaled point source.

June 21, 2000 earthquake

We have performed similar computations also for the second event.

The proposed finite-fault models are the following:

- Fault n° 1: 20×11 *km* fault dipping from the surface (from Wells and Coppersmith,1994)
- Fault n°2: 18×8 *km* fault dipping from the surface (da Stefánsson *et al.*, 2000)
- Fault n°3: 15×8 *km* fault dipping from 1 *km* depth (da Stefánsson *et al.*, 2003)
- Fault n°4: 18×10 *km* fault dipping from the surface (from aftershocks distribution)

In this case the scaled point-source approximation gave a very good misfit value of 33%.
On the other hand, a uniform tapered slip model worked best (misfit = 62%) for fault model number 1, but the results are worse than for the point-source case.
We have tried to model several non-uniform slip distributions.
A smooth two-asperity model worked best for fault model n.4 (misfit 111%), but with an even higher misfit. A smaller-base one-asperity model proved to be better, but the misfit remains still high (69%) with respect to both the uniform tapered slip model and to the simple scaled point-source model.
Also in this case the synthetic seismograms generated by a finite-fault source resemble by far better the observed ones than those of the scaled point source.
As a conclusion we can say that in order to further reduce the misfit on the PGA and obtain a close match also on the waveforms, we have to retrieve a slip distribution model by inverting the strong motion records.

B) STRONG GROUND MOTION PREDICTION

The characterization of the seismic source is of utmost importance in the strong motion prediction for seismic hazard assessment. In order to understand the physical process of the source and to describe realistic scenarios for earthquake prone areas, ground shaking scenarios are estimated.
The ground motion parameters, computed with a forward modeling, are the maximum horizontal displacements, velocities and accelerations, and they are used to assess the seismic hazard for a set of localities in the area. The computations are performed using a finite source model, applying a constant rupture propagation velocity model and varying the hypocenter position along the fault surface. In the realistic strong ground motion scenarios, the synthetic seismograms are computed using a kinematic approach for the representation of the finite source. The fracture process is described purely by the slip vector, as a function of the coordinates on the fault plane, and of the time.
On the basis of the best retrieved source model of the June 17, 2000 event, we have computed the acceleration field in all the SISZ and surrounding areas of southwestern Iceland. In this way a good estimate of the local shaking in all possible sites of interest has been obtained.
All the scenarios are computed in the hypothesis of a site lying on bedrock, and therefore possible wave amplifications due to site effects are not taken into account**.** However, the effects of local site conditions can be included by convolving the "bedrock" time series with the amplification curves at certain sites, if available.
Once the method is calibrated against observed strong motion records it is possible to predict the strong ground shaking due to possible future events in the area.

Acknowledgments

All the work described above has been published in the framework of a PhD thesis at the University of Trieste (Minigutti, F., 2003) and presented at the First-year project meeting in Reykjavik in January 2004. Thanks are due also to Angela Sarao' for her help with the modeling.
A close interaction with K. Vogfjord, and R. Stefansson from the Icelandic Metereological Office and with R. Sigbjornsson and S. Olafsson from the University of Iceland, Engineering Research Institute provided the necessary input data for this work.

References:
Du, Z.J., A. Michelini & G.F. Panza 1998. EurID: a regionalized 3-D seismological model of Europe. *Physics of the Earth and Planetary Interiors*, 105, 31–62.

Florsch, N., D. Fäh, P. Suhadolc & G.F. Panza 1991. Complete synthetic seismograms for high-frequency multimode SH-waves. *Pageoph*, 136, 529-560.

Laske, G., A. Dziewonski & G. Masters 2003 (Nov). The Reference Earth Model website. On Internet at: http://mahi.ucsd.edu/Gabi/rem.html.

Minigutti, F. 2003. Modellazione di forme d'onda accelerometriche dei due forti terremoti islandesi del giugno 2000. PhD thesis in Physics at the University of Trieste.

Panza, G.F. 1985. Synthetic seismograms: the Rayleigh waves modal summation. *J. Geophys*., 58, 125-145.

Panza, G.F. & P. Suhadolc 1987. Complete strong motion synthetics. In: Computational techniques, Vol. 4, Seismic strong motion synthetics, ed. by: B.A. Bolt, 153-204, Academic Press.

Stefánsson, R., G.B. Gudmundsson & P. Halldórsson 2000. The two large earthquakes in the South Iceland seismic zone on June 17 and June 21, 2000. *Vedurstofa Íslands – Report* VÍ-G00010-JA04, 8 pp.

Stefánsson, R., G.B. Gudmundsson & P. Halldorsson 2003. The South Iceland earthquakes 2000 - a challenge for earthquake prediction research. *Vedurstofa Islands - Report* 03017, 21 pp.

Suhadolc, P. 2003. EU Project PREPARED, Six Month Short Report, 11 pp.
http://hraun.vedur.is/ja/prepared/reports/suhadolc_pren_aug03.pdf
Wells, D.L. and K.J. Coppersmith 1994. New Empirical Relationships among Magnitude, Rupture Length, Rupture Width, Rupture Area, and Surface Displacement. *Bull. Seism. Soc. Am.* 84, 974-1002.

3 Socio-economic relevance

The social and economic impact of a destructive earthquake is enormous.
Knowledge of the expected characteristics of such an event implies various technical and social precautions and preparedness that can mitigate the impact of earthquake hazards in various ways. This work is economically and socially important for Iceland, and the European co-operation in carrying out the project will transfer the methods applied to other earthquake-prone areas of Europe.

4 Discussion and conclusions

The work in this package is progressing as planned, even if the lack of absolute timing of the majority of the records has delayed the inversion part, and it can be expected to fully comply with the objectives at the end of the project period.

5 Main objectives for the next period

The available data related to possible potential seismogenic sources, along with additional geomorphologic data and field observations, can be used for the computation of several realistic strong ground motion scenarios. We plan to perform some examples of such computations at the end of the second year of the Project, if the necessary data will be available.

WP 4.3 Surface fractures in the source region of the June 2000 events

In wp 4.3 we use differential GPS instruments to map in detail the remaining fractures of 2000 as well as all older fractures in the surrounding areas.
This work package consisted mainly of fieldwork in the source areas of the South Iceland Seismic Zone. Emphasis was put on three areas: The Flói district east of the town Selfoss, the Holt area in the centre of the zone, and the Land-Rangárvellir district near the eastern end of the zone. A field assistant, Bergur Einarsson, was hired for the summer months of 2003 to assist PE in the field. A summer student from the University of Lille, Jéremy Blieck, also participated in the fieldwork. Student groups from the University of Iceland contributed significantly to the mapping effort on field trips in October 2002 and October 2003. Teaching assistants were Dr. Maryam Khodayar and Steingrímur Þorbjarnarson. The work was mainly mapping previously known fractures, tracing them in the field with the GPS-mapping tools. With the experience and confidence gained during the 2000 earthquakes it was possible to identify considerably more fault structures than before. The fracture systems thus turned out to be more continuous than previously thought. Several fault segments were found that had not been identified before. These include segments belonging to the Austurkot fault in Flói, the Eastern Leirubakki fault in Land, and conjugate segments active in the 1912 earthquake in Rangárvellir. Surface faulting during one of the triggered earthquakes on June 17, 2000, was also found in the Holt district. The high rate of new discoveries suggests that further fieldwork may still be productive.

Work delivered so far:

1. All major, known surface fault segments of the South Iceland Seismic Zone have been field checked and mapped by differential GPS instruments.
2. Surface faulting of the 2000 earthquakes was more extensive than previously thought. Additional faults have been mapped and a paper submitted to Tectonophysics (Clifton and Einarsson, submitted 2004).
3. The general map base of the Icelandic Geodetic Survey has been incorporated into the mapping software. Detailed maps of faults can now be produced on that base for any sub-area.
4. A simplified map of all known surface faults of the SISZ has been prepared for general use. This map is already in use on the earthquakes information website of the Iceland Meteorological Office (vedur.is) as a background to the real-time earthquakes locations of the South Iceland Seismic Zone. The map is also to be seen on a public information sign of the Icelandic Road Department at the epicentre of the June 21 earthquake of 2000 (see Fig. 1).
5. Results of work under this work package were presented at a NorFa-NSF sponsored Summer School of the Nordic Volcanological Institute (Einarsson, 2003), the Spring Meeting of the Icelandic Geoscience Society 2003 (Einarsson et al., 2003), and the PREPARED Mid-term Meeting in Reykjavík 2004 (Einarsson, 2004)

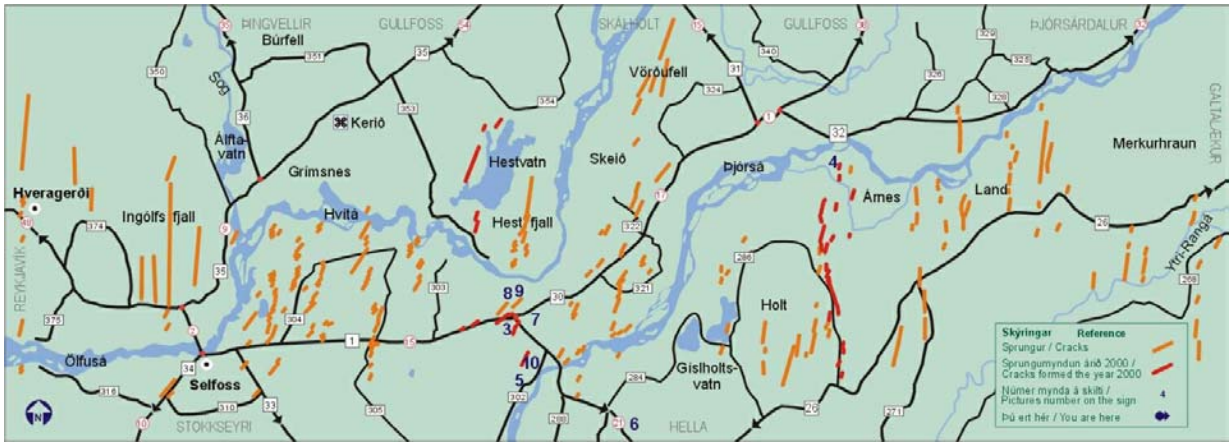

Figure 1. The main fracture systems of the South Iceland Seismic Zone. Fractures that are either known or suspected to be of Holocene age are orange. Red lines show fractures active in the 2000 earthquakes

Socio-economic relevance and policy implication

The earthquakes of June 2000 had many socio-economic implications. One of them was that structures in a seismically active region can be built to withstand earthquakes as long as reasonable building practices are used and the structures are not built directly across faults. A reliable fault map, one of our deliverables, is clearly of high importance here. An effort has been made to provide easy access to the fault data so that a fault map can be produced on the conventional map base for any area of the seismic zone. Recent examples show, however, that the construction community is still not ready to make use of this new knowledge. It should be one of the priority issues to publicise the new fault map and educate the construction sector about its use. It should also be mentioned that the National Energy Company (Landsvirkjun), who is planning two hydropower projects within the seismic zone, is making every effort to circumvent fractured bedrock as foundation for their structures.

Discussion and conclusions

The mapping effort under this work package has filled in the previously known picture of the South Iceland Seismic Zone. A more complete picture has been gained of the previously known faults and new fault segments have been discovered. With the new fault map in hand it is interesting to compare it to the distribution of hypocenters in the zone. This comparison has led to new insights into the connection between faults at depth and surface fractures.

Plan and objectives for the next period

Although significant progress has been made in the reconnaissance of the seismic zone, many aspects are still unclear and need attention.

1. *Mapping.* We recognise that not all faults have been found so far in spite of considerable effort. We therefore plan further fieldwork in the summer of 2004 in order to trace faults into difficult terrain. This is particularly in the Holt area, which is covered by glacial moraine material, and the Land district, where faults disappear to the north into a sandy lava flow. We have reason to believe that further fault segments can be found in these areas.

2. *Faults at depth.* We will work with other researchers of the PREPARED-project to correlate faults on the surface with faults at depth as shown by hypocenters.
3. *Reconstruction of historic earthquakes.* Assuming that the present background activity is a combination of late aftershocks of previous earthquakes and events due to stress accumulation in the interseismic period, one can make inferences about the source faults of the latest historic earthquakes. We have started work on the 1912 earthquake along these lines and plan to continue with the 1896 and 1784 sequences.

References:

Bjarnason, I. Þ., P. Cowie, M. H. Anders, L. Seeber and C. H. Scholz. The 1912 Iceland earthquake rupture: Growth and development of a nascent transform system. Bull. Seism. Soc. Am., 83, 416 - 435, 1993.

Clifton, A., and Páll Einarsson. Styles of surface rupture accompanying the June 17 and 21, 2000 earthquakes in the South Iceland Seismic Zone. Fall Meeting 2000. Abstracts of papers and posters. Icelandic Geoscience Society, p.1.

Clifton, A., and Páll Einarsson. Surface ruptures accompanying the June 17 and 21, 2000 earthquakes in the South Iceland Seismic Zone. Submitted to Tectonophysics 2004.

Einarsson, P. Fabric and systematics of the Icelandic rift zones. Lecture at the Summer School on Tectonic-Magmatic Interaction, Geysir, Iceland, Sept. 1-8, 2003, Nordic Volcanological Institute, 2003.

Einarsson, P. Surface fractures in the source region of the 2000 earthquakes. Lecture at PREPARED Midterm Meeting, Reykjavík, Jan. 30. 2004.

Einarsson, P., and Jón Eiríksson. Earthquake fractures in the districts Land and Rangárvellir in the South Iceland Seismic Zone. Jökull, 32, 113-120, 1982.

Einarsson, P., S. Björnsson, G. Foulger, R. Stefánsson and Þ. Skaftadóttir. Seismicity pattern in the South Iceland seismic zone. Í: Earthquake Prediction - An International Review (ritstj. D. Simpson and P. Richards). American Geophys. Union, Maurice Ewing Series 4, 141-151, 1981.

Einarsson, P., M. Khodayar, S. Þorbjarnarson, C. Pagli, R. Pedersen, and student groups of the courses Tektóník (09.60.52) and Current Crustal Movements (09.24.81), 2002. New fault maps of the Hestfjall and Leirubakki areas of the South Iceland Seismic Zone. Icelandic Geoscience Soc. Spring Meeting 2003. Abstracts of papers and posters, p. 54.

Jónsdóttir, K., Páll Einarsson and Vala Hjörleifsdóttir. Fractures active in the 1630, and 1784 earthquakes in South Iceland. Spring Meeting 1999. Abstracts of papers and posters. Icelandic Geoscience Society, p. 42.

Pedersen, R., Amy Clifton, Páll Einarsson, Freysteinn Sigmundsson, and Guðmundur H. Guðfinnsson. Styles of surface rupture accompanying the June 17 and 21, 2000 earthquakes in the South Iceland Seismic Zone. American Geophysical Union, Fall Meeting, San Francisco, Eos 81, p. 1171, 2000

.

Section 3: Detailed report on workpackages (months 1-12)

WP 4.4 Deformation model for the June 2000 earthquakes from joint interpretation of GPS, InSAR and borehole strain data

a) Objectives

The objectives of the work package are to evaluate the 3D co-seismic deformation associated with the June 2000 earthquakes and derive a deformation model for the earthquakes based on joint interpretation of all the available geodetic data.

b) Methodology and scientific achievements related to workpackages

We have completed the analysis of InSAR and GPS data to derive the co-seismic displacement field for the June 17 and June 21, 2000, earthquakes. The data have been analysed and modelled separately (Árnadóttir et al., 2001; Pedersen et al., 2001) and a joint inversion of the InSAR and GPS data for fault geometry and slip distribution has been completed (Pedersen et al., 2003), assuming rectangular dislocations in an elastic half-space. In the inversion procedure the InSAR data is first unwrapped, and then the number of InSAR data is reduced by quadtree partitioning algorithm to speed up model computations. Figure 1 shows the dataset used in the joint inversion and Table 1 gives the model parameters obtained.

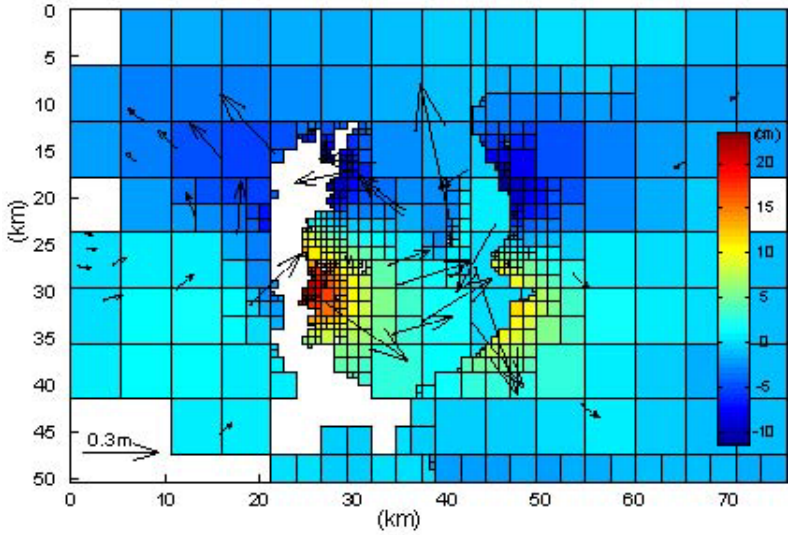

Figure 1. Quadtree partitioned InSAR data from Track 52 and Track 95 covering the June 2000 earthquakes. Co-seismic GPS displacements are shown with black arrows.

First we use a non-linear inversion algorithm to estimate the fault geometries and locations, for the June 17 and 21 dislocation models, assuming uniform slip on two rectangular faults. Then we fix the geometry and location and allow the slip to vary over the dislocation surface, assuming only right-lateral strike slip motion. Figure 2 shows the slip distribution obtained from the inversion (Pedersen et al., 2003). The preferred model indicates two simple 15 km long, near vertical faults extending from the surface to approximately 10 km depth. The model locations and geometries are in good agreement with preliminary aftershock locations. The fault model shown in Figure 2 has been used to calculate the static Coulomb stress change due to the June 17 and June 21, 2000, earthquakes in South Iceland (Árnadóttir et al., 2003). We find that the June 17 earthquake increased the static Coulomb stress by about 1 bar in the area of the June 21 hypocenter, promoting failure on the second fault. Figure 3 shows the predicted displacements for the GPS and InSAR data (A and B) and the residuals (C and D).

Table 1: Fault parameters for the June 2000 events estimated from different datasets. Latitude and Longitude is for the center of the fault plane at the upper edge. From Pedersen et al. (2003).

June 17	Length (km)	Width (km)	Depth (km)	Dip (°E)	Strike (N°E)	Lon (°)	Lat (°)	Strike slip (m)	Dip slip (m)	Rake (°)	M_0 (Nm)×10^{18}	M_w
Uniform slip	10.6	7.9	0.0*	87*	1	-20.347	63.973	1.7	0	180	4.4	6.4
Distributed slip	~15	~10	0.0	87*	2*	-20.347	63.973	0.0-2.6	0*	180	4.5	6.4
Árnadóttir et al. [17]	9.5	9.8	0.1	90*	3	-20.351	63.970	2.0	0.2	174	5.6	6.5
Pedersen et al. [18]	16.0	10.0*	0.0*	86*	5*	-20.342	63.979	0.3-2.4	0.0-0.2	175	5.4	6.5
NEIC [9]	-	-	-	75	-1	-20.487	63.966	-	-	173	4.3	6.4
Harvard CMT [33]	-	-	-	87	4	-20.47	63.99	-	-	-164	7.1	6.5
June 21	**Length (km)**	**Width (km)**	**Depth (km)**	**Dip (°E)**	**Strike (N°E)**	**Lon (°)**	**Lat (°)**	**Strike slip (m)**	**Dip slip (m)**	**Rake (°)**	**M_0 (Nm)×10^{18}**	**M_w**
Uniform slip	11.9	8.2	0.0*	90*	0	-20.705	63.987	1.8	0	180	5.3	6.4
Distributed slip	~15	~10	0.0	90*	0*	-20.705	63.987	0.0-2.9	0*	180	5.0	6.5
Árnadóttir et al. [17]	12.3	8.0	0.0*	90*	0.5	-20.691	63.984	1.5	0	180	4.5	6.4
Pedersen et al. [18]	15.0	9.0*	0.0*	90*	0*	-20.703	63.982	0.5-2.2	0	180	5.1	6.4
NEIC [9]	-	-	-	79	-4	-20.758	63.980	-	-	-173	5.0	6.4
Harvard CMT [33]	-	-	-	85	2	-20.85	63.98	-	-	-167	5.4	6.5

* parameter held fixed in the modeling

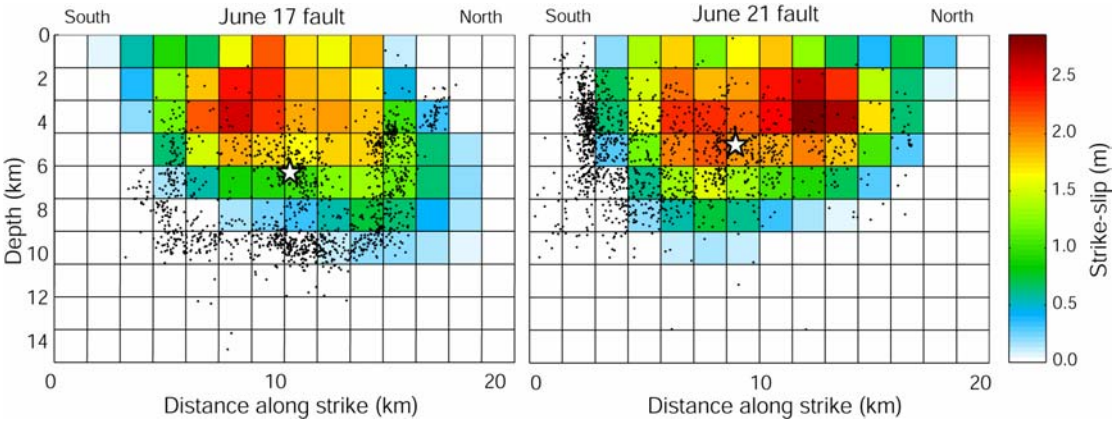

Figure 2. Right-lateral strike slip distribution estimated for the June 17 and June 21 earthquakes. Hypocenters are shown with white stars, and aftershocks in the immediate vicinity of the modelled faults as black dots.

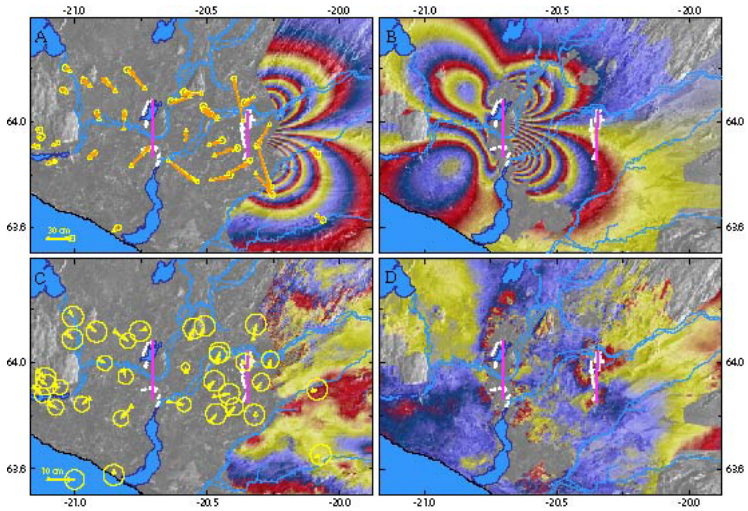

Figure 3. Model predictions for the Track 52 and Track 95 interferograms (A, B) calculated from the distributed slip models (Figure 2). One color cycle or fringe corresponds to 2.83 cm of range change. Observed (yellow) and predicted (orange) GPS displacements are shown in A. (C,D) Residual interferograms, with residual GPS vectors in C. Note the different scales for GPS displacements in A and C. Surface ruptures are shown with white lines. The upper edges of the uniform slip model are shown with pink lines.

An important new discovery was made when interpreting the residual signal seen around the June 17 rupture in Figure 3D. The signal can be explained by poro-elastic rebound due to ground water flow in the 2 months following the June 2000 main shocks (Jónsson et al., 2003).

The non-linear inversion algorithm has also been implemented in a paper by Pagli et al. (2003) using InSAR data to constrain models of triggered fault slip on the Reykjanes Peninsula in 2003 (Clifton et al., 2003).

We have participated with P1 and P6 in studies of the volcanoes Katla and Eyjafjallajökull (Sturkell et al., 2003), to examine links between volcano deformation and tectonic activity in the SISZ. Revised analysis and interpretation of these data show that the SISZ earthquakes were precieded by unrest at these volcanoes (Sigmundsson, 2004). Similarily, unrest at Hengill volcano, at the western edge of the SISZ, occurred in the decade before the June 2000 earthquakes.

c) Socio-economic relevance and policy implication.

The deliverables of this workpackage are the first detailed estimates of co-seismic slip distribution on faults in the South Iceland seismic zone. They provide important information that can be used in estimation of seismic hazard in the area. The algorithm we have developed can be adapted for use for similar scenarios of events, in other hazardous areas in Europe.

d) *Discussion and conclusions*

We have modeled the co-seismic surface displacements due to the June 17 and June 21, 2000, main shocks. We have used the fault models to calculate static Coulomb failure stress changes, as well as poro-elastic rebound due to post-seismic ground water pressure changes. The models obtained from geodetic data can be compared with similar models obtained in other workpackages (e.g. WP4.2), and are already implemented in the dynamic stress calculations in WP6.2.

e) *Plan and objective for the next period*

We are collaborating with P10 (Kurt Feigl) to refine the model of the June 2000 SISZ earthquakes, using finite element modelling techniques. We are also collaborating with P10 in re-processing the GPS data using the GAMIT/GLOBK software to estimate pre- co- and post-seismic deformation in the SISZ. We have also formed an improved interferogram capturing the co-seismic range changes due to the June 17, 2000, main shock, with better coherence in the area west of the rupture. These new data can be used to refine the deformation models of the June 17 and June 21 earthquakes. We plan to use the relative relocations of the aftershocks (results from WP5.1) to refine the fault geometries. We will also examine relationships between areas of surface rupture (WP5.2), refined aftershock locations and high fault slip. We plan to continue our studies of links between volcano unrest and tectonic activity in the SISZ.

References:

Árnadóttir,Th., Hreinsdóttir,S., Gudmunsson, G., Einarsson, P., Heinert, M., and C. Völksen, Crustal deformation measured by GPS in the South Iceland Seismic Zone due to two large earthquakes in June 2000, *Geophys. Res. Lett., 28*, 4031-4033, 2001.

Árnadóttir,Th., S. Jónsson, R. Pedersen and G. Gudmundsson, Coulomb stress changes in the South Iceland Seismic Zone due to two large earthquakes in June 2000, *Geophys. Res. Lett.*, vol. 30, doi:10.1029/2002GL016495, no. 5, 2003.

Clifton, A.E., C. Pagli, J.F. Jónsdóttir, K. Eythórsdóttir, and K. Vogfjörd, Surface effects of triggered fault slip on Reykjanes Peninsula, SW Iceland, *Tectonophysics 369*, 145-154, 2003.

Jónsson, S., P. Segall, R. Pedersen, and G. Björnsson, Postseismic poroelastic deformation in S Iceland observed with radar interferometry: Implications for aftershock decay, *Nature, 424*, 179-183, 2003.

Pagli et al., Triggered fault slip on June 17, 2000 on the Reykjanes Peninsula, SW Iceland captured by radar interferometry, *Geophys. Res. Lett., 30(6),* 1273, doi:10.1029/2002GL015310, 2003.

Pedersen, R., S. Jónsson, Th. Árnadóttir, F. Sigmundsson, and K.L. Feigl, Fault slip distribution of two Mw=6.5 earthquakes in South Iceland estimated from joint inversion of InSAR and GPS measurements, *Earth and Planetary Science Letters, 213*, 487-502, 2003.

Pedersen, R., F. Sigmundsson, K. Feigl, and T. Árnadóttir, Coseismic interferograms of two Ms=6.6 earthquakes in the SISZ, June 2000, *GRL*, 28, 3341-3344, 2001.

Sigmundsson, F., Widespread increase in magma pressure precedes major failure along the plate boundary in Iceland, Abstract volume for the 26th Nordic Geological Winter Meeting, GFF, vol. 126, part 1, page 51-51, 2004

Sturkell, E., F. Sigmundsson, and P. Einarsson, 1994 and 1999 unrest and magma movements at Eyjafjallajökull and Katla volcanoes, Iceland, J. Geophys. Res., 108, 2369, doi: 10.129/2001JB000917, 2003.

WP 5 New hazard assessment/New methods for improving assessment of probable earthquake effects

Objectives

On basis of the unique observations made in relation to the June 2000 earthquakes in the SISZ as well as on basis of results of modelling the earthquake sources in time and space we aim towards a more detailed hazard assessment both as concerns the location and severity of probable earthquake hazard. This improvement is very significant basis for a general risk assessment.

Methodology and scientific achievements related to workpackages including contribution from partners

Probable faults of future large earthquakes will be mapped in detail. Following the June 2000 earthquakes an area of 100 km length along the SISZ and the Reykjanes peninsula, and to some extent towards north, was activated by triggered activity of small earthquakes, reflecting faults movements on numerous faults, which either were not known before or not accurately known. Data and methodology is now available for accurate mapping of these faults at depth by microearthquakes information, to be compared with geological mapping of faults on the surface.

Digital strong motion records near the origin complemented with information on surface effects mapped by geologists and intensities on basis of questionnaires will improve the basis for detailed expected hazard mapping.

Drastic changes in ground water and geothermal water systems in the area were observed, especially following the June 2000 earthquakes. These will be analyzed and compared to the detailed models of the earthquakes to understand better the relation between such earthquakes and hydrological changes.

New intepretation of historical information: A significant part of the workpackage is to compare the detailed information which we have about the June 2000 earthquakes with historical informaton and thus to try to confirm or modify earlier interpretations of the historical activity.

WP5 will operate like a forum consisting of representatives from WP5.1-5.6 and WP4.2 for integrating the results from the multidisciplinary work. Most of the workpackages of the project will produce results which can be applied here, not least the modelling packages WP6.1 and WP6.2.

Up to the end of the first year the work in WP 5 has been limited to discussion with the participants in this workpackage and other partners that will render results which are significant for the WP5 objectives, mainly in WP5.1-5.6, WP4.2 and WP6.1, as well as start the integration work of these packages. Work is going according to schedule in these WPs, and it is expected that work in merging together the results in WP5 can start early in 2004. Significant progress has been made in mapping of surface faults in SW Iceland, especially faults of historical earthquakes. Surface faults and other surface effects of the 2000 earthquakes have been mapped in detail. These faults will be compared with mapping of faults with seismic methods at depth.

Socio-economic relevance and policy implication

Information of what ground motions can be expected at various places in populated areas is socially and economically significant.. Where will the faults rupture the surface and when is of huge significance in any earthquake-prone country.

Social and economic impacts of a destructive earthquake or the knowledge that a destructive earthquake is to be expected is enormous and can be of such an effect to break up communities.

Knowledge of what can be expected leads to direct precautions in where and how man made structures are built, or leads to strengthening or removal of existing vulnerable buildings. It implies various technical and social precautions and preparedness that can mitigate the impact of earthquake hazards in various ways, on people and on society. To realize such precautions a spacially more detailed and time dependent hazard assessment is significant.

Discussion and conclusion

The multidisciplinary fault mapping together with progress in modelling the earthquake processes in the SISZ will help to make a more detailed and secure hazard assessment for the whole region. A special application will be a real-time hazard assessment, for nowcasting and short-term warnings, when the probable location is detected of a probably impending earthquake.

Plan and objectives for the next period

The objective of WP5 for the next period is to encourage the fulfillness of the objectives of the individual workpackages as well as to merge together the results in a common new detailed hazard map and a WP5 report near the end of the period.

WP 5.1 Mapping subsurface faults in southwestern Iceland with the microearthquakes induced by the June 17th and June 21st earthquakes

Objectives

To map sub-surface fault planes and slip directions on faults in south-west Iceland that were illuminated by the microseismicity induced by the June 17th (J17) and June 21st (J21) earthquakes. This includes faults within and around the South Iceland seismic zone (SISZ), as well as within the rift zone on Reykjanes peninsula. Thousands of smaller earthquakes followed J17 and J21, induced either by seismic waves propagating from the two, or by the slower propagating change in stress field, resulting from the large (roughly 1m) slips on their several kilometer long faults. The resulting map is a significant input to the detailed hazard map, which will be prepared in the project, as closeness to active faults is critical for the ground motion of shallow earthquakes in South Iceland. The map is also a necessary input for models of stress field changes in time and space.

Methodology and scientific achievements related to workpackages including contributions from partners

About sixteen thousand microearthquakes recorded by the SIL seismic network between June and December 2000 have already been interactively analyzed. Approximately half of them occured outside the two main faults. In this workpackage a multi-event relative relocation method is applied to this dataset in order to increase the location accuracy to such a degree that individual fault patterns become resolvable.

The method uses cross-correlation of similar wave forms at each station to determine relative travel times of waves from events to station with increased accuracy. The matrix of differences between these relative travel times and theoretical travel times is inverted to minimize the time residuals. Joint interpretation of the event distributions with focal mechanisms allows the determination of slip directions on individual faults. It is possible to analyze up to 1800 hundred events at a time.

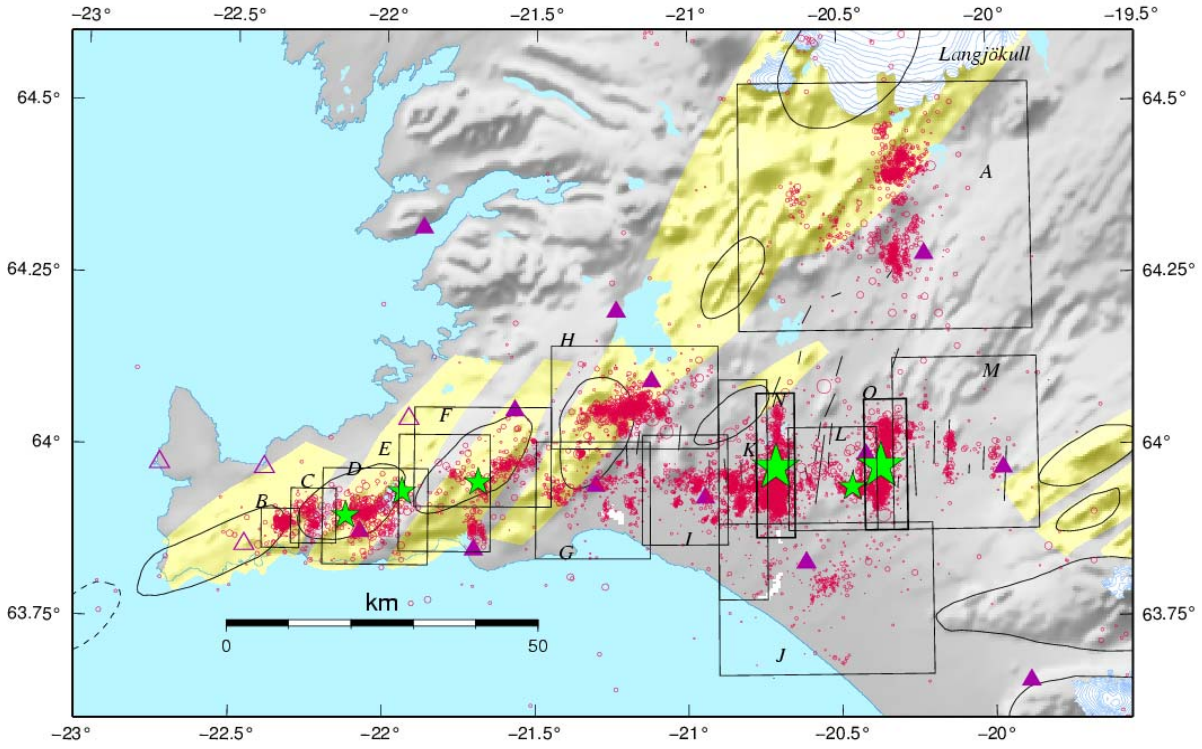

Figure 1. *Overview of the study area. Seismicity (red circles) in Januar-December 2000. Green stars show largest events. The triangles show SIL-stations. Yellow areas are volcanic systems (From Einarsson and Sæmundsson, 1987).*

The study area includes the SISZ, the Reykjanes Peninsula and an area around the Geysir-geothermal system on the eastern edge of the Western Volcanic Zone. The area has been divided into fifteen boxes, each containing a sufficient number of events. Figure 1 shows south-west Iceland and the division of the area. Two of the boxes include the J17 and J21 faults, which are a part of WP 4.1 and not discussed here. Since the relocation software has been under constant developement and the latest version not extensively tested before, it was decided to run some tests in area A-Geysir to see its reliability and to get an estimate of how accurate the results can be, as well as to examine the quality of the data.

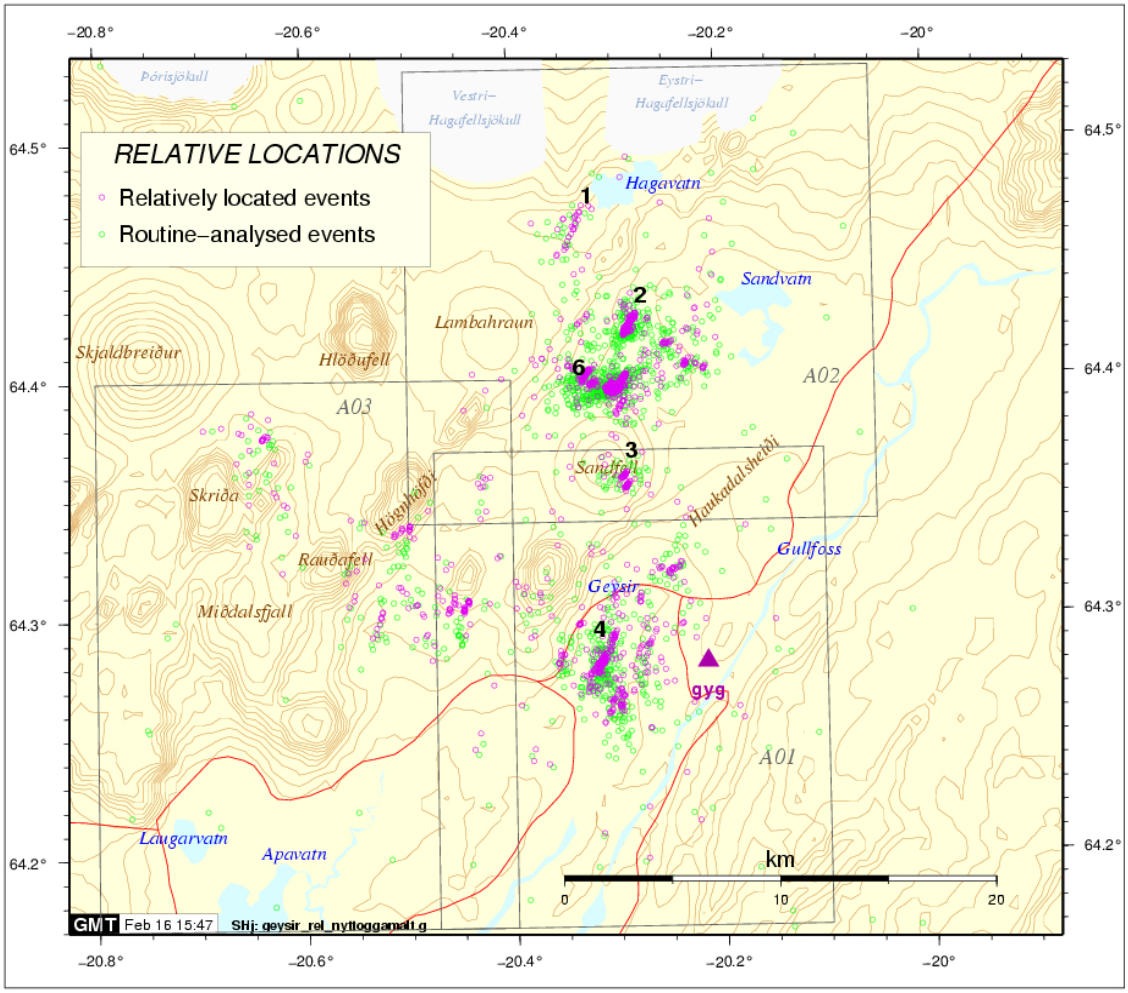

Figure 2. Area A, the Geysir area. Several faults can be seen clearly after the relocaion.

In the Geysir area (A) around 1300 events larger than zero occured during the time period. The green circles in figure 2 show the seismicity before relocation. Based on the seismic clustering the area was divided into three subareas, two main clusters south of and north of Geysir (A01 and A02) and a less active area on the western side (A03). The tests were run on subareas A01 and A02. Before the inversion the events are ordered into groups of predefined minimum and maximum number. The division of events into groups is also dependent on a predefined spatial extent of the groups and the allowed distance between the group centres. We first tried running with area radius 3km and distance 3km. Then it was decided to decrease the group dimension down to 2.8km radius and allow more overlap (distance 2.2km). Most faults did not alter their shape between the two runs, although some groups as a whole moved. Using the latter values for the spatial parameters, different group sizes were tested. The minimum number allowed was held constant at 6 but maximum number varied between 48, 44 and 40. To estimate the difference between two runs, the relative errors in latitude, longitude and depth were calculated according to:

$$err_{lat} = lat_r(grz1) - lat_i(grz1) - [lat_r(grz2) - lat_i(grz2)] \quad \text{for i=1,...,n and r}\in[1,...,n],$$

where *grz1* and *grz2* are maximum group sizes in two different runs.The relative error measures the change in distance between the reference event and all other events in the data set. Figure 3 shows the relative error in latitude between group sizes of 48 and 40 in area A02, using the first event in this data set for reference (r=1, *grz1*=48, *grz2*=40). From a total of 799 events, around 79% had an error value in latitude within 100m. Relative errors in longitude

and depth were very similar and of similar size. Most of the events with large relative error occur early in the time period. In most cases, the wave forms of these events were disturbed by interference with close events and thus were poorly correlated. The southern area, A01, was mainly active early in the time period, in June and early July, and the results turned out to be more unstable, with more outliers and not as many clear structures. More tests included running on best events only, and weighting down absolute times. The best events seemed to remain stable, except for a few which had earlier correlated with events now removed from the data set. Changing the weights had little effect on the results.

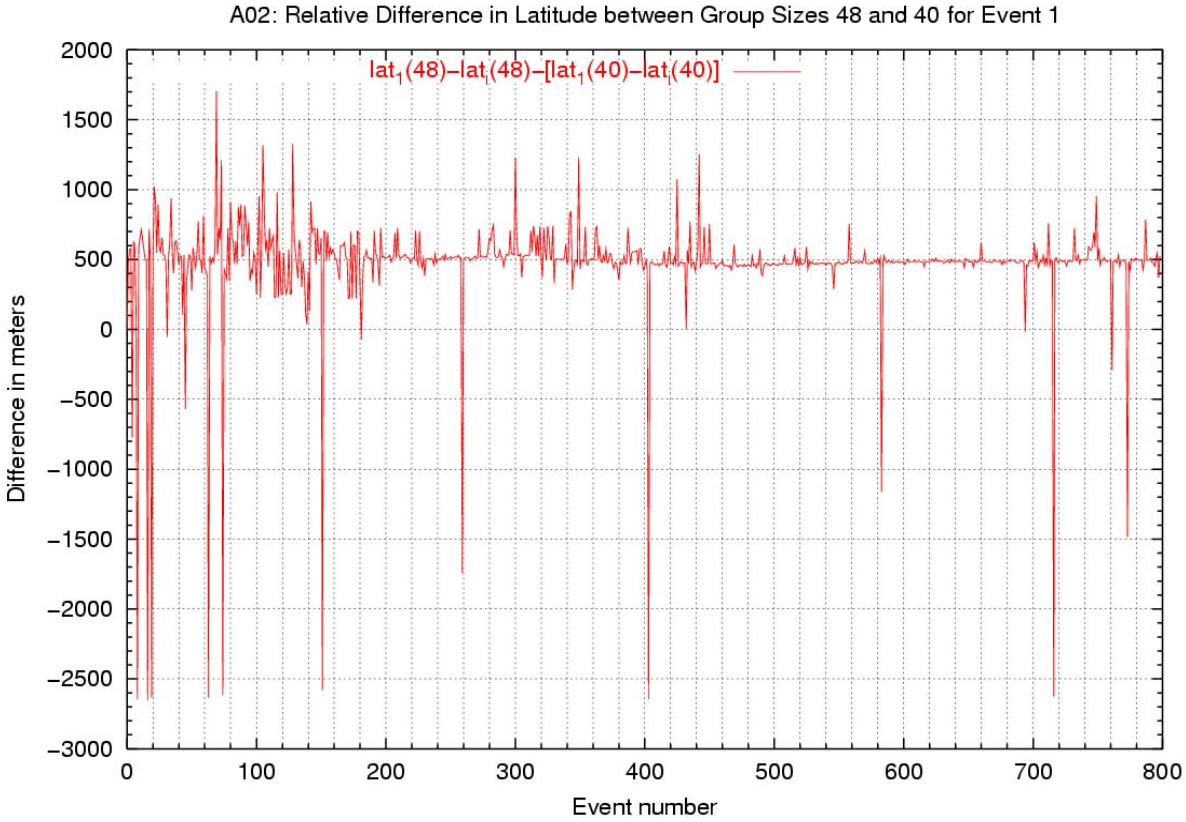

Figure 3. *Relative error between group sizes 40 and 48 for event no. 1 in the data set.*

The purple circles in figure 2 show the improvement after relative relocation. We clearly see how the earthquakes form linear clusters (faults), most of them striking SW-NE. A closer view of the one labelled 2 is shown in figure 4.
In the upper figure we see on the left the fault in map view and on the right a vertical view along strike. The angle of view is shown on the small circle in the lower right corner of the map view. We are looking approximately in the SW-direction, as indicated by the thin black line on the circle. Each disk represents an event and is scaled according to its fault radius. The best fitting plane through the 123 events is shown by a thin black line, striking N28°A and dipping 85° to the south-east. In map view the line shows where the best fitting plane intersects the surface. In the lower figure again we have map view on the left and vertical cross section perpendicular to the fault plane on the right. The tick marks on the disks indicate the direction of slip, according to the best fault plane solution chosen with respect to the best fitting fault plane. Most of the ticks indicate a slip direction to the NE, i.e. the western side is moving to the left, hence we have a fault with a dominant right lateral movement.

A few faults have also been mapped in the Hengill-area (box H), but there we seem to have a more complicated fault pattern, due to a more complicated stress field, as the area lies on a triple junction connecting the rift zone on Reykjanes Peninsula, the SISZ and the Western

Volcanic Zone. In box B, on Reykjanes Peninsula, a pattern of intersecting NS and NE-SW striking faults is observed.

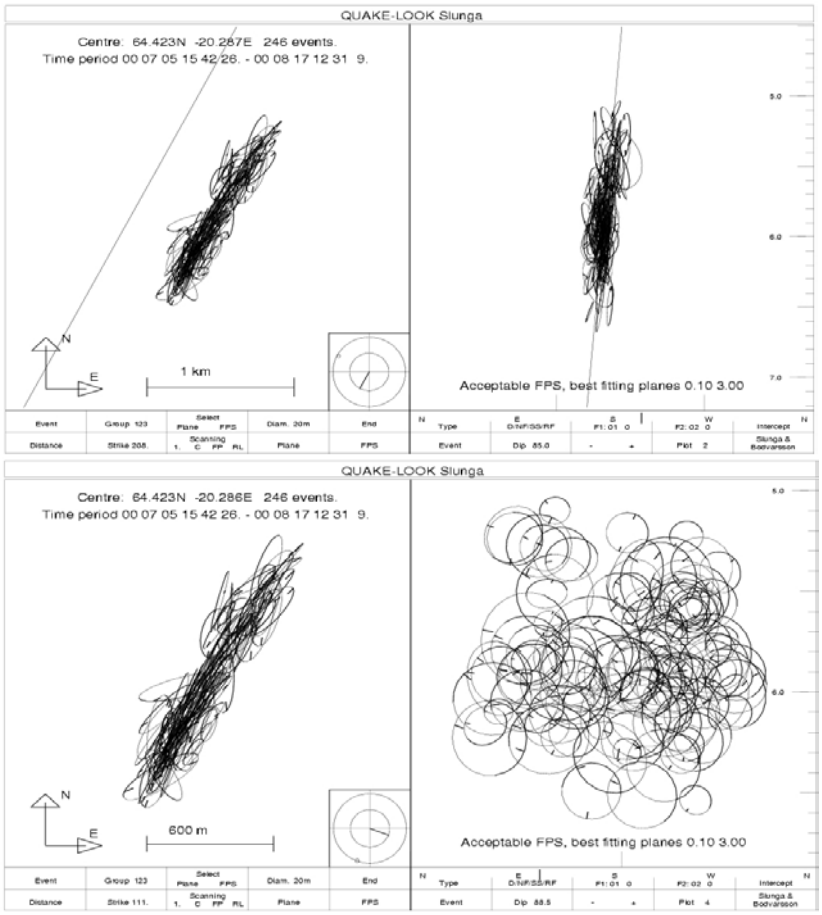

Figure 4. *Fault no.2 in figure 2. Map view (left) and vertical view (right)from NE, along strike (upper) and from NW, perpendicular to the fault plane (lower).*

Socio-economic relavance and policy implication

A detailed map of subsurface faults and slip directions on them will be an important input to a tectonic map of the study area, along with surface features mapped in the Reykjanes Peninsula (WP 5.2) and in the SISZ (WP 4.3). The tectonic map will also be used to evaluate the stress field in the SISZ. It will be interesting to link subsurface fault planes to surface ruptures to learn more about the rupture process. The fault map may also have great value for geothermal power companies and water suppliers in southwestern Iceland, as it reveals the plumbing systems delivering fluid into the geothermal systems in the Hengill area (Nesjavellir and Hellisheiði), the Svartsengi area and Geysir, as well as water wells.

Discussion and conclusions

We have shown that by applying the relocation algorithm to the microearthquakes induced by J17 and J21 events, locations can be significantly improved such that fault patterns become resolvable. By testing the effect of various parameters in the programs, we see that the fault patterns are quite stable but do of course depend on the quality of the raw data. Some events will not define clear fault patterns, since their waveforms are disturbed by other close events and thus have large uncertainty. In difficult areas, we can choose smaller subareas to run on and even use the output as input to a second run to sharpen our image, if necessary.

Plan and objectives for the next period

The relocation method has already been applied to events in all thirteen boxes. These first results give a basis to identify fault patterns and faults have already been identified and

worked on in three boxes. The objectives for the coming months are to continue the search for fault patterns in all areas and rerun the algorithm on selected areas were needed. Furthermore, to obtain an estimate of the average slip direction on each fault. The slip direction is extracted from the best matching focal mechanisms of the events defining a common fault plane. A catalogue of relocated earthquakes is due by M18 and a map of subsurface faults and slip directions on them by M20.

WP 5.2 Mapping and interpretation of earthquake rupture in the Reykjanes peninsula and other surface effects there and in the SISZ

Field work in the area of the three triggered earthquakes on Reykjanes Peninsula was completed before month 6. A complete map of primary rupture and secondary effects from shaking has been completed, and a report published as a journal article in the publication Tectonophysics.

a) Objectives

The objectives of this workpackage are to identify distant faults (on the Reykjanes peninsula) whose movement was triggered by the 17 June, 2000 earthquake in the South Iceland lowland, map the extent of surface rupture along these distant faults and other surface effects (rock fall and slope failure) in the entire area of SISZ and the Reykjanes peninsula, and characterize the faults along which motion was triggered in order to determine future predictability of minor fault movements.

b) Methodology and scientific achievements related to workpackages including contribution from partners

A GIS database has been established for the entire Reykjanes Peninsula. A new fault and fracture map has been generated from a combination of field mapping and mapping from georeferenced digital air photos. Other layers incorporated into the GIS as separate layers include earthquake location point data (in collaboration with P1), digital geologic map data, resistivity data and GPS vector data. Thematic layers showing slope and aspect have been generated within the GIS.

c) Socio-economic relevance and policy implication.

The making of a hazard map for Reykjanes Peninsula will be of great value to plans of future development. As the population grows and development proceeds, it will become increasingly important to take hazards into account, in order to save lives and property.

d) ***Discussion and conclusions***

Conclusions at this stage in the project are mainly qualitative. From visual inspection of the fracture map, it is clear that faults and fissures are unevenly distributed and that the stress field across the peninsula from west to east is non-uniform. It also appears that strike-slip faults are more numerous than previously recognized and that these faults are either longer or extends farther to the north than previously recognized.

When earthquakes are plotted over the fault map it can be seen that earthquake swarms are often occurring at the tips of mapped surface fault traces along strike-slip faults, indicating that these faults are still active and pose a potential hazard. A number of these swarms occurred in the weeks preceding the 4 June 1998 Hengill earthquake and again in the weeks preceding the 17 June 2000 earthquakes. Further study may allow us to use this information to better predict where larger earthquakes will occur.

e) ***Plan and objective for the next period***

The database will be used to develop a geologically realistic model of the behavior of the plate boundary during the earthquake sequence of June 2000, and to put it in the context of the cumulative deformation that has occurred during all of post-glacial time (10,000 years). Methods of GIS analysis will be applied to the existing data and a hazard map will be the outcome.

References:

Clifton, A.E., C.Pagli, J.F. Jónsdóttir, K. Eythorsdóttir, K. Vogfjörð, 2003. Surface Effects of Triggered Fault Slip on Reykjanes Peninsula, SW Iceland. Tectonophysics 369, p.145-154.

Clifton, A.E. and Einarsson, P., 2003. Styles of Surface Rupture Accompanying the June 17 and 21, 2000 Earthquakes in the South Iceland Seismic Zone, has been submitted for review to the journal Tectonophysics in 2003.

WP5.3 Study of the strong ground motion, acceleration and intensities of the two large earthquakes

a) Objectives.

The main objectives is to study the strong motion and the attenuation of the two large earthquakes in South Iceland in June 2000. The applied models can be used for earthquake hazard estimation and simulation of realistic input records for computational structural models.

b) Methodology and scientific achievements related to workpackages including contributions from partners.

The mathematical models applied are based on an analytical approach in contrast to an empirical approach that are most commonly used to model the attenuation of strong ground motion.

Using the far-field model by Brune, extended with an exponential term to account for high frequency decay, a closed form attenuation formula can be derived using the Parseval theorem, that describes the attenuation of rms-accelaration a_{rms} with respect to distance from source, R, and seismic moment, M_o:

$$\log_{10}(a_{rms}) = \log_{10}\left(\frac{(2\sqrt{7})^{2/3}}{2\sqrt{\pi}}\frac{C_P\, R_{\theta\phi}\, \Delta\sigma^{2/3}}{\beta\rho\sqrt{\kappa}}\right) + \frac{1}{2}\log_{10}\left(\frac{\Psi}{T_d}\right) + \frac{1}{3}\log_{10}(M_o) - \log_{10}(R)$$

where T_d is the duration of shaking, C_P is the partitioning factor, □□ is the stress drop, □ is the shear wave velocity, □is the crustal density, R□□ represent the mean radiation pattern, □□R/□Q is the spectral decay factor. Here Ψ denotes a dispersion function for which a closed form solution is readily obtained. The peak ground acceleration can be related to the rms ground acceleration by applying the theory of locally stationary Gaussian processes. The result is: $a_{peak} = p\, a_{rms}$ where p is the so-called peak function, which depends on the strong motion duration, T_d, and the predominant period of the strong motion phase of the acceleration.

Applying the near field model of Brune, the following attenuation formula has ben derived for the a_{rms} for strong motion close to the source:

$$\log_{10}(a_{rms}) = \log_{10}\left(\frac{1}{\sqrt{\pi}}\frac{7}{8}\frac{C_p}{\rho\beta r^3\sqrt{\kappa_o}}\right) + \frac{1}{2}\log_{10}\left(\frac{\Psi_o}{T_o}\right) + \log_{10}(M_o)$$

Here, the duration is denoted by T_o and Ψ_o is a dispersion function which can represented in closed form, r is the radius of the fault plane.

Figure 4 shows the models fitted to the horizontal peak ground accelerations recorded in the two earthquakes, represented by solid circles. The horizontal dotted line represent the near field model and the solid curve represent the model for intermediate distances. The break in the solid curve is due to the use of a geometrical spreading function where the spreading

function takes a value of 1/R2 at intermediate distances and 1/R further from the source. Plus and minus one standard deviation from the model is represented by thin dotted curves.

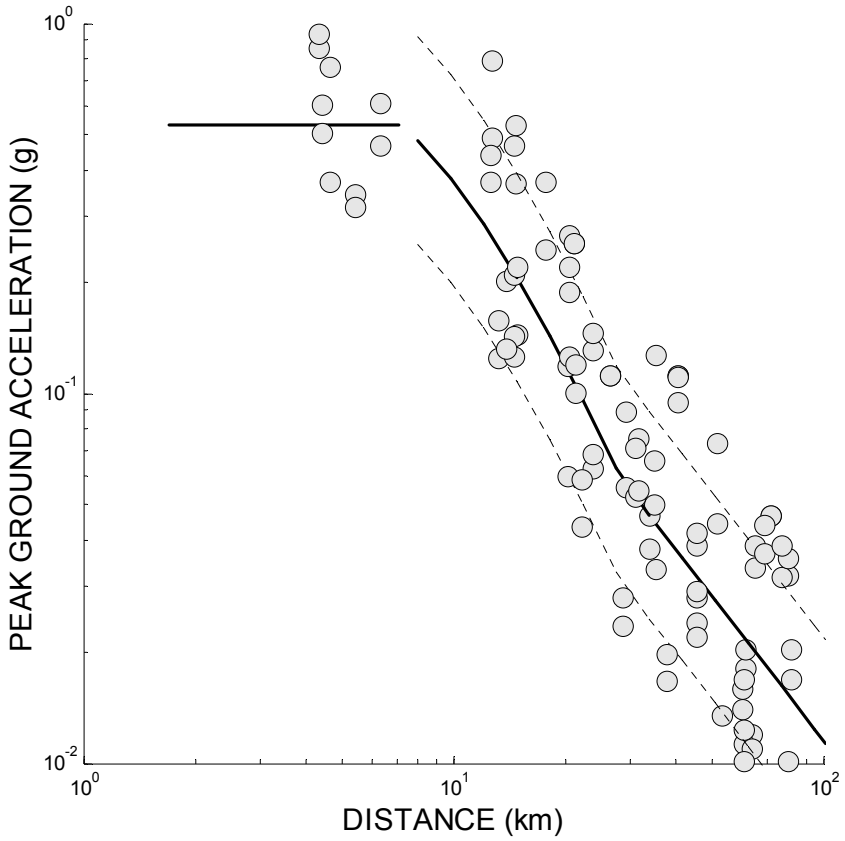

Figure 4 *– Attenuation of horizontal peak ground acceleration. The solid line represents the far- and intermediate-field model, the horizontal dashed line gives the near-field model, and the circles represent data from the South Iceland earthquakes on 17 and 21 June 2000. Dotted lines indicate the deviation of the data from the model by ± one standard deviation.*

c) Socio-economic relevance and policy implication.

To obtain improved ground motion models for seismic hazard assessment and seismic design by using the data gathered in the two large earthquakes. This improves the safety of structures in strong earthquakes in the area and strives to reduce the risk of personal injury and economic loss due to damage to structures.

d) Discussion and conclusion.

We consider the analytical modelling approach used for the attenuation of strong ground motion in this study more fitting than the empirical approach, due to the lack of data in this region. The model uses parameters that have physical meaning and accounts for the variability of the ground motion. The models can also be applied to simulate an ensemble of input records to computational structural.

e) Plan and objectives for the next period.

The plan is to estimate the soil amplification at each measurement site as well as studying the intensity data. The attenuation model will be tested and developed further. All model parameters will be re-evaluated based on the site amplification data.

WP 5.4 Reevaluation of the historical earthquakes in light of the new observations

Objectives
The aim of the project is to reevaluate magnitudes, locations and possible fault sizes for historical events in the South Iceland seismic zone back to 1700.

Methodology and scientific achievements related to workpackages including contributions from partners
According to the description of WP5.4 the start month is M12 and the only milestone is the final deliverable of the package: A revised historical earthquake catalogue for SW Iceland. Therefore no results are available yet.

As described in the Description of Work the previous estimates of magnitudes and locations of historical seismic events in Iceland are based on: 1) the area of damage zone (defined where at least half of all houses collapsed); 2) the Icelandic formula for attenuation of intensities and finally; 3) the instrumentally observed magnitude (Ms=7.0) of an earthquake in the SISZ 1912.

Now can we add the experience from the events in June 2000. For this we have detailed information about the earthquakes, exact locations, fault geometry and slip. The effects of the earthquakes (surface faulting and intensities) are also far better known than for the historical events and now we have in addition acceleration records.

A comparison of detailed information from the 2000 earthquakes with incomplete data from the historical events gives the possibility to reevaluate magnitudes, locations and fault sizes of the historical events.

It is also necessary to reevaluate the historical sources we have used to estimate intensities and damages caused by earthquakes.

At the beginning of the work a new attenuation formula for Iceland was developed and some historical documents have been reanalysed and reinterpreted for estimating intensities. This work will take up to third part of the project.

Socio-economic relevance and policy implication
The main socio-economic implication of the project is the possibility to improve the seismic hazard assessment for the area.

Discussion and conclusions
As mentioned before the work is in the starting phase. Therefore it is not timely to draw conclusions or discuss the progress of the work.

Plan and objectives for the next period

The next period is in fact the first period of the project. The plan is to continue the work and publish a new catalogue of historical earthquakes for SW Iceland in the beginning of the year 2005.

WP5.5 Hydrological changes associated with the June 2000 earthquakes

a. Objectives

The main objectives in the early part of the period were to start work on the overall structure of the South Iceland Seismic Zone (SISZ) and to analyse fracture data related to the June 2000 earthquakes so as to be able to put the results from the geothermal changes and related aspects of the 2000 earthquakes into a general tectonic and hydrogeological framework. In the latter part of the period, the focus was on data analysis (including establishing contacts with persons who will collaborate in the data analysis) and numerical modelling.

The main aim in all these studies is to understand the mechanics of the June 2000 earthquakes and the associated hydrological changes. A second aim is to develop further the model that the volcanoes in the vicinity of the SISZ can be used as precursors to large earthquakes in the SISZ. In particular, that crustal deformation, seismicity and changes in geothermal fields in volcanoes such as Hengill and Eyjafjallajokull, and abrupt changes in the eruption frequency of the Hekla Volcano, can be related to the loading to failure of the SISZ. A third aim, related to the mechanics of the earthquakes, is to provide understanding as to how stress transfer from the nearby volcanoes and volcanic zones may trigger, or suppress, seismogenic activity in the SISZ.

b. Methodology and scientific achievements

During the period, a comparison was made between the surface features, faults and visible crustal structure of the SISZ and its adjacent parts (the West Volcanic Zone and the East Volcanic Zone) and the deeply eroded features observed in the nearby Pleistocene and Tertiary lava piles in Southwest and Southeast Iceland. There is no doubt that the SISZ is underlain by a layered crust, and the dips and mechanical properties of these layers have effects on the faults that developed during the June 2000 earthquakes as well as the associated changes in the geothermal fields during the earthquakes. Furthermore, in Southwest Iceland, and particularly in Southeast and East Iceland, extinct magma chambers that are presumably similar to those that currently exist (or have existed) in the central volcanoes adjacent to the SISZ, such as Hengill, Hekla and Eyjafjallajokull, can be observed and used as a basis for numerical models similar to those presented in Gudmundsson and Brenner (2003).

When these extinct magma chambers were active, they gave rise to geothermal fields, presumably similar to those that are currently active in the Hengill Volcano. It is believed that the intense seismic activity in the Hengill Volcano and its surroundings that was a precursor to the June 2000 earthquakes (Gudmundsson and Brenner 2003) is largely related to fluid-pressure changes in the associated geothermal field during loading of that field by the SISZ. It is also observed that most of the inactive faults in the Pleistocene and Tertiary lava pile have mineral veins (extinct hydrofractures) along the fault cores and in the damage zones, suggesting a close correlation between fluid-driven fractures and seismogenic faulting in the SISZ as well as in Hengill.

The field studies in 2003 were carried out in collaboration with two assistant scientists, Sonja L. Brenner (Germany) and Ines Galindo (Spain). Both are experts on fractures, in particular faults and associated geothermal fluid transport, and one (SLB) has already worked on numerical models of the SISZ (cf. Gudmundsson and Brenner 2003).

All these field observations, together with studies of the active geothermal fields in South and Southwest Iceland, will be used for making numerical models to explain the hydrological changes associated with the June 2000 earthquakes, as well as to extend and develop further the model of the SISZ and its adjacent volcanoes, presented in Gudmundsson and Brenner (2003).

To complement the field studies, aerial photographs were ordered of selected areas within, and adjacent to, the SISZ, in particular areas in Southwest Iceland (Hengill, Reykjanes Peninsula), and in South Iceland (Hekla, Eyjafjallajokull). These are being studied in detail and the results used to provide further constraints on the numerical models.

Studies at the National Energy Authority (Grimur Björnsson, subcontractor), including a televiewer measurements and analysis of the geothermal boreholes in the SISZ, are progressing. The new data gathered from the subcontractor, as a well as the new results obtained during the fieldwork the summer of 2003 will be added to and analysed in more detail in the summer of 2004. This part of the project is in collaboration with Ms Amy Day-Lewis, a Ph.D. student in the Department of Geology and Geophysics, University of Connecticut, USA. She is an expert on crustal stresses and associated fluid transport. Ms Day-Lewis will come to Iceland in the summer of 2004 to work with Grimur Bjornsson and Agust Gudmundsson in connection with stresses and fluid transport in the SISZ.

The main achievements during the reporting period may be summarised as follows: about 1000 measurements of fractures and push-ups generated during the June 2000 earthquakes have been classified and put into files suitable for analysing. These fractures and fracture patterns are generated in the same fault-related stress fields that were responsible for the changes in the hydrothermal and geothermal fields in South Iceland before and after the June earthquakes.

Also, many new numerical models of the SISZ fault zones have been made indicating abrupt changes in the local stress fields nearby, and within, the fault zones of the SISZ when they are loaded to failure. These local stresses largely control the hydrological changes associated with the June earthquakes. In addition, numerical models have been made on the local stress fields in the layered crust in the SISZ and in the nearby volcanic zones. The results indicate how sensitive the stresses around volcanoes and fault zones are to mechanical layering, and how stress transfer between the volcanic and seismic zones may trigger or suppress earthquakes in the SISZ. All these results have important implications for earthquake mechanics and fluid transport in the SISZ.

c. Socio-economic relevance

The work made in this package has great socio-economic relevance, in particular in the following fields (both as regards South Iceland and in general):

- Earthquake hazard analysis
- Earthquake risk analysis
- Fracture-generated and maintained permeability and transport of crustal fluids (gas, oil, groundwater, geothermal water)
- Understanding and using geothermal reservoirs
- Interaction between volcanic and seismogenic zones
- Understanding volcanic unrest and hazards
- Evaluating volcanic risk

d. Discussion and conclusions

The work in this package is progressing essentially as planned. However, the work has already lead to many new ideas and models concerning the mechanics of seismogenic faulting in the SISZ and the related fluid transport. In particular, the effects of mechanical heterogeneities and layering on faulting and fluid transport appear to be of fundamental importance for understanding the mechanics of earthquakes, and associated changes in geothermal fields and permeability, in the SISZ. The implications of these findings will be explored in the second year of the Prepared project.

e. Plan and objectives for the next period

These may be briefly summarised as follows:

- Stress, fracture and fluid transport analysis in the SISZ in the summer of 2004. Participants Agust Gudmundsson, Grimur Bjornsson, Amy Day-Lewis, and assistants and students.

- Continuation and refinement of numerical models on fault zones, volcanic systems, and fluid transport in relation to the mechanics of the June 2000 earthquakes in the SISZ.

- Testing of some of the models results on fracture and fluid data from the June 2000 earthquakes.

- Development of more general seismo-volcano-tectonic models of Iceland with a view of understanding stress transfer and triggering of earthquakes (and associated fluid transport) in the SISZ.

- Presentation of the results at conferences and meetings, and publication of the main results in international scientific journals.

WP5.6 Paleo-stress fields and the mechanics of faulting

1. Objectives

The main purpose of the WP 5.6 is the description of the stress field and understanding of the mechanical behaviour of an active seismogenic zone, the South Iceland Seismic Zone (SISZ). In that way, our first aim was to determine how the stresses are distributed along the active faults and their evolution. We deals with the case of the Hestfjall fault, associated with the magnitude 6.6 earthquake of June 21. In a second time, to recognise the parameters which could control the nature and the distribution of the surface rupture traces induced by major earthquakes, we carried out field measurements of recent faults and a detailed GPS mapping along selected parts of major historical active faults. All these works deal with analysis of faulting in terms of geometry and mechanics, based on both the inversion of focal mechanisms of earthquakes and of fault slip data analysis, and the analysis of surface deformations associated to major earthquakes.

2. Methodology and scientific achievements

The main methodologies used in the WP 5.6 are:
- Inversion of fault slip data to obtain the stress tensor and of double-couple earthquake focal mechanisms (from the SIL-network) to obtain the stress tensor without choice among nodal planes.
- Analysis of surface features of faults (mapping and geometrical analysis).
- Numerical modelling (distinct-element, finite-element).

A first field work has been carried out in the SISZ, 28th April – 15th May, 2003 (F. Bergerat, J. Angelier, C. Homberg and M. Bellou) for fault slip data collection , accurate GPS mapping with a kinematic GPS equipment and measurements of characteristic features, along the historical fault associated to the 1630 earthquake.
The focal mechanisms of earthquakes analysis has been carried out, during this first year, on the 21 June 2000 earthquake sequence.

2.1. Fault slip data analysis and stress tensor reconstructions

The collection of data has been carried out in 10 sites, in the eastern part of the SISZ.

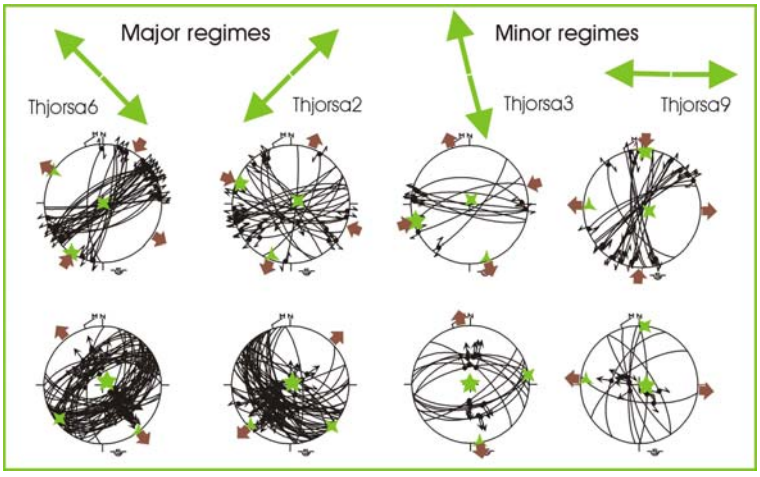

Figure 1 *– Examples of selected sites illustrating the major (on the left) and minor (on the right) stress regimes characterised by strike-slip (upper line) and normal (lower line) fault slip data analysis*

The detailed analysis of the collected data, in terms of stress tensors indicates 4 main paleo-stress fields including both normal and strike-slip faulting (Fig. 1). The two major regimes (in terms of number of faults) are: NE-SW compression/NW-SE extension, NW-SE compression/NE-SW extension; the two minor regimes are: N-S compression/E-W extension, and E-W compression/N-S extension.

2.2. Surfaces features of seismic faults

This part of the work has already been developed in the 6th month report (July 2003), therefore we just summarise herein the main results.
We focused our study on the 1630 earthquake located in the eastern part of the SISZ. Some segments of the fault have been mapped: a left-lateral segment trending N47°E and about 1386 m long, located in the northwest part of the fault, a right-lateral segment trending N10°E and about 943 m long, located North of the Thjorsa river, and two sub-parallel branches. The eastern one oriented N17°E and 825 m long, and the western one of about 1700 m long and oriented N2°E. We mainly focused our study on the segmentation pattern and on the measurements of push-ups structures in order to obtain information on the mechanical process of faulting and calculation of magnitude of the earthquake.

2.3. Inversion of focal mechanisms

A new inverse method to determine the stress that best accounts for a set of double couple focal mechanisms of earthquakes has been developed in the framework of the PRENLAB, SMSITES and PREPARED projects (Angelier, 2002). It is based on the SSSC criterion (Slip Shear Stress Component). The sum of the SSSC values is maximised as a function of four unknowns that describe the reduced stress tensor, including the orientations of principal stress axes and the ratio between principal stress differences. No choice between the nodal planes is needed, because of the intrinsic SSSC properties. The runtime is negligible regardless of the size of the data set, because the inverse problem is solved by analytical means. Thus, the SSSC-based inversion can easily be included in a variety of processes to refine the data and to separate multiple states of regional stress.

2.3.1. Stress distribution around the June 21st earthquake strike-slip fault : The Hestfjall fault.

This part of the work has already been developed in the 6th month report (July 2003), therefore we just summarise herein the main results.

We aimed at characterising the stress evolution along the Hestfjall fault. Thus we selected a shallow zone between the longitudes 63,87°N-64,08°N and latitudes 20,75°W-20,65°W representing a total set of 6518 nodal planes, from June 21st to August 31st 2000.
We divided the Hestfjall area into several boxes (6 or 12 boxes) located on the two sides of the fault, and we carried out stress inversion of all the boxes separately. Such tensor calculations give us a good idea of the space evolution of the stress direction along the fault and illustrates the perturbations in stress trajectories (σ_3 axis shown in Fig. 2).

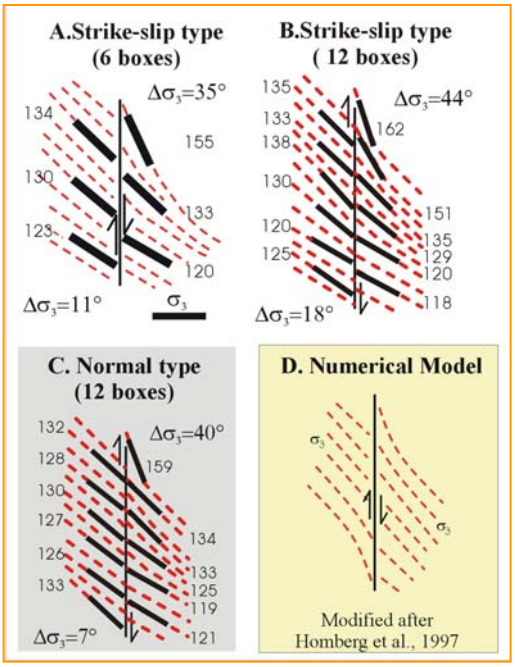

Figure 2 – Results of the stress inversion of focal mechanisms of earthquakes for strike-slip (A-B) and normal (C) mechanisms.

2.3.2. Can instantaneous inversion of large sets of focal mechanisms be carried out to reconstruct regional states of stress?

Because major sources of stress perturbation are expected in the brittle crust, whether or not a significant average stress state may emerge from regional-scale inversion of large sets of focal mechanisms is subject to doubt. Stress inversion of double couple focal mechanisms recorded by the SIL network is carried out within a set of 126,588 shallow earthquakes from July 1991 to July 1999 (Fig. 3).

Box	Subset	Number of nodal planes with ω<40%	Number of nodal planes with ω>40%	σ1 axis trend (deg)	σ1 axis plunge (deg)	σ2 axis trend (deg)	σ2 axis plunge (deg)	σ3 axis trend (deg)	σ3 axis plunge (deg)	Stress ratio Φ	Average ω (%)
K	major	8	34	222	77	31	13	121	3	0.88	78
	minor	0	18	110	10	19	3	270	79	0.07	78
T	major	4096	14900	155	3	23	86	245	3	0.64	74
	minor	2810	2576	59	1	157	81	329	9	0.53	64
S	major	24974	87172	232	17	30	72	140	6	0.61	72
	minor	14736	16916	320	3	89	85	229	4	0.65	61
R	major	6	34	128	6	232	66	35	23	0.22	86
	minor	8	18	43	13	228	77	133	1	0.65	84

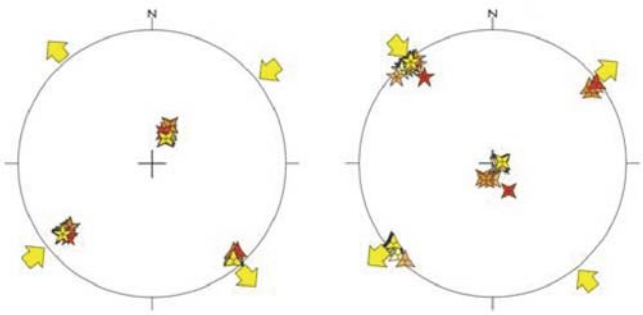

Major subset
96,112 accepted data (86%)
16,033 rejected data (14%)

Minor subset
25,635 accepted data (81%)
6,018 rejected data (19%)

Figure 3 – Summary of the inversion results of focal mechanisms of earthquakes (1991-1999) for the Kolbeinsey (K) Tjörnes (T), South Iceland (S) and Reykjanes (R) zones (see Angelier *et al.*, 2003, for details). The two diagrams illustrate the stress axes σ1, σ2 and σ3 and the directions of compression and extension for the major and minor sets of the South Iceland Seismic Zone.

Inversion is performed for two main data sets of 12,191 and 71,889 focal mechanisms in the transform zone areas of N and S Iceland. The inversion reveals surprisingly high levels of consistency with regard to uncertainties and dispersion. Adopting a reasonable threshold value for individual fit, the proportion of acceptable data is as high as 78% for 65,571 focal mechanisms of the major regime in these two areas. The major stress regimes show nearly vertical σ_2 axes. The azimuths of extension are 065° in the right-lateral transform zone of N Iceland and 140° in the left-lateral one of S Iceland. With respect to the 105° azimuth of plate separation, these directions show nearly symmetrical angular deviations, 40° anticlockwise in N Iceland and 35° clockwise in S Iceland (Fig. 4). This reveals first-order stress perturbation in areas where major rift offset resulted from Late Cenozoic rift jumps related to plate boundary migration with respect to the Iceland Mantle Plume.

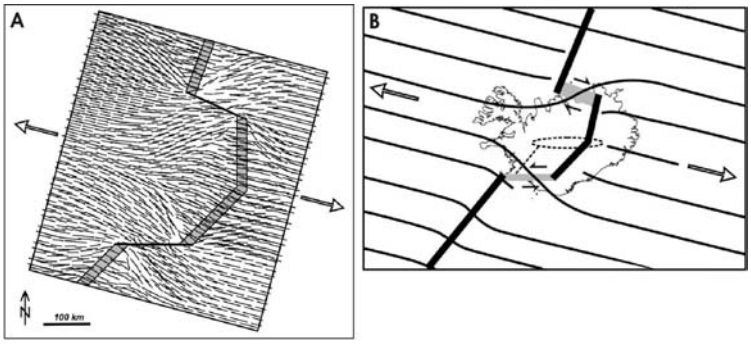

Figure 4 – Two-dimensional model of stress distribution for the simplified present-day pattern of rifts and transform zones in Iceland, based on the distinct-element method (A) and schematic interpretation of the present-day first order extension pattern across the Mid-Atlantic Ridge in and around Iceland (B) [after Angelier *et al*., 2003].

3. Socio-economic relevance

This study contributes to a better understanding of earthquake processes and mechanisms in the SISZ. Associated with the studies carried out in the other WP of the PREPARED project, the WP 5-6 is socially and economically important for Iceland and other seismic areas.

4. Discussion and conclusions

The study of recent (slips), historical (surface ruptures) and present-day faulting (focal mechanisms) allow a better understanding of the mechanics of earthquakes. The analysis of focal mechanisms, the comparison with the pre-historical fault slip data and historical surface traces highlight the crustal processes leading to large earthquakes.

5. Plan and objectives for the next period

In agreement with the proposed project, the second year work will include:

- Field work in the SISZ (planned May 2004) including: fault slip data measurements and geometrical analysis of surface features.
- Inversion of fault slip data and of focal mechanisms of earthquakes for the SISZ

- Numerical modelling (distinct-element, finite-element)
- Participation to the PREPARED meetings and to international meetings (e.g., EGU, Nice, April 2004)
- Preparation of papers to be published in international journals

WP 6 Modelling and parameterizing the SW Iceland earthquake release and deformation processes

Objectives

Modelling and parameterizing the strain build-up and strain release in the SW Iceland earthquake zones on basis of all available relevant multidisciplinary data.

Methodology and scientific achievements related to workpackages including contribution from partners

WP 6 is based on inputs from progress and results of WP6.1 and WP6.2, as well as results of other workpackages parameterizing or modelling on basis of various observations.

Several models have been created to describe faulting in the SISZ models which explain significant observations of geophysics and geology. The June 2000 earthquakes yield new information which constrain such a model.

WP6.1 and WP6.2 will continue modelling work carried out within the PRENLAB projects, fulfilling more multidisciplinary information, and especially observations of the June 2000 earthquakes.

The workpackage leaders together with representatives of WP6.1 and WP6.2 will create a forum with other partners of the consortium to discuss and to merge a general model of the area. It will inform the participants about emerging results regarding the general characteristics of the SISZ and the linked Reykjanes peninsula, so they can be applied directly in the various workpackages.

The WP6 is a forum for communication of results and discussion between the lead contractors in WP6.1-6.2, GFZ Potsdam as well as DF.UNIBO, IMOR, SIUI and CNRS-UMR 5562. Based on historical seismicity since 1700 and an elastic/viscoelastic layered model, GFZ Potsdam in WP6.1, tries by Coulomb stress modelling to approach time dependent earthquake hazard assessment for the area as a whole, i.e. where along the zone is most probable that the next earthquake will strike. For this purpose it needs improved geoparameters that probably will emerge from other WPs. CNRS-UMR 5562 tries a parallel and complementary approach, WP6.2 adds new input to this modelling by studying the effects of pore fluids permeating the crust, which may help to answer the question where inside the area of highest earthquake probability an earthquake will strike. Also WP6.2 has modelled dynamic stress transfer which can explain the “immediate” release of a series of earthquakes at 100 km from the main earthquakes of year 2000.

Socio-economic relevance and policy implication

The objective of this WP is significant for all other efforts for risk mitigation in the area, the general hazard assessment, the time dependent hazard assessment, for the warning algorithms and for nowcasting for risk mitigation purposes.

Discussuion and conclusions

Conclusions so far are that for a general modelling and parameterizing the SW Iceland earthquake release and deformation processes results from most other WPs are needed, and new knowledge is emerging in the various workpackages that may lead to new understanding of the South Iceland seismic zone earthquake processes.

Plan and objectives for the next period

Intensive work for merging together the outcome of the various WPs rending information, significant for the WP6 objectives. Meetings during the period, EGU General Assembly in Nice in April 2004, ESC General Assembly in Potsdam in September 2004, and the PREPARED final meeting.

WP 6.1 Earthquake probability changes due to stress transfer

a) Objectives

Damaging earthquakes (i.e. Ms ≥ 6) in the South Iceland seismic zone (SISZ) occur fairly regularly and as a series of events with time lags of generally only a few days between them. Generally, the first event in the series is the most eastward one, the subsequent events occur farther and farther west in the SISZ. All earthquakes occur as NS-oriented right-lateral strike-slip events. Stress build-up by plate motion as well as stress changes caused by volcanic eruptions and seismic events, but also lateral inhomogeneities and the variation in crustal thickness determine the magnitude, location, and time of the impending event. The objective of WP 6.1 is to use the past of the SISZ, i.e. the historical events, in order to understand where future earthquakes might strike. This can be done of course only in a probabilistic sense. We aim at improving the probabilistic earthquake hazard assessment through modelling of the stress field in the SISZ, whereby the time-lagged reaction of the viscoelastic lower crust and mantle to stress changes is taken into account. This property calls for a time-dependent hazard analysis since the probability of future earthquakes will change with time as the viscoelastic lower crust and mantle relax.

b) Methodology and scientific achievements related to workpackages including contributions from partners

Seismic recordings and therefore reliable data on location, magnitude, average slip, and rupture dimensions have been only available since the beginning of the 20^{th} century. Therefore, the parameters of historical events have to be estimated based on a comparison of damage reports from chronicles with recent damage observations. We use results published by Stefánsson et al. (1993), but will in future benefit from the re-evaluation of the historic events by WP 5.4. We employ the viscoelastic-gravitational extension of the elastic stress modelling software published by Wang et al. (2003), which computes the stress field for a layered halfspace based on dislocation theory. For model construction we therefore need P- and S-wave velocity depth profiles (e.g. the SIL model; Stefánsson et al., 1993), as well as density and viscosity profiles. So far, for the latter two parameters we used only three different values, one for the elastic upper crust (0-6 km depth), one for the viscoelastic lower crust (6-24.5 km) and one for the mantle. Density and average lower crust-mantle boundary values were taken from Menke (1999), while the viscosity (identical for the lower crust and mantle) was taken from Árnadóttir et al. (2003). The rather low value of 10^{18} Pas results in a rapid relaxation over only 30 years (approximately 95% of the final value) in the model. Input from other work-packages will hopefully help to form an undisputed opinion on an appropriate value.
Our modelling software produces individual stress fields (normal and shear) caused by each of the 13 events considered since 1706. We combine these results for obtaining the temporal shear stress variation in the SISZ and we compute Coulomb stress changes to detect the possible triggering of events due to positive stress changes caused by earlier events as well.

Temporal shear stress variation*:*

The exceedance of a critical shear stress level determines the location and time of an impending event. We assume that the SISZ is pre-stressed due to plate motion (background field) and stress release and accumulation takes place co- and post-seismically for each of the

13 events. Further annual stress build-up due to continuing plate motion needs to be taken into account, but other stress transfer mechanisms (volcanic activity) are not considered yet explicitly. Unfortunately, we have no knowledge of the stress field prior to the event in 1706. However, we stipulate that the area on which the largest historical event on August 14, 1784, occurred must have been pre-stressed with at least the same amount of shear stress released during this event. The background field is based on the more elaborate modelling of Roth (2004) copying its shape with a simple strike-slip event all along the SISZ. This background field was also scaled to mimic the yearly stress build-up by plate motion. So far, we did not check the pre-stress levels at the location of each of the 13 ruptures, but compared the results gained for an elastic model with those for the viscoelastic one. Differences occur mainly outside the centre of the SISZ, where the magnitude of the background field drops off rapidly (Figure 1). There seems to be a bias for more stress relaxation in the northern part of the SISZ, but this effect is probably due to having located the stress field representing the background model too far south.

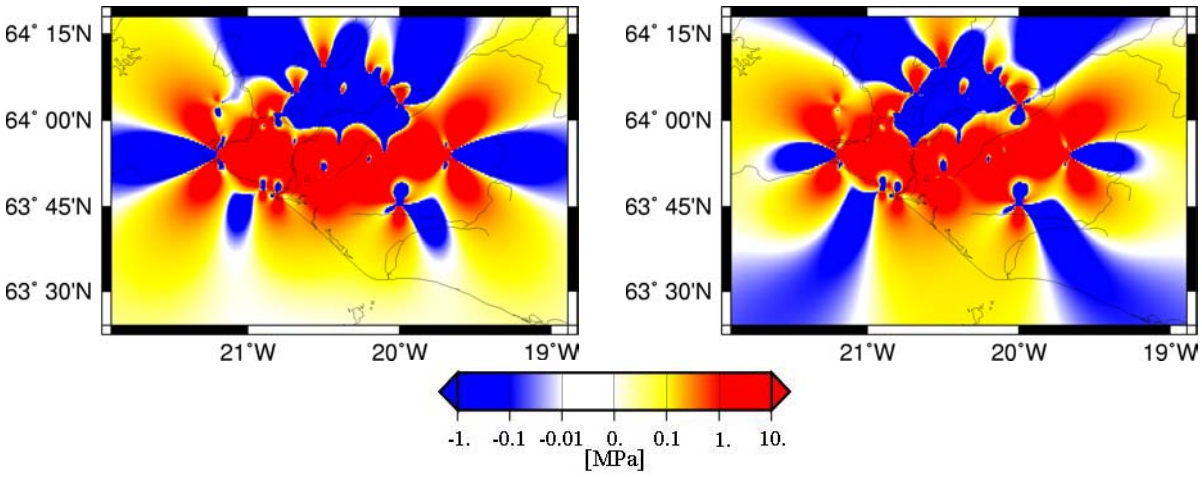

Figure 1. **Elastically (left) and viscoelastically (right) modelled shear stress fields in the year 2004.**

Coulomb stress changes:

Assuming that pre-existing vertical right-lateral strike-slip faults trending NS are present throughout the SISZ, we can compute Coulomb stress changes due to a causative event. Positive values are interpreted as bringing the pre-existing faults closer to failure (clock advance), negative ones as removing them from failure (clock delay, stress shadows). The stress changes due to successive events may be summed up. If we neglect other stress transfer mechanisms (e.g. plate-tectonic motion, volcanic activity) and if we assume the Coulomb stress changes to be static, no event should be located in a stress shadow. Consequently, if we sum up the elastic Coulomb stress changes for all 13 events, assuming for convenience that 1706 was the first event ever to have happened in the SISZ, the result is that not more than 3 events should have happened at all after 1706. Obviously, the Coulomb stress change approach cannot be applied under such assumptions. However, for short periods of time, i.e. for the subsequent events, the Coulomb approach should be applicable. We tested this hypothesis and found in 6 out of 7 cases that (visually) more than half of the respective rupture lengths lay in regions with positive Coulomb stress level, even above the assumed threshold for stress triggering of 0.01 MPa (King et al., 1994; e.g. Figure 2, right), while the first event of each series lay in 4 out of 5 cases in the stress shadow of the previous series (e.g. Figure 2, left). This suggests that if events are separated by more than a few days other stress

transfer mechanisms are needed for retrospectively explaining the location of the successive event.

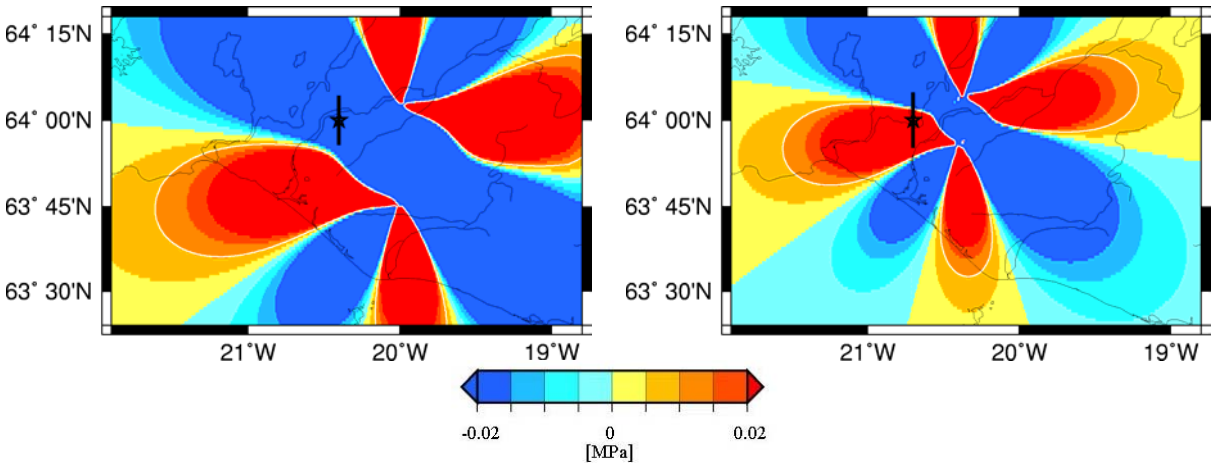

Figure 2. *Coulomb stress changes caused by the event in 1912 (left) with location of June 17, 2000, event indicated by the solid line and the star (epicentre). Coulomb stress changes due to the June 17, 2000, event are shown on the right with the June 21, 2000, event indicated as well. The white line indicates the 0.01 MPa contour in both figures.*

c) Socio-economic relevance and policy implications

Our work will aid in the long-term earthquake warnings through time-dependent hazard assessments. It will allow for directing risk mitigating efforts, research, and monitoring towards areas with increased hazard. In case of future events the modelling of Coulomb stress changes (triggering of subsequent events) might help to indicate areas of increased aftershock activity.

d) Discussion and conclusions

Apart from imperfect knowledge on the parameters (location, rupture area, exact mechanism, slip) of historical earthquakes - which will be improved by work from other workpackages - and apart from neglecting heterogeneities in the SISZ (e.g., increase of crustal thickness from West to East) and modelling it as a layered halfspace, we face the crucial question on an appropriate threshold for earthquake triggering. Shear stress modelling permits insights into pre-stress levels at historical sites that may lead to conclusions on probable areas for impending events. However, the influence of the background field is obvious and needs to be carefully investigated. If we neglect the background field and other stress transfer mechanisms and compute only Coulomb stress changes we are able to find a correlation between positive stress change and occurrence of subsequent events inside a series (i.e., events occuring inside a time window of a few days). However, the question why the subsequent event has taken place at the exact spot cannot be answered.

e) Plan and objectives for the next period

Based on results from other workpackages (e.g. WP 5.4) we will revise the parameters of the historical events used so far. Results from WP 2.3 (long term observations) and WP 4.4 (observations since 2000) will help to improve our average layered model of the SISZ,

especially the viscosity. Then we will re-compute the temporal shear stress variations and using the pre-stress analysis improve the background field. We will consider other stress transfer mechanisms than seismic events and assess the Coulomb stress changes for the viscoelastic model to check whether we can then explain the occurrence of the respective first event of each series. Finally, both the shear stress as well as the Coulomb stress variations will be converted into an increase/decrease of changes in the occurrence probability of future earthquakes.

WP 6.2 Model stress in the solid matrix and pressures in fluids permeating the crust

Objectives

WP 6.2 addresses three major objectives through theoretical modelling: (1) Lithosphere-asthenosphere interaction under the SISZ, taking into account viscoelastic constitutive relationships and intrusive events across rheological discontinuities; (2) Fault instability in the SISZ, taking into account poro-elastic constitutive relationships; (3) triggered seismicity and the interaction between the two large earthquakes of year 2000 in the SISZ.

1. Dislocation models in heterogeneous media (D-98)

We have studied the singular behaviour of strike-slip faults crossing a material discontinuity, employing the asymptotic theory of generalized Cauchy integral equations. Planar crack surfaces across interfaces are characterized by jump discontinuities in the dislocation density distribution which must be accompanied by stress drop discontinuities (Bonafede et al. 2002); instead, non planar surfaces, bent across an interface, are characterized by algebraic singularities in the dislocation density, which might be responsible for unbounded singularities in some components of the stress field at the interface. Previous studies have shown that the stress drop discontinuity condition cannot be fulfilled in several cases for planar surfaces: in such cases a planar strike-slip fault across the interface is in conflict with the welded-boundary conditions. A simple way out of the mentioned problem is assuming that the fault surface is affected by a sharp change of the angle of dip at the intersection with the interface (see Fig. 1).

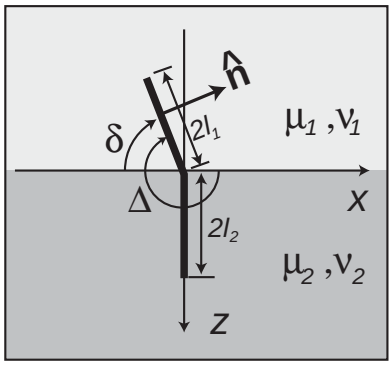

Figure 1. *Scheme of strike-slip fault bent across the welded interface between two media with different rigidities and Poisson ratios (μ1, ν1 in the upper medium, μ2, ν2 in the lower medium). The upper crack section has length 2l1, the lower section has length 2l2. The dip angle of the upper section is* $\delta = \Delta - \pi$.

The problem can be addressed in terms of a deep vertical planar crack interacting with a shallower inclined planar crack. An asymptotic study of the singular behaviour of the dislocation density at the interface reveals that (1) the density distribution has a singularity at the interface of degree ω, obeying the following transcendental equation

$$\left\{\cos\pi\omega + \Gamma\cos\left[2\left(\frac{3}{2}\pi - \Delta\right)(\omega+1)\right]\right\}\left[\cos\pi\omega - \Gamma\right] + \left(\Gamma^2 - 1\right)\cos^2\left[\left(\frac{3}{2}\pi - \Delta\right)(\omega+1)\right] = 0 \quad \text{with}$$

$$\Gamma = \left(\frac{\mu_1 - \mu_2}{\mu_1 + \mu_2}\right);$$

(2) only one solution exists for ω in the interval (-1,0) of admissible values; (3) ω values depend on both, the dip angle $\delta = \Delta - \pi$ of the upper crack section and on the rigidity contrast between the two media (see Figure 2).

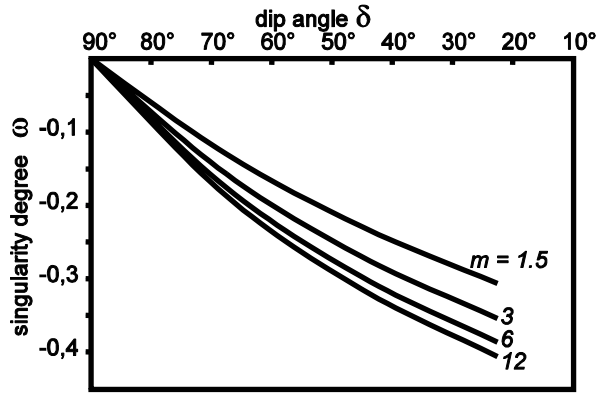

Figure 2. *Singularity degree ω of the dislocation distribution density for an antiplane crack (transform fault) as a function of the dip angle δ of the upper fault section, for different values of the rigidity contrast $m=\mu_2/\mu_1$. Only a planar crack cutting perpendicularly the interface ($\delta = 90°$) is non-singular.*

A semi-analytical scheme has been worked out to obtain approximate analytic expansions for the two dislocation distributions and from these the displacement and the stress fields can be computed all over the layered medium. From the welded boundary condition at the interface a generalized stress drop discontinuity condition is obtained,

$$\frac{\Delta\sigma_1}{\Delta\sigma_2} = \frac{\mu_1}{\mu_2}\sin\delta$$

which can be fulfilled if the stress drop in the upper medium is lower than required for a planar trough-going surface: as a corollary, a vertically dipping strike slip fault at depth may cross the interface with a sedimentary layer, provided that the shallower section is suitably inclined (fault "refraction"); this results has important implications for our understanding of the complexity of the fault system in the SISZ (WP 5.6); in particular, we may understand the observed offset of surface fractures (WP 4.3) w.r. to seismic faults, imaged through accurately relocated of aftershocks.

2. Role of Fluid migration in the preparatory stage of earthquakes (D95 and D-100)

Existing models of triggered seismicity assume that pore pressure changes are induced by stress changes following an earthquake, assuming undrained conditions for the fluid. Similar models neglect several aspects which may be important in the earthquake nucleation process and in the post-seismic phase. It is well known from laboratory experiments and from indirect in-field evidence that dilatancy (i.e. localized increase of microcrack density) takes place when a rock is subjected to increasing deviatoric stress, before a through-going fracture develops in a rock. Thus porosity changes are expected to take place in the source region of an impending earthquake and fluid migration may start suddenly if, following the increase of microcrack density, an interconnected pattern of microcracks develops in the medium, leading to a transition from impervious to pervious conditions. It is also known that the pore pressure field in the crust is often characterized by a transition from a nearly hydrostatic gradient at shallow depth, where meteoric water circulates, to a nearly lithostatic gradient at greater depth, where water (released by deep magma or by metamorphic processes) is in thermal and mechanical equilibrium with the surrounding rock.

We shall assume very schematically that water released by magma below the crust gradually accumulates at depth, building up a reservoir of hot pressurized fluid topped by an impervious cap which separates the lithostatic from the hydrostatic domain. We investigated the role of fluids in the preparatory stage of earthquake nucleation, assuming that this nearly impervious barrier is gradually eroded by dilatancy, until the rock suddenly becomes permeable, and a transient upflow of deep fluids takes place. Then, two strictly related processes take place: pore pressure increases in the layer between the high-pressure reservoir and the hydrostatic meteoric aquifer and the thermal gradient also changes from the conductive regime to the advective regime, which is characterized by higher temperatures.
The equations employed to describe this coupled thermo-poro-elastic problem were obtained by Mc Tigue (1986) and Bonafede (1991); for a 1-D configuration, in which the dependence on time t and depth z are considered, the governing equations reduce to an energy balance equation

$$\rho c \frac{\partial T}{\partial t} - k_T \frac{\partial^2 T}{\partial z^2} = -\frac{\rho_f c_f K}{\mu(T)} \left(\frac{\partial T}{\partial z} \right) \left(\frac{\partial P}{\partial z} \right)$$

where ρ is the density and c is the specific heat of the saturated rock, k_T is the thermal conductivity of the saturated rock, ρ_f is the density and c_f the specific heat of the fluid, K is the rock permeability, $\mu(T)$ is the fluid viscosity, which is assumed temperature dependent, according to the relation: $\mu = a\ exp\{-b(T-T_0)\}$, with $a = 3 \cdot 10^{-4}$ Pa s and $b = 7 \cdot 10^{-3}$ °C^{-1}, T is temperature, P is fluid pressure in excess of the hydrostatic value $\rho_f gz$.
To this, a diffusion equation for pore pressure adds, which takes into account fluid mass conservation and the equilibrium equation

$$\frac{\partial P}{\partial T} - \frac{\partial}{\partial z} \left(\kappa_f \frac{\partial P}{\partial z} \right) = \frac{S}{T_0} \frac{\partial T}{\partial t}$$

where κ_f is the hydraulic diffusivity, which is proportional to KG/μ (Rice & Cleary 1976, McTigue 1986), G is rock rigidity, T_0 is a reference temperature (the temperature of the deep reservoir), S is a material coefficient incorporating knowledge of the thermal expansion of the rock and the fluid, and the mechanical interaction between pore pressure and stress (S may be interpreted as the pressure increase that would be induced by a temperature increase T_0 in an impervious medium (Bonafede and Mazzanti 1997). The previous system of equations incorporates the Darcy law governing fluid flow, the equilibrium equation and the constitutive equation in thermo-poro-elastic media (see Bonafede 1991).
From the previous equations, since water viscosity is strongly temperature-dependent, the pore-pressure also increases within the advectively heated layers, so that the Coulomb failure function increases considerably, with two different time scales: one related to the hydraulic diffusivity governing the diffusion of pore pressure and one related to temperature migration following advection processes. The change in temperature and pore pressure between the initial configuration (conductive and hydrostatic) and the final stationary configuration (advective and super-hydrostatic) may be best appreciated from figure 3, computed for sandstones (high permeability rocks) and a granites (low permeability rocks). It may be stressed that connected permeability lines develop before a connected fracture surface develops, i.e. much before faulting occurs. Thus, the pore pressure increase related to the onset of fluid migration and to the thermally activated viscosity decrease generates a positive feedback mechanism, leading to increasing Coulomb failure function, increasing permeability, faster advection, higher temperature, higher pressure and so on, until eventually macroscopic faulting may take place; rupture of a fault surface increases enormously the permeability along the fault surface and fluid migration accelerates in the post-seismic phase. Eventually, exhaustion of the deep fluids brings the pore pressure gradient back to hydrostatic, the Coulomb failure function decreases and the medium strength increases: the seismic cycle is over. The next earthquake in the region will not take place on the same fault

because shear stress was released in the volume surrounding the fault but also because deep fluids were exhausted below its base. Solutions of the previous problem can be obtained analytically for the stationary regime in a bounded medium. Solutions were obtained for the self-similar problem in an unbounded medium obeying suitable B.C. The set of PDE's can be put into a self-similar form employing the similarity variable $\zeta = z/2\sqrt{\kappa_T t}$. This reduces the equations to a set of ODE's which can be solved employing standard numerical methods (Runge-Kutta of 4-th order). In this case no stationary regime is attained and, in spite of the very different Temperature fields, pore pressure is very similar among media endowed with different permeabilities. This is due to the temperature front lying well behind the pressure field.

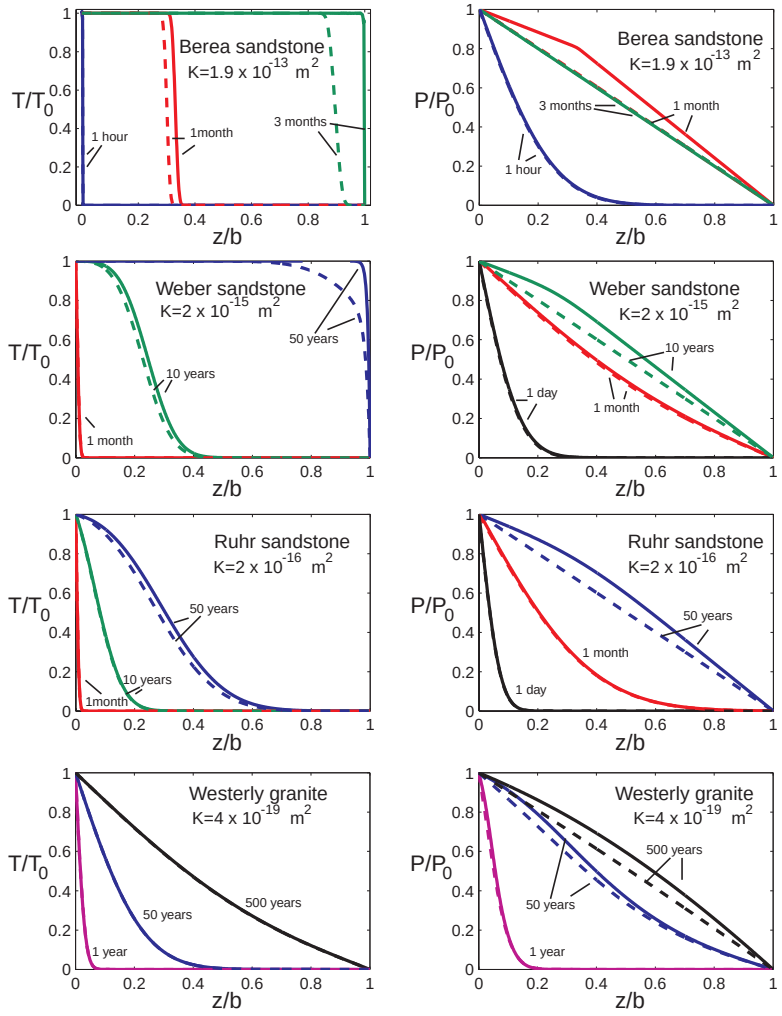

Figure 3. Temperature (left) and pressure (right) fields for several materials, characterized by different permeability values K (shown in each panel). The layer undergoing transition from conductive to advective regime has thickness b=1 km. Fluid density and specific heat are assumed to be constant and pertinent to water at 200 °C and 100 MPa. Solid lines show solutions when the temperature dependence of fluid viscosity is accounted for; dashed lines show solutions for constant viscosity. In the high permeability sandstones the temperature field in the long term deviates significantly from a linearly decreasing (conductive) geotherm. The pore pressure is significantly affected by the temperature change, particularly if the temperature dependence of viscosity μ is accounted for: in high permeability media, pressure increases in the transient phase beyond the stationary linear trend typical of isoviscous fluids. In the low permeability granite, the temperature field tends to approach a linear conductive profile (advection is negligible) but the pore pressure is significantly affected by the greater thermal expansion of water

w.r to the solid matrix; this effect is emphasized when the temperature dependence of viscosity $\mu(T)$ is accounted for.

Transient solutions were also obtained numerically employing the method of lines: the trial solutions were written as combinations of cubic Hermite polynomials and the time-dependent coefficients were obtained through the collocation method by imposing that the trial solutions satisfy the differential equations at selected points within the mesh. The pore pressure during the transient phase is found to be significantly higher than in the stationary regime! This is essentially due to the temperature dependence of fluid viscosity. The present model has important implications for the interpretation of time-dependent seismic tomography (WP2.4), Radon anomalies (WP 3.2), hydrological changes associated with earthquakes (WP 5.5) and probability changes due to stress transfer (WP6.1).

D-102. Fault interaction by dynamic stress transfer

Fault interactions studies provide a contribution to the understanding of the physical processes at the base of earthquakes sequences. In particular, the explanation of short-term and long-range interactions can rely upon the study of the dynamic stress redistribution during the sequence studied. After the first magnitude 6.6 earthquake of year 2000, here called the main event, a series of earthquakes followed immediately to a distance of 100 km along the SISZ and its prolongation along the Reykjanes peninsula (RP). We considered in particular two of the largest events recorded by the digital local seismic network SIL after the main shock, within 1 minute of its occurrence. These events were localized in the RP, about 60 km to the West of the main event. We computed the dynamic Coulomb Failure Function variation ΔCFF produced by the main event in the region where the two aftershocks occurred. To this aim, we preliminarily assumed a 4 layers crustal model (Table 1) that reproduces the main features obtained by tomographic studies West of the Hengill location in the SISZ, within the first 20 km of depth (Vogfjörð,, personal communication). The code used to compute dynamic stress is based on the discrete wave-numbers and the reflectivity method (Cotton and Coutant, 1997).
Our preliminary results are shown in Figure 4, where we plot the variation of the ΔCFF as a function of time t in the location of the hypocenter of the two aftershocks. It is clear from Figure 4 that both the two aftershocks did not occur immediately at the arrival time of the seismic waves generated by the main event, as confirmed by seismological observations (Vogfjörð, 2003). From Fig. 4 it is also evident that the aftershocks occurred close to a peak of ΔCFF.

Table 1. Crustal model used for modeling the CFF variation

Depth (km)	V_p (km/s)	V_S (km/s)	ρ (kg/m^3)
0-3.1	3.30	1.85	2300
3.1-7.8	6.00	3.37	2900
7.8-17	6.85	3.88	3100
>17	7.50	4.21	3300

These results support the idea of dynamic triggering for both the two aftershocks, recently suggested by Pagli et al., 2003. We tested the stability of these results with respect to small variations of the rise time, main fault orientation and slip distribution, and using another crustal model (that reproduces the main structural features observed East of Hengill, Vogfjord personal communication). We still obtained that the aftershocks occurred during a time interval of high ΔCFF, as evaluated at their hypocenter. We are also analyzing the response of a fault modelled as a spring-slider with rate- and state-dependent friction, to the computed time dependent shear and normal stress perturbation shown in Fig. 4, in order to verify the

possibility of instantaneous triggering due to transient stress changes (Belardinelli et al., 2003).

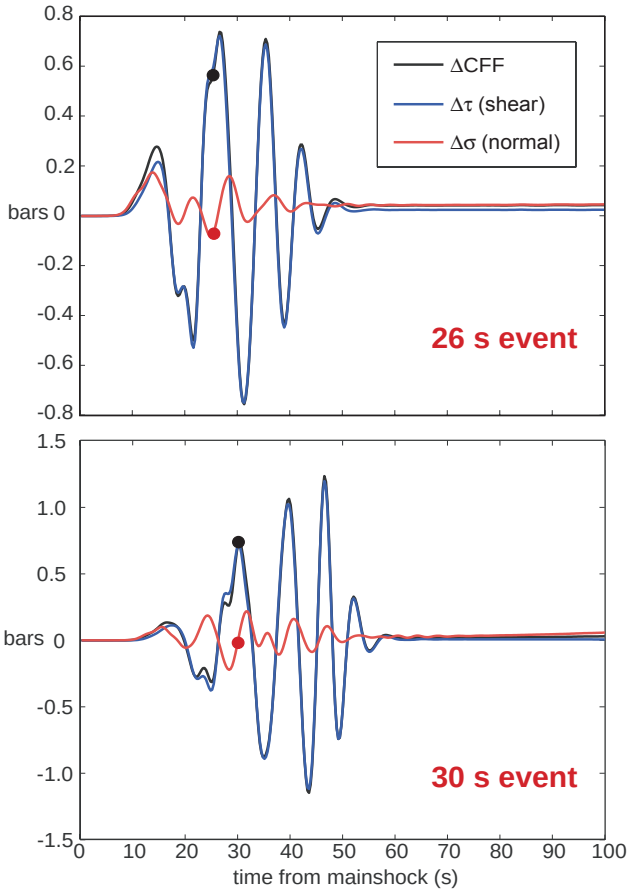

Figure 4. *Variations of Coulomb Failure Function, shear stress and normal stress due to the main event of 17/06/2000 as functions of time and evaluated at the hypocentral locations given by the SIL network for aftershocks occurred after 26s and 30s from the mainshock. The ΔCFF is evaluated assuming right-lateral strike-slip faults oriented N-S.and an apparent friction coefficient equal to 0.4 (Beeler et al., 2002 and references therein). Time is computed starting from the origin time of the main event. The value of the normal stress and the CFF variations at the origin time of the aftershock is evidenced by solid circles. For the mainshock we assumed a Haskell source model, with a bilateral rupture (Minigutti, personal communication), a 1.8 s rise time, and a 2.5 km/s rupture velocity. The main event source is a right lateral fault (180° rake) with 7° strike, 86° dip, as suggested by the aftershocks distribution (Stefansson et al, 2003). We took the slip distribution on the main fault inferred by geodetic data (Arnadottir et al., 2003).*

References

Arnadottir, T, S. Jonsson, R. Pedersen and G.B. Gudmundsson, 2003. *Geophys Res. Lett.,* 30 (5), 10.10292002GL016495.
Belardinelli M.E., Bizzarri A., Cocco, M., 2003. *J. Geophys. Res.*, 108 (B3), 10.1029/2002JB001779.
Beleer N. M., Simpson R. W., Hickman S. H. and Lockner D. A., 2000. *J. Geophys. Res.*, 105, 25,533-25,542.
Bonafede, M., 1991. *J. Volcanol. Geotherm Res.*, 48, 187-198.
Bonafede, M., Mazzanti, M., 1997. *Geophys. J. Int.*, 128, 383-398.
Bonafede, M., Parenti, B. and Rivalta, E., 2002. *Geophys. J. Int.*, 149, 698-723.

Cotton, F., and O. Coutant, 1997. *Geophys. J. Int.*, 128, 676-688.
Mc Tigue, D.F., 1986. *J. Geophys. Res.*, 91, 9533-9542.
Pagli, C., R. Pedersen, F. Sigmundsson and K. Feigl, 2003. *Geophys Res. Lett.*, 30 (6), 10.10292002GL015310.
Rice, J.R., and Cleary, M.P., 1976. *Rev. Geophys. Space Phys.*, 14, 227-241.
Stefansson, R., G. Gudmundsson and P. Haldòrsson, 2003. URL: http://hraun.vedur.is/ja/prepared/SouthIcelandEarthq2000/.
Vogfjörð, K., S., 2003. Abstract Book CD-ROM 'Geophysical Research Abstracts' Volume 5, 11251, 2003.

Annex

Contributions of Partner 10 - CNRS.DTP (Toulouse)

Work packages in which CNRS.DTP (Toulouse) participates

CNRS.DTP (Toulouse) participates in the following work packages:

- WP 2.3 Long-term deformation in SISZ from joint interpretation of GPS, InSAR & borehole strain data
- WP 4.4 Deformation model for the June 2000 earthquakes from joint interpretation GPS, INSAR and borehole strain data
- WP 6.1 Earthquake probability changes due to stress transfer

WP 2.3 Long-term deformation in SISZ from joint interpretation of GPS, InSAR & borehole strain data

Objectives

From proposal.

Methodology and scientific achievements related to Work Packages including contribution from Partners.

The contribution from Toulouse has been mostly technical support in for INSAR and GPS data analysis.

For the INSAR data analysis to date, we have used version 1.0 of the DIAPASON/PRISME software developed at the French Space Agency (CNES) and the associated open-source scripts DTOOLS developed by CNRS.DTP. The results from the INSAR analysis have been published. The primary conclusion in terms of the INSAR technique is that C-band SAR correlation breaks down in less than one year in the vegetated lowlands where the June 2000 earthquakes occurred.

Articles in the international, peer-reviewed literature :

Pagli, C., R. Pedersen, F. Sigmundsson, and K.L. Feigl, Triggered seismicity on June 16, 2000 on the Reykjanes Peninsula, SW Iceland captured by radar interferometry, Geophys. Res. Lett., 30 (6), 1273, doi:10.1029/2002GL015310, 2003.

Jonnsson, S., P. Segall, R. Pedersen, and G. Bjornsson, Post-earthquake ground movements correlated to pore-pressure transients, Nature, 424 (10 July 2003), 179 - 183, 2003.

Pagli, C., R. Pedersen, F. Sigmundsson, and K.L. Feigl, Triggered seismicity on June 16, 2000 on the Reykjanes Peninsula, SW Iceland captured by radar interferometry, Geophys. Res. Lett., 30 (6), 1273, doi:10.1029/2002GL015310, 2003.

Pedersen, R., S. Jónsson, T. Árnadóttir, F. Sigmundsson, and K.L. Feigl, Fault slip distribution derived from joint inversion of InSAR and GPS measurements of two June 2000 Mw 6.5 earthquakes in South Iceland, Earth Plan. Sci. Lett., 213, 487-502, 2003.

Pedersen, R., F. Sigmundsson, K.L. Feigl, and T. Árnadóttir, Coseismic interferograms of two MS=6.6 earthquakes in the South Iceland Seismic Zone, June 2000, Geophys. Res. Lett., 28, 3341-3344, 2001.

Presentations at international symposia:

Sigmundsson, F., R. Pedersen, K.L. Feigl, E. Sturkell, P. Einarsson, S. Jonsson, K. Agustsson, A. Linde, and F. Bretar, Joint Interpretation of Geodetic Data for Volcano Studies: Evaluation of Pre- and Co-eruptive Deformation for the Hekla 2000 Eruption from InSAR, Tilt, GPS and Strain Data, in AGU fall meeting, San Francisco, USA, 2001.

Jonsson, S., R. Pedersen, P. Segall, and G. Björnsson, Postseismic poro-elastic deformation in South Iceland observed with radar interferometry: Implications for aftershock decay, in AGU Fall Meeting, San Francisco, 2002.

Feigl, K.L., L. Dubois, D. Komatitsch, R. Pedersen, T. Arnadottir, K. Vogfjord, and F. Sigmundsson, Finite element models of co- and post-seismic deformation from two M 6.6 earthquakes in Iceland, in EGS, Nice, 2003.

Socio-economic relevance and policy implication

The deformation field estimated in this work package is one of the inputs for WP 6.1 (Earthquake probability changes due to stress transfer).

Discussion and conclusion

This work package is on schedule.

Plans and objectives for the next period

For the GPS analysis, we continue to work on a solution including all the data available (continuous and campaign) in the SISZ from 1992 through the end of 2003. We plan to estimate displacements for punctual events at discrete epochs and velocities (displacement rates) for intervals of time. Currently, we estimate displacement parameters for the following events:

- Earthquake of Nov 1998
- Earthquake of 2000-JUN-17
- Earthquake of 2000-JUN-21

In addition, we estimate velocities for the following intervals:

- Pre-seismic (1992 through 2000 JUN 16)
- Early post-seismic (2000-JUN-22 through 2000-OCT-01)
- Middle post-seismic (2000-OCT-01 through 2001-OCT-01)
- Late post-seismic (2001-OCT-01 through 2003-DEC-31)

WP 4.4 Deformation model for the June 2000 earthquakes from joint interpretation GPS, INSAR and borehole strain data

Objectives

From proposal.

Methodology and scientific achievements related to Work Packages including contribution from Partners

We have developed a 2-step estimation process. First, we solve a non-linear inverse problem to estimate the following parameters related to fault geometry: strike, dip, rake, easting, northing, depth, length, and width. Next, we solve a linear inverse problem to estimate the distribution of slip (rupture) on the fault plane. The results have been published in the international, peer-reviewed literature :

Pedersen, Rikke., Sigurjon Jónsson, Thora Árnadóttir, Freystein Sigmundsson, and Kurt L. Feigl, Fault slip distribution derived from joint inversion of InSAR and GPS measurements of two June 2000 Mw 6.5 earthquakes in South Iceland, *Earth Plan. Sci. Lett. 2003.*

Socio-economic relevance and policy implication

The slip distribution estimated in this work package is one of the inputs for WP 6.1 (Earthquake probability changes due to stress transfer).

Discussion and conclusion

This work package is on schedule.

Plans and objectives for the next period

In Toulouse, we plan to improve the estimated slip distribution by improving both the data in the inversion and by improving the parameterization.

The analysis of the geodetic data input to the inversion can be improved in several respects. The partners in this work package have agreed in principle on the following Proposal for a chapter in the Ph.D. thesis of Cristina Catita, to be entitled, "Application of SAR interferometry and correlation to deformation associated with the earthquake sequence of June 2000, south Iceland". We expect that this thesis chapter will lead to a publication in the international, peer-reviewed literature.

The work requires the following inputs:

- GPS estimates of June 2000 co-seismic displacements from Thora, Weipeng and Kurt
- Matlab scripts for inversion as used in Pedersen et al. 2003 (Rikke to make archival CD-ROM)
- Raw ERS and ENVISAT data as shared between CNRS and NORVOLC
- Elevation model of SISZ in UTM coordinates at 50 m posting.
- Diapason/PRISME version 3.0 Linux (in beta test now). Univ. Lisbon & Norvolc should both purchase at 2000 euros.
- DTOOLS scripts, including ps_filt2.c and stackamp.c

The first step will be a complete re-analysis of available ERS images using INSAR, with the following improvements:

- high resolution DEM in UTM coordinates
- temporal adjustment
- orbital corrections
- permanent scatterers

The next step will be to estimate the "azimuth offsets" for co-seismic displacements of June 2000 earthquakes from the available co-seismic pairs of images. This represents a feasibility study using existing ERS data, above and beyond the description of work. On the other hand, we will not attempt to analyze the data from the strain meters. If useful results are available (from S. Jonsson?), we can include them in the inversion. Similarly, we do not intend analyze the seismograms directly, preferring to use derivative products (e.g., focal mechanisms and hypocentral locations of aftershocks) to constrain the solution.

Once the data analysis is complete, we will proceed with interpretation and validation, including:

- geodetic analysis of improvements, including error budget
- repeat joint inversion for co-seismic parameters

- starting with matlab scripts used for solution published in EPSL
- adding azimuth offsets
- sensitivity analysis to different GPS inter-seismic rates
- considering surface rupture?
- considering aftershock locations?
- validation using available models for co-seismic, inter-seismic and post-seismic deformation

We also plan to improve the parameterization for the co-seismic model using Finite Element Modeling, as described under WP 6.1

WP 6.1 Earthquake probability changes due to stress transfer

Objectives

From Description of Work

- Improving probabilistic earthquake hazard assessment through stress field models for media with both elastic and inelastic layers.
- Achieving a time-dependent hazard analysis by deducing changes in the probability of future earthquakes due to stress transfer.

Contribution of CNRS.DTP in Toulouse

- Developing a model capable of calculating displacements, velocities and stress in an elastic, poro-elastic, or visco-elastic medium with arbitrary geometry from boundary and initial conditions specified in terms of displacement using a finite-element approach.

Methodology and scientific achievements related to Work Packages including contribution from Partners

To date, we have accomplished the following tasks :

Choose FEM package

We have selected the TECTON package developed by Charles Williams of Renssalaer Polytechnical Institute (U.S.A.) because it possess the following desirable attributes:

- split nodes describe by *Melosh and Raefsky*, 1981
- hexahedral elements (“bricks”)
- open source
- arbitrary rheology (elastic, viscous, plastic, etc.)

We have obtained the Fortran source code directly from Williams. Note that William’s code is now distinct from the TEKTON (spelled with a “K”) package developed by J. Melosh that is freely available over the Internet.

Develop scheme to densify mesh near fault

To achieve acceptable accuracy, we need boundary conditions 200 km from the fault and elements of the order of 1 km near the fault. To meet both these requirements in a reasonable sized-mesh, we chose a mesh with a variable density shown in Figure 1.

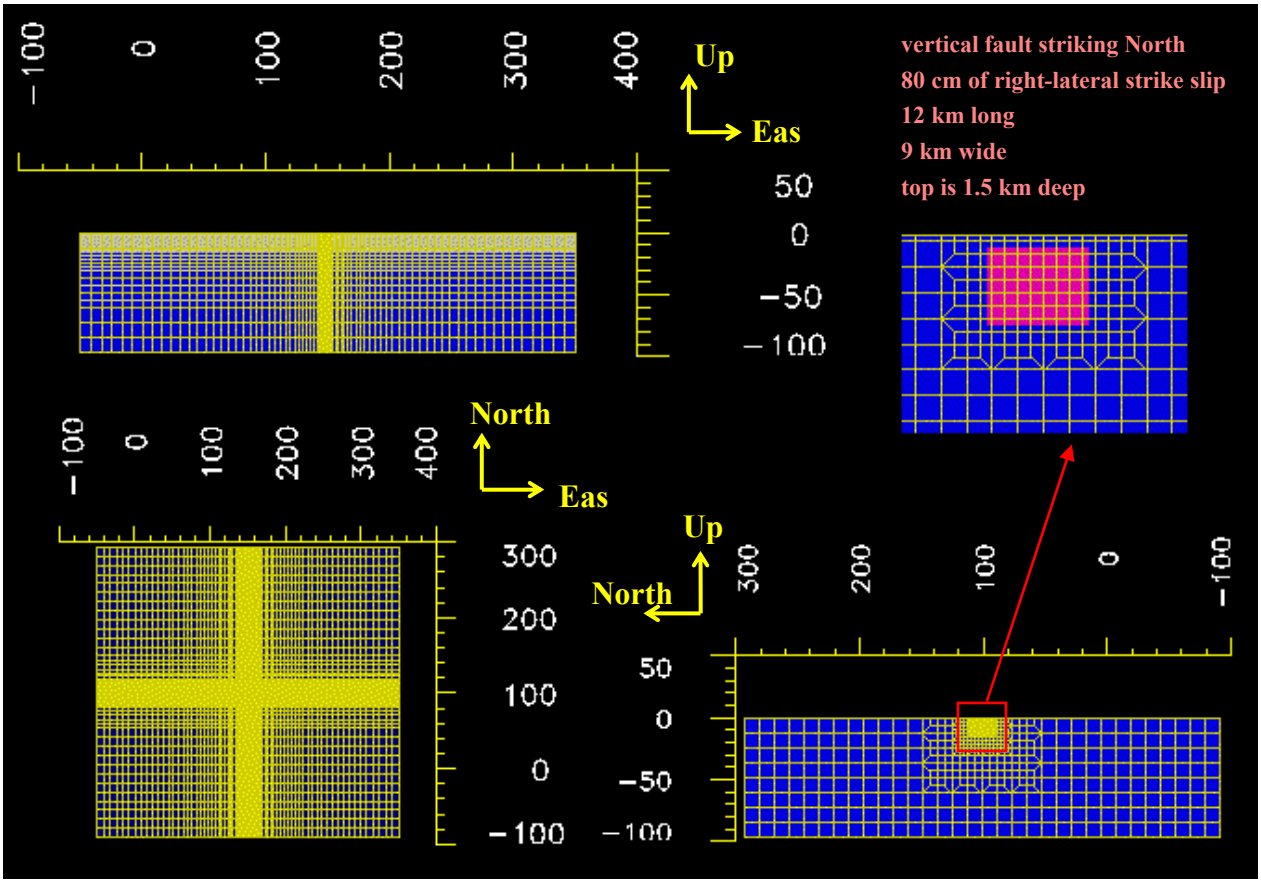

Three views of the finite element mesh which consists of 400 km x 400 km x 100 km volume. The size of the elements increases in East direction with the distance from the fault. The elements are coarsened in the North and Up direction with the distance from the fault. The upper-right corner shows a zoom on the fault.

Develop post-processing module (POSTECTON)

Starting with William's routine UCD3D in Fortran 77, we have written a post-processing routine called POSTECTON in Fortran 90. It performs the following functions :

- Read binary output file from a TECTON run
- Calculate quantities of interest (e.g. displacement, Coulomb Failure Stress) at specified (arbitrary) "observation" points
- Output in formats suitable for visualization with OpenDX, Matlab6 and GMT

Test A

- elastic half-space (no layering)
- vertical fault striking North, 80 cm of right-lateral strike slip, 12 km long, 9 km wide, top is 1.5 km deep (Figure 1)
- compare to Okada's (1985) analytic solution (Figure 2)
- displacement accuracy is good : the average error is less than 1 mm and the maximum error (near fault) is less than 10% of Okada's (1985) analytic solution

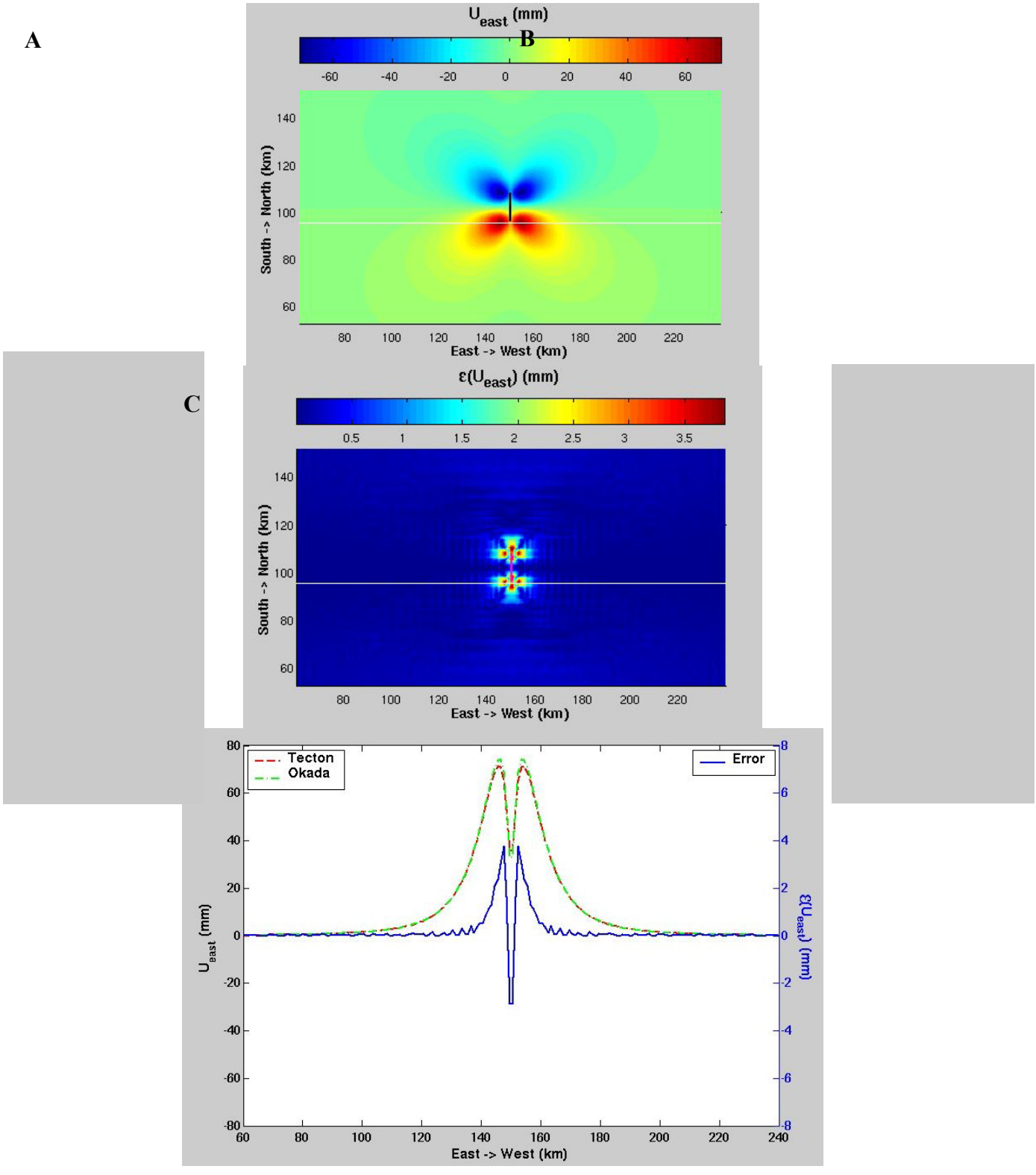

Coseismic surface displacement in East direction due to the dislocation defined in Figure 1. A **shows the result from TECTON in map view. The black N-S line is the projection of the fault onto the surface.** B **gives the difference from the comparison between the TECTON solution and Okada's analytic solution from RNGCHN (*Feigl and Dupré*,1999). The magenta N-S line is the projection of the fault onto the surface.** C **shows the displacement from TECTON and Okada's solutions and the difference between them (solid blue line, right hand scale) along an E-W profile (white line drawn in** A **and** B**).**

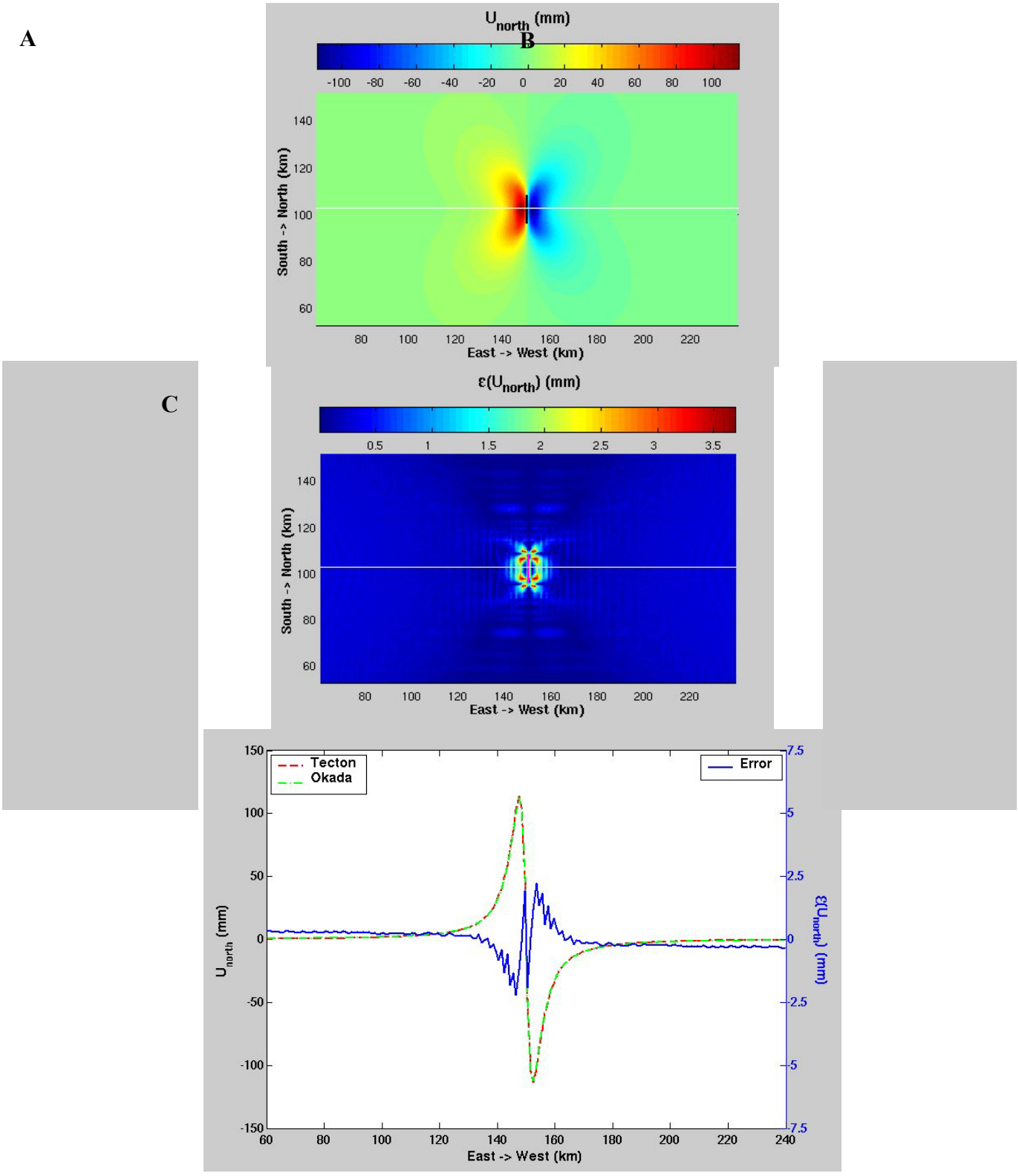

Coseismic surface displacement in North direction due to the dislocation defined in Figure 1. Plotting conventions as in previous figure.

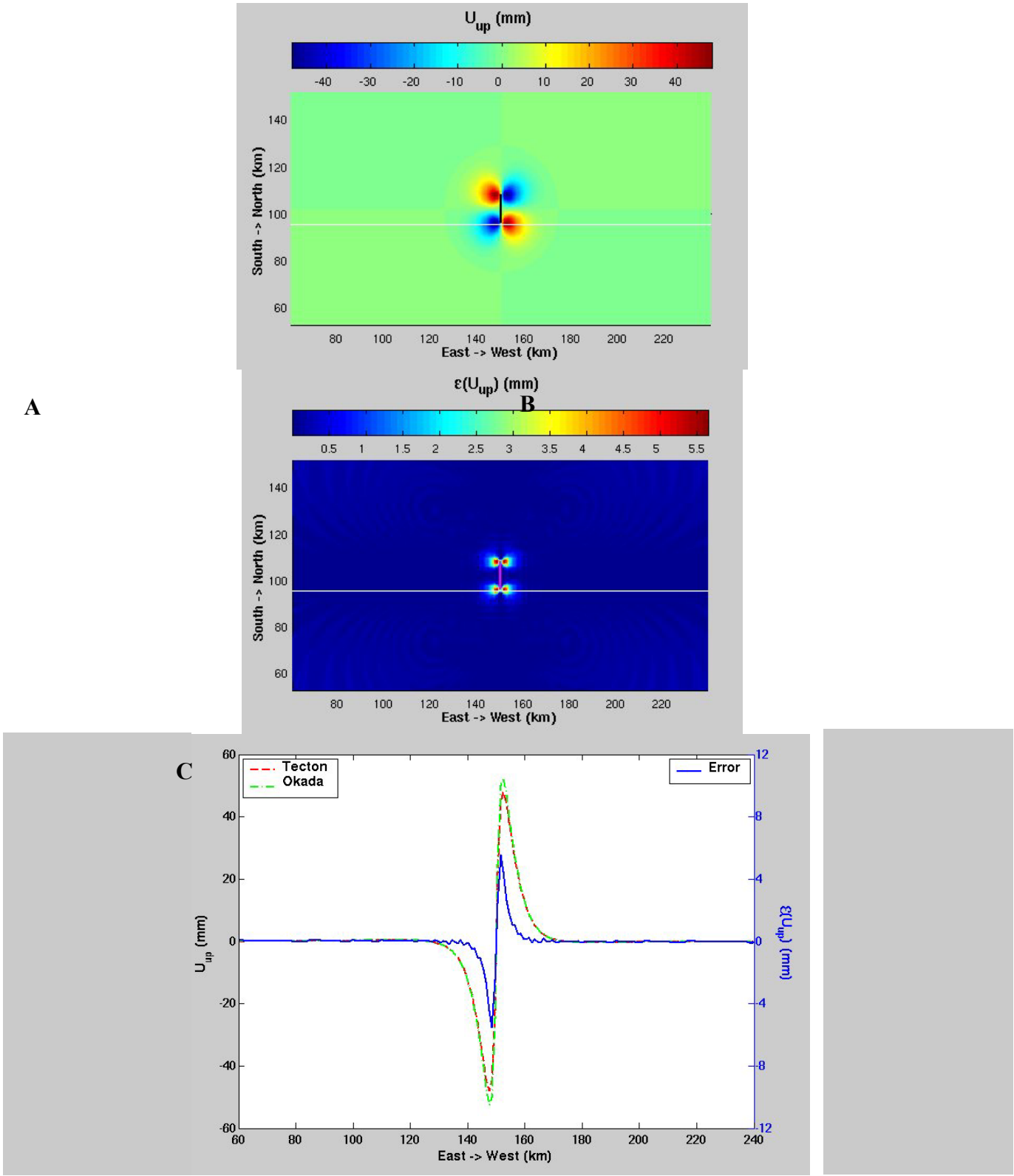

Coseismic surface displacement in Up direction due to the dislocation defined in Figure 1. Plotting conventions as in previous figure.

Test B

- poro-elastic case, compares Okada to TECTON (Figure 5)

A

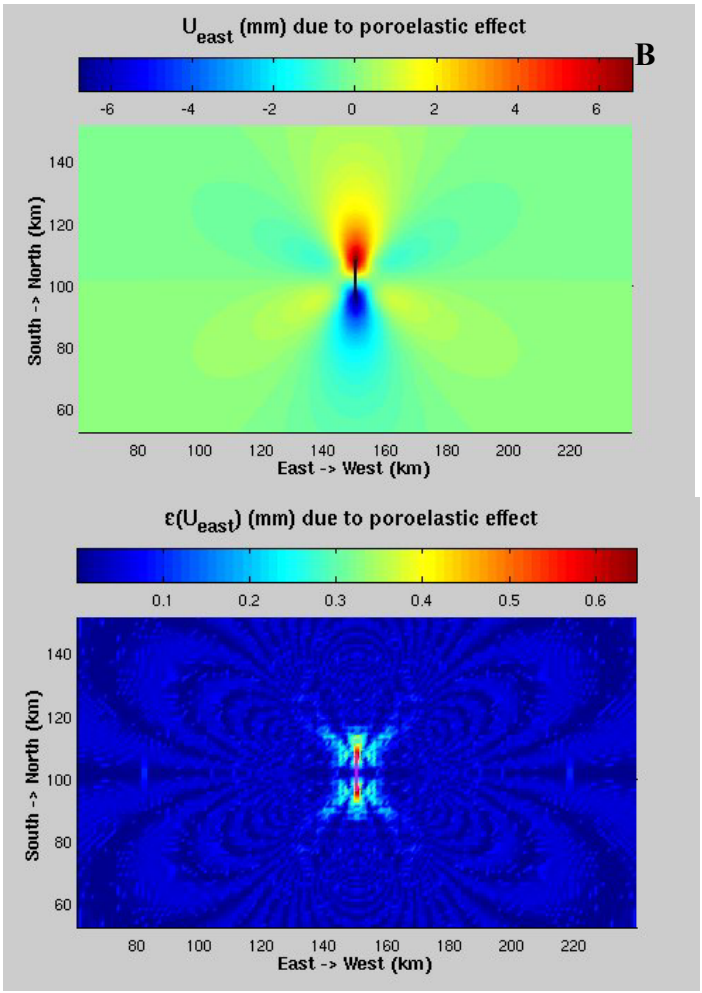

B

C

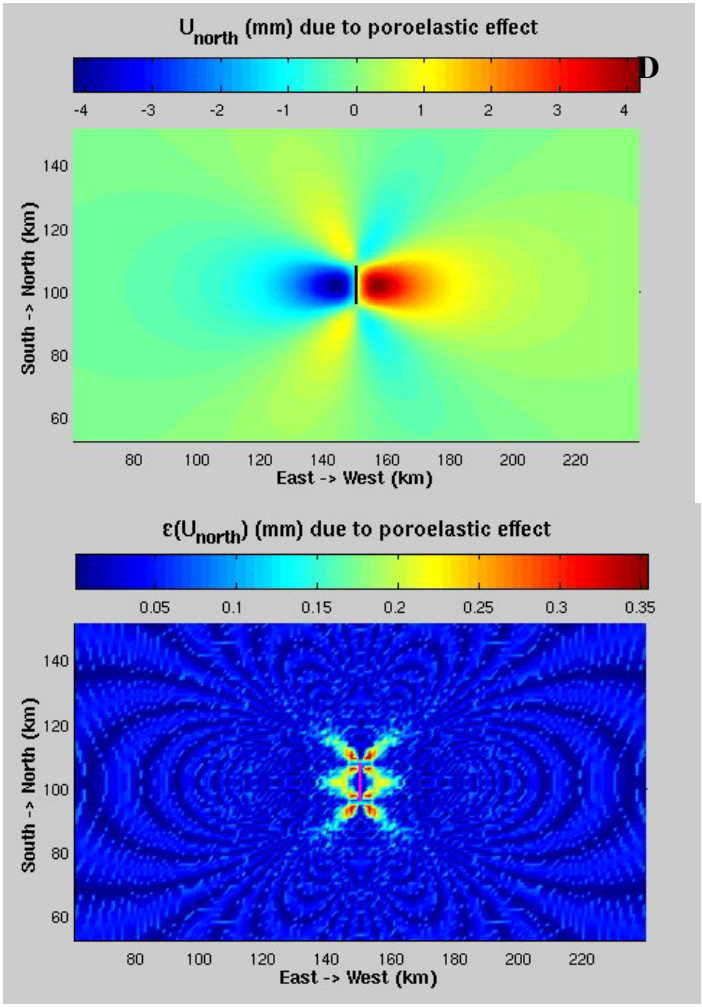
U_{north} (mm) due to poroelastic effect
-4 -3 -2 -1 0 1 2 3 4
South -> North (km)
140 120 100 80 60
80 100 120 140 160 180 200 220
East -> West (km)
$\varepsilon(U_{north})$ (mm) due to poroelastic effect
0.05 0.1 0.15 0.2 0.25 0.3 0.35
South -> North (km)
140 120 100 80 60
80 100 120 140 160 180 200 220
East -> West (km)

D

E

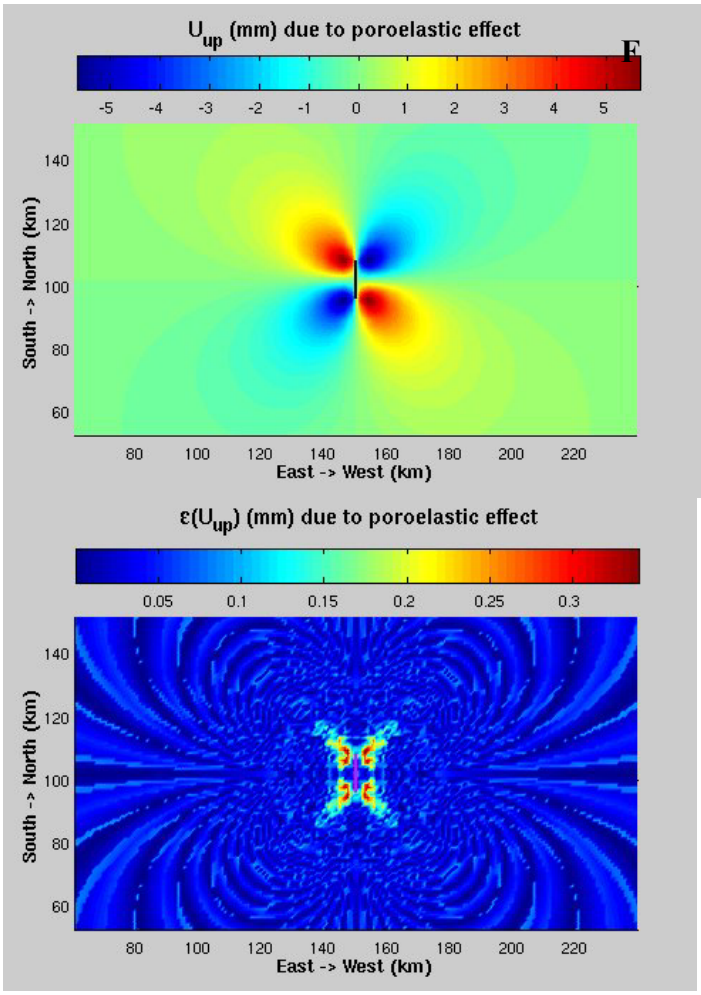

F

Poro-elastic surface displacement comparison between the TECTON solution and Okada's solution from RNGCHN with the dislocation defined in Figure 1. The method here is the application of the approximation presented in *Coco and Rice*, 2002. These figures are obtained by subtracting coseismic displacements from two run with different Poisson's ratio, $\upsilon = 0.33$ and $\upsilon = 0.27$. A, C and E result from TECTON runs and correspond respectively to the East, North and Up displacements. The black N-S line is the projection of the fault onto the surface. B, D and F show the error compared to Okada's analytic solutions. The magenta N-S line is the projection of the fault onto the surface.

Socio-economic relevance and policy implication

The stress fields calculated here will contribute to changes in estimates of Earthquake probability.

Discussion and conclusion

For the elastic cases, the difference between the Finite Element (TECTON) and analytic (Okada, RNGCHN) solution is less than 1 mm except near the fault. For the poro-elastic case, the difference is also submillimeter, but represents a larger fraction of the signal. In both cases, the agreement appears acceptable for the applications planned for PREPARED. By rigorously comparing two completely independent approaches, we have validated our complete Finite Element suite, including mesh, solver and post-processing interpolator.

Plans and objectives for the next period

In Toulouse, we plan to finish the validation tests.

Test C

- horizontal elastic layers
- compare to EDGRN/EDCMP (*Wang et al.*, 2003)

Test D

- elastic layer over viscous layer
- compare to *Yu et al.*, 1996 and/or *Savage*, 2000 solutions
- compare to Potsdam solutions in WP 6

Afterwards, we will be able to apply the finite element model to the analysis of the June2000 events with more realistic geometry, multi-layering and complex rheology. The objectives will be :

- the fault slip distribution with complex assumptions
- the comparison of the coseismic change of the Coulomb stress and the aftershocks locations
- the poro-elastic case with different permeability distributions

We will also use these finite element calculations to predict the GPS observations of the following quantities :

- Earthquake displacements of 2000-JUN-17
- Earthquake displacements of 2000-JUN-21
- Pre-seismic velocities (1992 through 2000 JUN 16)
- Early post-seismic velocities (2000-JUN-22 through 2000-OCT-01)
- Middle post-seismic velocities (2000-OCT-01 through 2001-OCT-01)
- Late post-seismic velocities (2001-OCT-01 through 2003-DEC-31)

References

Coco, M., J.R. Rice, Pore pressure and poroelasticity effects in Coulomb stress analysis of earthquake interactions, J. Geophys. Res., 107 (B2), doi: 10.1029/2000JB000138, 2002.

Feigl, K.L., E. Dupré, RNGCHN : a program to calculate displacement components from dislocations in an elastic half-space with applications for modelling geodetic measurements of crustal deformation, Computer & Geosciences, 25, 695-704, 1999.

Melosh, H.J., A. Raefsky, A simple and efficient method for introducing faults into finite element computations, Bull. Seismol. Soc. Am., 71, 1391-1400, 1981.

Okada, Y., Surface deformation to shear and tensile faults in a half-space, Bull. Seismol. Soc. Am., 75 (4), 1135-1154, 1985.

Savage, J.C., Viscoelastic-coupling model for earthquake cycle driven from below, J. Geophys. Res., 105 (B11), 25525-25532, 2000.

Wang, R., F.L. Martin, F. Roth, Computation of deformation induced by earthquakes in a multi-layered elastic crust – FORTRAN programs EDGRN/EDCMP, Computer & Geosciences, 29, 195-207, 2003.

Yu, T.T., J.B. Rundle, J. Fernandez, Deformation produced by a rectangular dipping fault in a viscoelastic-gravitational layered earth model. Part II: Strike-slip fault – STRGRV and STRGRH Fortran programs, Computer & Geosciences, 22, 751-764, 1996.